UNIVERSITY OF SOUTHAMPTON

OBSERVATIONS ON THE PHARMACOKINETICS, PHARMACODYNAMICS AND PULMONARY DEPOSITION OF NEDOCROMIL SODIUM

by

QUENTIN SUMMERS

A thesis submitted for the degree of
Doctor of Medicine

Medicine 1
Southampton General Hospital

March 1991

TABLE OF CONTENTS

UNIVERSITY OF SOUTHAMPTON

ABSTRACT

FACULTY OF MEDICINE

MEDICINE I

DOCTOR OF MEDICINE

OBSERVATIONS ON THE PHARMACOKINETICS, PHARMACODYNAMICS AND PULMONARY DEPOSITION OF NEDOCROMIL SODIUM

by Quentin Summers

Nedocromil sodium (NS) is a small hydrophilic molecule active in the treatment of asthma. NS pharmacokinetics are governed by absorption of the drug across the respiratory mucosa. In asthmatics, NS inhibits bronchoconstriction induced by inhaled adenosine-5'-monophosphate (AMP). When delivered by inhalation, by mouth or by intravenous infusion to 9 atopic asthmatics, only inhaled NS conferred significant protection against inhaled AMP. In 2 subjects, both highly atopic and highly reactive to inhaled AMP, all 3 routes of NS administration provided equivalent protection, and overall there were correlations between response to AMP and the protective efficacy of NS. Therefore the preferred route of administration of NS is by inhalation, and in those with greater degrees of airways inflammation, NS may exert some effect by delivery to sites of action via the bronchial circulation.

In normal subjects, both multiple forced expirations and a single deep inspiration with a prolonged breath-hold produce sudden rises in plasma NS. The likely mechanism is disruption of epithelial tight junctions, allowing the more rapid paracellular egress of drug into the bronchial circulation. Probenecid premedication did not alter the overall kinetic profile of NS, but was associated with greater rises in plasma NS after the respiratory manoeuvres. This may be a consequence of that fraction of NS absorption through the transcellular route being retarded by probenecid, resulting in more NS being available at the mucosal surface for paracellular transport, the first time that a probenecid-sensitive facilitated transport mechanism has been shown for a drug in the human lung. Inhaled methoxamine did not alter the induced rises in plasma NS, suggesting that changes in respiratory mucosal blood flow are unlikely to be responsible for these rises, although changes in bronchial-to-pulmonary blood flow cannot be excluded.

A method was developed to add a radioisotope (technetium-99m as pertechnetate) to NS delivered by metered-dose inhaler. This produced an aerosol in which drug and label distributed together and which preserved the aerosol size characteristics. Coarse and fine radiolabelled aerosols of NS were inhaled by 10 normal subjects, and intra-pulmonary deposition studied by planar and tomographic γ-camera imaging. No differences in deposition or pharmacokinetics were found, although the fine aerosol tended to be deposited more peripherally. New techniques were developed to describe the 3-dimensional (or volume) deposition of the aerosols, both in terms of the intensity of deposition and of the dose deposited, to allow an accurate assessment of the total dose delivered to definable sites within the lung. 50% of the intrapulmonary dose of these aerosols was in the lung periphery, and in 9 subjects, the dose increased linearly from the lung hilum to periphery, but not in another subject who had predominantly central deposition. Tomographic imaging is a valuable tool for showing the volume deposition of aerosols in the lung, and provides an opportunity to relate drug deposition and pharmacokinetics.

ACKNOWLEDGEMENTS

I wish to thank Professor Stephen Holgate for his great enthusiasm, invaluable guidance and encouragement to persist, and for enabling me to grow in the highly stimulating and challenging environment that his group provides. I would also like to thank Dr Michael Nassim and Mr Andy Clarke, both of Fisons plc, for their equally invaluable support and guidance, and for their stimulating conversations which helped maintain and increase my own enthusiasm and interest. Dr Andrew Renwick provided sound pharmacokinetic expertise, as well as a good deal of general and specific experimental advice.

Although I carried out the bulk of the work in this thesis, I would like to thank Richard Honeywell for performing the nedocromil sodium radioimmunoassay. Anne Hollingsworth performed the nedocromil sodium spectrophotometric estimations in the labelling experiments, and travelled regularly to Southampton with Mr Clarke during the development of the method. Dr John Fleming and Mr Stephen Perring provided enthusiastic practical and theoretical support and help with the nuclear imaging procedures, and Kate Wallace and Dr Richard Blacquiere provided assistance in obtaining thoracic CT scans. Yahlei Dai provided great assistance during the SPECT study, particularly with the repeated blood collections. Dr Duncan Ackery and the staff of the nuclear medicine department were always supportive and helpful. Mr Andy Tuck and Dr Lowes of the Microbiology department kindly performed the probenecid assays.

I am grateful to Fisons plc for their financial support and for supply of materials for the nedocromil radioimmunoassay and the nedocromil metered-dose inhalers, and to the Lillian Roxon Memorial Asthma Research Travel Grant (The Asthma Foundation of Victoria, Australia). Mr Philip Hemes and Mr Ian Shuttlewood of Vitalograph kindly provided the Vitalograph Compact. Dr Frank Clewes of the Department of Medical Electronics and Dr Ray Bacon of the Department of Medical Engineering both gave essential help in the design and manufacture of the apparatus used for the remote actuation of metered-dose inhalers.

I am especially grateful to the staff of Medicine I, who not only extended their friendship and support, but also eased the process of arriving and settling in a new country. My colleagues in the department were also of great help, particularly with discussions regarding experimental and statistical design. My thanks also go to all of

my subjects without whom none of this work would have proceeded. Dr Richard Tarala provided long-range support and encouragement.

Finally I would like to thank my family, Julie and Vyvyan, for their unfailing support, and their encouragement to persist, especially during those times when everything seemed to be going wrong.

Chapter 1. Introduction.

1.1 Inhaled drugs and the lung.

1.1.1 Historical review.

Inhalation therapy is the mainstay of treatment of diseases causing airflow limitation, such as asthma, chronic bronchitis and emphysema. Such therapy is not new, and was employed by ancient civilisations, by Hippocrates (460-370 BC) and by Galen (139-199 AD) (Newman & Clarke, 1983). The first specific inhalation therapy for asthma was the inhalation of the fumes of the leaves of *Datura stramonium*, which has atropine-like properties. Modern asthma therapy began with the discovery of 'adrenal substance' (Sollis-Cohen, 1900) and the subsequent isolation of adrenaline (Takamine, 1902). Ephedrine, derived from the plant *Ephedra equisetina*, was described by Chen and Schmidt in 1926, and the first synthetic adrenergic agent, isoprenaline, was produced in 1940 (Konzett). The development of the more specific β-agonists followed after a relatively short time. The utility of inhalation therapy was recognised in 1935, when Graeser and Rowe found that the inhalation of adrenaline vapour produced bronchodilatation with minimal side-effects.

The advantages of inhaled over systemic drug delivery are the ability to deliver active substances directly to the site of disease with the avoidance of systemic side-effects (thus increasing the therapeutic index), the ability to produce a more rapid clinical response and the circumvention of barriers to therapeutic efficacy such as poor absorption from the gastro-intestinal tract and first-pass metabolism in the liver (Paterson et al, 1979). More recently, parenchymal diseases of the lung such as *Pneumocystis carinii* pneumonia in immunocompromised subjects and sarcoidosis have also been treated with therapeutic aerosols (Van Gundy et al, 1988; Miller et al, 1989; Selroos, 1986).

It is now appreciated that the treatment of extrapulmonary disorders by administering drugs into the lung is a possibility, thereby utilising the large absorptive surface area of the pulmonary epithelium. Such therapy has been used in cardio-pulmonary arrest to deliver cardioactive agents such as adrenaline and atropine directly into the lung as a fluid bolus through the endotracheal tube (Redding et al, 1967), although direct intra-tracheal administration produces a much poorer intrapulmonary distribution when compared to aerosol administration (Brain et al, 1976). Other inhaled substances such as morphine (Young et al, 1989) and insulin (Wigley et al, 1971) have been

investigated for systemic therapeutic efficacy, and there is clearly a need for further work in this area.

Despite the widespread use of inhaled agents, little is known about the optimal site of deposition for maximum therapeutic response, the factors that determine drug absorption or retention within the lung, and the role of the bronchial (systemic) circulation in redistributing inhaled drugs to other sites of activity within the lung. Moreover, few studies have attempted to establish the relationship between deposition of drugs and their subsequent pharmacokinetics and pharmacodynamics, principally because of the great difficulties that exist in accurately determining the pulmonary deposition of drugs and their concentrations within the lung and airways, coupled with the problems of preparation of radiolabelled drugs. It is often stated that increasing the peripheral penetration of drugs into the lung will result in optimal drug action, although there is little information available on which to make this assumption.

This introduction will deal with the factors that influence drug deposition, retention and absorption within the lung, concentrating particularly on the therapeutic aerosols used to treat asthma, and will examine the contention that drug efficacy is enhanced by greater lung penetration.

1.1.2 Aerosols.

1.1.2.1 Properties of single particles.

An aerosol can be defined as a two-phase system consisting of a gaseous phase (usually air) and a discontinuous phase of individual particles (Swift, 1985). The rate at which an aerosol particle settles in air is an important property that depends upon particle size and shape. The terminal settling velocity (V_{TS}) of an aerosol particle is given by the formula:

$$V_{TS} = \frac{\rho d^2 G}{18 \eta C}$$

where d = particle diameter (cm), ρ = particle density (g/cc), G = gravity constant (980 cm/sec^2), η = gas viscosity (g/cm/sec) and C = correction for gas slip. This relationship is the basis for the concept of aerodynamic equivalent diameter of a particle (d_{AED}), which is defined as the diameter of a unit density sphere having the same settling velocity in air as the particle in question. This concept allows comparisons of different particles as particles with the same d_{AED} have similar

dynamics. Particles possess two other important properties which determine their behaviour, that of Brownian motion and of acquired net electric charge (see 1.1.2.3.3).

1.1.2.2 Collective properties of aerosols.

The collective property of an aerosol that is related to single particle size is the size distribution. When an aerosol is sized, the particles are counted and placed in size range intervals. The resultant distribution can then be displayed as a histogram, with the height of each size range representing the number of particles in that range. If the distribution of particles falls into a small range, the aerosol can be said to be monodisperse. The uniformity of size is an important collective property of an aerosol because of the strong size dependence of many particle properties. The size distribution of particles within an aerosol can be described in terms of the arithmetic mean value and the standard deviation.

Most aerosols have a log-normal particle size distribution (Morrow, 1974), and are better described by the count median aerodynamic diameter, the particle diameter above and below which 50% of the number of particles are distributed, and the geometric standard deviation (GSD), a dimensionless parameter which is the ratio of the 84th percentile diameter (or the 16th percentile) to the median diameter (Marple & Rubow, 1980). Most therapeutic aerosols have a GSD $>$ 1.5; it is possible to produce monodisperse aerosols having a GSD $\leq$ 1.22, although these aerosols are usually confined to research laboratories. As mass equals volume multiplied by density, and volume is proportional to the cube of diameter multiplied by π, the mass and volume of an aerosol are heavily affected by large particles. Thus, the mass median diameter (MMD) of an aerosol is related to the count median diameter (CMD) by:

$$\ln (MMD) = \ln (CMD) + 3 (\ln GSD)^2$$

As the action of therapeutic aerosols depends on the mass of drug delivered to the respiratory tract, the size distribution of such aerosols is best described by the mass median aerodynamic diameter (MMAD).

1.1.2.3 Deposition mechanisms of aerosols.

The respiratory system acts as a filter so that a significant proportion of an inspired aerosol is removed during its movement in and out of the respiratory tract. There are two main mechanisms active in this filtering process.

1.1.2.3.1 Inertial impaction.

This is probably the most important mechanism responsible for particle deposition within the proximal respiratory tract. When a particle travels in a stream of air towards an airway bifurcation or bend, its inertia will tend to carry it toward the airway wall. Countering this is the force on the particle exerted by the airstream as it bends at the bifurcation, thereby tending to keep the particle in the airstream. If the momentum of the particle is too great for its direction of travel to change with that of the airstream, it will carry on and impact on the airway wall. Because momentum depends upon mass and velocity, inertial impaction will be greatest for heavy particles or for particles travelling rapidly. In addition, a particle of low density with the same mass as a particle of high density will be affected more by airflow because such a low density particle has a greater surface area upon which the airflow can act (Heyder, 1982).

1.1.2.3.2 Gravitational sedimentation.

As particles traverse an airway, they fall under the influence of gravity. Whether a particle will make it through to the other end of the airway depends upon its density and size, the airway width and the length of time that the particle is within the airway. Sedimentation rate is proportional to particle density and length of time within the airway, and is inversely proportional to particle size and airway calibre. This deposition mechanism is predominant in the more distal airway generations.

1.1.2.3.3 Other mechanisms.

Particles may also deposit as a result of Brownian motion, interception and electrostatic forces. Brownian motion is the random movement of a particle in a gas as a result of collisions between the particle and gaseous molecules. Brownian motion increases with decreasing particle size, and is therefore of importance when small particles ($< 1\ \mu m$) are being studied, especially in areas of non-turbulent (laminar) airflow. Interception occurs when the physical dimension of a particle is sufficient to bring it into contact with an airway wall. Because aerosol particles are generally much smaller than even the smallest airways, interception is not an important factor. Some particles may carry an electrostatic charge; when such particles are in proximity to a surface, they engender the development of an opposite charge on that surface, which therefore brings about their attraction to that surface and subsequent deposition. Again, this mechanism is not an important one for therapeutic aerosols.

1.1.2.4 Deposition of aerosols.

Therapeutic aerosols are generated by a range of devices which aim to provide an aerosol that can be deposited in the lungs. The majority of the work studying the effect of aerosol particle size on lung deposition has been performed by environmental scientists, generally using monodisperse aerosols, in order to better understand the relationship between the development of pulmonary disorders and inhalation of toxic aerosols such as coal dust and asbestos fibres (Task Group on Lung Dynamics, 1966). Thus, it is well appreciated that particles > 10 μm in diameter are unlikely to deposit in the lungs, while those between 2-10 μm in diameter will deposit with varying degrees of efficiency (Stahlhofen et al, 1980). Small particles (< 4 μm) are likely to deposit preferentially in the small airways and alveoli as a result of gravitational sedimentation, whilst larger particles deposit in more central (larger) airways due to inertial impaction.

Factors other than particle size may influence the site of particle deposition within the lung. Increased central deposition by impaction occurs with increasing inspiratory flow rate or particle size (Ryan et al, 1981a); a breath-hold of up to ten seconds after inhalation enhances drug deposition by allowing longer for sedimentational deposition (Newman et al, 1980); and increasing inspired volume enhances the depth of lung penetration (Pavia et al, 1977). In both normal subjects and asthmatic patients, a decrease in airway calibre may increase central airway deposition by increasing turbulent airflow and thus inertial impaction at these sites (Pavia et al, 1977; Chung et al, 1988; Laube et al, 1986). Small sub-micronic particles do not deposit well in the lung because they are exhaled. However, it has been shown both experimentally (Melandri et al, 1977) and theoretically (Chan & Yu, 1982) that it is possible to enhance the alveolar deposition of such aerosols by imposing an electrostatic charge on the particles.

1.1.2.5 Generation of aerosols.

1.1.2.5.1 Metered dose inhalers.

The major device used for delivering aerosols to the respiratory tract is the metered-dose inhaler (MDI). This consists of an aluminium canister containing drug suspended in a chlorofluorocarbon propellant mixture, often with the addition of a surfactant both to prevent agglomeration of drug particles and as an aid to valve lubrication, or drug dissolved in a co-solvent (such as ethanol) and propellant. Upon actuatation, a small metered volume, ranging from 25 - 100 μl is released into the

atmosphere, and the exposure to atmospheric pressure causes the propellant to evaporate explosively (flashing), thus creating an aerosol cloud of drug particles contained within larger droplets of propellant. Ideally, a propellant droplet will contain one drug particle, but it is possible that a propellant droplet can contain multiple drug particles, or no drug at all. Once emitted, the aerosol cloud evolves rapidly by virtue of continued evaporation of the propellant mixture. It is commonly stated that the MMAD of aerosols delivered by metered dose inhaler is within the so-called respirable range (< 5 μm), and indeed many studies support this statement (Hiller et al, 1978; Kim et al, 1985; Dolovich et al, 1981b; Bouchikhi et al, 1988). However, this information is probably misleading as in all of these studies the aerosol cloud was sized after the propellant had been allowed to evaporate wholly or partially, leaving only drug particles, and thus is unlikely to represent the aerosol size at first entry to the respiratory tract. That such an aerosol is emitted at a velocity of 30 m/s (70 mph) (Rance, 1974) may be the major cause of the poor pulmonary deposition efficiency of such aerosols, which is of the order of 10-15% of the delivered dose, the majority of the aerosol impacting in the oropharynx (Newman et al, 1989a).

Clearly this is not the only reason for such a small deposition efficiency, as the MMAD of terbutaline delivered by metered dose inhaler is 36 μm at the actuator orifice, decreasing to 12 μm at a distance 10 cm from the actuator (Morén & Andersson, 1980). Perusal of Newman's data (1989a) reveals that the MMAD of a sodium cromoglycate aerosol emitted by metered dose inhaler (Intal 1) is greater than 22 μm. A wide spread of droplet sizes ensures that a proportion of the aerosol is of a suitable size to enter the lung. The deposition of such aerosols is thus determined both by the size distribution of the propellant droplets rather than the size distribution of the drug particles, and the high velocity at which the aerosol travels.

The mechanisms which underlie the droplet size reduction of an aerosol by spacer devices so as to enhance pulmonary drug deposition are therefore the impaction of large droplets on the spacer walls, the evaporation of propellant with a resulting fall in particle size and a reduction in aerosol cloud velocity (Newman et al, 1981a). A finer aerosol can be emitted from metered dose inhalers if changes are made during the manufacturing process, by decreasing the drug particle size and concentration, decreasing the valve stem orifice, decreasing the actuator orifice, or increasing propellant vapour pressure, concentration or temperature (Dolovich, 1989).

1.1.2.5.2 Nebulisers and dry powder inhalers.

Therapeutic aerosols are also produced by jet or ultrasonic nebulisers, and by dry powder inhalers. The aerosol cloud generated by these devices is much more stable than that emitted by metered dose inhalers because of the absence of the highly volatile propellant gas mixtures.

Jet nebulisers produce an aerosol by use of the Bernoulli effect. A high velocity air stream is produced by channelling air through a narrow nozzle adjacent to one end of a tube, the other end of which is placed into the fluid within the nebuliser. A negative pressure area is created at that end of the tube adjacent to the nozzle which sucks fluid through the tube into the airstream and disrupts it into particles. Large particles are broken up further by their impaction on internal baffles, or they may impact on the walls of the nebuliser and return to the fluid, while smaller particles are carried by the airstream out of the nebuliser. Jet nebulisers generally produce aerosols with MMAD's between 1 - 8 μm (Newman et al, 1986). Smaller particles can be generated by increasing the driving gas flow rate, by decreasing inspiratory flow rate, by increasing environmental temperature and by decreasing relative humidity (Lewis, 1984). The MMAD of these aerosols falls during nebulisation in concert with the profound fall in temperature which occurs within the nebuliser because of evaporation of the nebuliser solution in order to saturate with water vapour the gas used to generate the aerosol (Phipps & Gonda, 1990).

Ultrasonic nebulisers produce aerosols by passing an ultrasonic wave generated by a piezo-electric crystal through the fluid. Standing waves are induced in the fluid, and because the tips of the standing waves are unstable they disrupt into small droplets. The size of these droplets depends upon the power and frequency of the crystal. Unlike jet nebulisers, these devices generate heat, which, together with the fact that these nebulisers may degrade some nebulised compounds limits their use for the delivery of therapeutic agents, although they deliver aerosols of similar or larger size than the jet nebulisers (Gale, 1985; Newman et al, 1986).

Dry powder systems produce aerosols by utilising the inspiratory flow rate developed by the patient to disperse the powder into small particles. The dose deposited in the lung depends upon the inspiratory flow rate; a low flow rate will produce a bigger aerosol than a higher inspiratory flow, and therefore less will penetrate into the lungs (Richards et al, 1987). There is little information relating the particle size distribution

and lung deposition of drugs delivered as dry powders, excepting that for terbutaline delivered from the breath-actuated Turbuhaler® device (Newman et al, 1989b). Deposition studies showed a mean 14.5% of the inhaled dose within the lungs, when inhaled at an inspiratory flow rate of 56 l/min, compared with the sizing data that 32% of the terbutaline powder aerosol was less than 10 μm. However, because these workers have also shown that an aerosol generated by a metered dose inhaler with a similar size distribution, but emitted at high velocity, has a similar lung deposition (Newman et al, 1989a), the dry powder work suggests that particle size rather than aerosol velocity is the major determinant of lung dose.

1.1.2.6 Radiolabelled aerosol studies.

The most effective way to determine the deposition of an inhaled drug is by the use of radioactive substances attached to or carried with the drug enabling an image of the activity within the lung to be obtained. However, it is difficult to radiolabel drugs delivered by metered dose inhaler or in dry powder form as the contents may be inaccessible, and because of the problems inherent in the preparation and handling of such drugs. Only one study has been performed in which a drug has been directly labelled (Spiro et al, 1984). In this case, a cyclotron was used to label the bromide moiety of ipratropium bromide to enable gamma-emission images of its pulmonary distribution to be obtained.

The radioactive isotope most commonly used is technetium-99m (Tc^{99m}), which has a suitable energy for gamma-ray emission detection and a short half-life of decay (six hours). Most studies have utilised monodispersed Teflon particles labelled with Tc^{99m} and delivered by metered dose inhaler, yielding valuable information regarding the deposition of the particles, but such studies cannot substitute for information regarding the pulmonary deposition of drug solutions delivered by metered dose inhaler. Many investigators have used radiolabelled aerosol delivered by jet nebuliser as this is a more accessible system. Recently, a technique for the easy addition of Tc^{99m} to metered dose inhalers has been described (Köhler et al, 1988), and a similar method has also been utilised to add label to sodium cromoglycate (Newman et al, 1989a). Because Newman's technique preserves the particle size distribution of the aerosol, and because the radiolabel is closely associated with the drug, it allows the study of the lung deposition of such radiolabelled drugs, coupled with the study of drug pharmacokinetics and pharmacodynamics. Even so, it should be noted that, once deposited, the factors that determine dissolution and clearance may affect the drug and

co-deposited label differently.

Once radiolabelled drugs have been inhaled, it is possible to obtain images of the distribution by scintigraphic recording of gamma-emission within the chest. Conventionally, these images have been planar views of the chest, following which computer-generated regions of interest are superimposed on the image to represent 'central' and 'peripheral' areas of the lung. The relative amounts of activity within the two regions can be estimated, and information can be gained about factors affecting deposition. The information derived from planar images is not accurate, because the central region invariably contains large areas of overlying peripheral lung. Moreover, the definition of the limits of the regions is arbitrary, and the information contained within lung between the central and peripheral regions is often not used. Phipps and colleagues (1989) have recently utilised single photon emission computed tomography (SPECT) to obtain more detailed information regarding the sites of deposition of inhaled aerosols, and have shown that the technique is a better discriminator than planar gamma-emission imaging for demonstrating differences in radioaerosol deposition in central and peripheral lung regions. SPECT allows the acquisition of tomographic images of the lung, and when these are reconstructed by computer, images similar to those obtained by conventional x-ray thoracic CT imaging can be generated showing radioaerosol deposition in transverse, coronal and sagittal planes. In addition, this technique allows the generation of three-dimensional images of the whole lung. By linking SPECT to conventional CT images it is possible to obtain detailed anatomical information enabling precise localisation of radioaerosol deposition (Logus et al, 1984). The main limiting factor of this procedure is the resolving power of the gamma-camera used to obtain the images; most cameras cannot resolve structures less than 1 - 1.5 cm in diameter, and therefore it is not possible accurately to separate radiolabel deposited in the trachea and oesophagus, for example, or to identify small airways.

Notwithstanding the technical limitations of conventional planar gamma-emission imaging, there have been a number of studies which have examined the distribution of inhaled radio-aerosol in subjects with and without airways obstruction. Some studies have found no difference in the amount of aerosol deposited in the lung, or in the intra-pulmonary deposition pattern when comparing normal subjects and those with airflow limitation (Spiro et al, 1984; Trajan et al, 1984; Gillett et al, 1989), whereas others report that in airways disease there is reduced peripheral penetration of aerosol (Laube et al, 1986; Chung et al, 1988).

1.1.2.7 Drug retention and absorption.

Once deposited, inhaled drugs are either cleared from the lung or absorbed into the circulation. Substances which impact in the conducting airways may be cleared by the mucociliary escalator or absorbed through the epithelium. The mechanisms underlying the absorption of drugs from the lung are poorly characterised. Substances that deposit in the alveoli may be taken up by alveolar macrophages, or absorbed into the pulmonary circulation.

The bronchial epithelium is highly specialized, mucus-lined and pseudostratified. Cells that line the airway lumen have an apical membrane in contact with the periciliary fluid beneath the mucus sheet, and a basolateral membrane which forms the sides and basal surface of the cell. The apical membranes are joined by tight junctions which act as barriers to fluid flow, controlling the passage of ions and neutral species through the intercellular space which forms the paracellular pathway. Tight junctions are fundamental to the organisation of the transcellular pathway, which mediates transport of substances through the cell, by dividing the cell membrane into functionally distinct apical and basolateral domains (Gumbiner, 1987). Non-polar molecules with high lipid- and low water-solubility (lipophilic molecules) pass easily through the cell membrane, whereas polar ionic compounds which are hydrophilic permeate through the tight junction. Active transport mechanisms exist that are responsible for molecular transport via endo- and exocytosis, one-way pumps and exchange pumps. Such intercellular organisation and junctional complexes are also a feature of the alveolar epithelium (Jones et al, 1982), and it has been shown that absorption of substances from the alveolar epithelium is more rapid than from airways epithelium (Bennett & Ilowhite, 1989).

Little is known concerning specific factors that influence airways epithelial permeability, although more is known about the factors that influence alveolar epithelial permeability. The clearance of Tc^{99m}-labelled diethylenetriaminepenta-acetate (Tc^{99m}-DTPA), a small hydrophilic molecule (mw 492 daltons) believed to move principally through intercellular junctions, has been widely used as an index of epithelial permeability (O'Brodovich & Coates, 1987). Thus, when delivered as a small (micronic) aerosol, absorption (measured as clearance from the lung) is increased in the upper lobes compared with the lower lobes, in smokers compared with non-smokers (Dusser et al, 1986), as a result of raising intra-thoracic pressure and/or volume (Marks et al, 1985; Nolop et al, 1986), during exercise (Meignan et al, 1986) and after the

inhalation of histamine (Elwood et al, 1983). The most likely explanation for these increases in Tc^{99m}-DTPA clearance is suggested by the work of Egan (1980) and Lorino et al (1989), who consider that stretching and deformation of the tight junctions are important determinants of the enhanced passage of Tc^{99m}-DTPA.

Mucosal inflammation is one of the pathological hallmarks of the airways epithelium of asthmatics (Beasley et al, 1989), and as a consequence airways epithelial permeability would be expected to increase. This has been confirmed in guinea-pig models, where airways inflammation induced both by cigarette smoke (Simani et al, 1974) and allergen inhalation (Ranga et al, 1983) have been accompanied by increased airways epithelial permeability to macromolecules. Moreover, in guinea-pigs histamine and methacholine inhalation also led to increased airways permeability, considered to be due to the opening up of the tight junctions by the chemical agents (Boucher et al, 1978). In human studies, the prior inhalation of histamine has been found to increase the absorption of the hydrophilic drug, sodium cromoglycate (Richards et al, 1988a), again considered to be due to the opening up of tight junctions. However, only one study has shown such an increase in human asthma (Ilowhite et al, 1989). By taking care to deliver an appropriately sized aerosol for optimal airways deposition, and by taking into account the contribution of mucociliary clearance to overall lung clearance, a 250% increase in airways epithelial permeability in asthmatics was demonstrated when compared with normal subjects. By contrast, other studies which have reported no difference in permeability in asthmatic subjects were flawed by the delivery of sub-micronic aerosols which would not deposit primarily in the airways (O'Byrne et al, 1984) or by failure to account for mucociliary clearance (Elwood et al, 1983). A recently described technique for the investigation of airways permeability is the measurement of the appearance in sputum of a radioactive tracer administered intravenously. This procedure has been used to examine the airways permeability of asthmatics and bronchitics (Honda et al, 1988). However, while the bronchitics had greater amounts of radiolabelled albumin in their sputum than the asthmatics, no comparison was made with normal subjects.

There is no information available regarding the permeability of human respiratory epithelium to drugs used in the treatment of lung diseases, although some data is available from animal work. Gardiner & Schanker (1974) have reported that the absorption of sodium cromoglycate (SCG) across the rat lung is mediated partly by a saturable active transport process, and partly by passive diffusion. They found that the

active transport of SCG was partially inhibited by anionic drugs such as probenecid, penicillin and cephalothin. It also seems likely that the absorption of substances across the respiratory epithelium may be modulated by airways mucus and alveolar surfactant, although the only evidence to suggest this is indirect. The clearance of Tc^{99m}-DTPA is increased following surfactant depletion by lung lavage (Evander et al, 1987), and airways mucus can bind the same molecule with such affinity that it has been suggested that all measurements of lung epithelial permeability using Tc^{99m}-DTPA reflect alveolar permeability (Cheema et al, 1988).

1.1.2.8 The bronchial and pulmonary circulations.

One other factor that must be taken into account when considering the relationship between intra-pulmonary drug deposition and efficacy is the role of the circulation in drug delivery and clearance. The bronchial arteries arise from the aorta and supply the bronchial tree down to the respiratory bronchioles where they anastomose with the pulmonary circulation, which supplies blood to the alveolar structures. As much as 30% of the venous drainage of the lungs returns from the proximal bronchial tree to the right atrium, and from the rest of the lungs blood drains via the bronchopulmonary anastomoses into the pulmonary veins (Clarke, 1984; Baier et al, 1985; Deffebach et al, 1987). There is little doubt that drugs delivered to the lung by the circulation can be effective in treating airways or parenchymal diseases, but whether the bronchial circulation can influence the efficacy of inhaled drugs is not known with any certainty. It may be that inhaled drugs are absorbed into the bronchial circulation and redistributed downstream and peripherally to other sites of activity within the lung, in which case they need only to pass the draining watershed in the lung to be effective. While there has been no experimental work in humans investigating this hypothesis, results from studies in sheep have shown that pulmonary artery obstruction reduces the clearance of Tc^{99m}-DTPA from the alveoli (Rizk et al, 1984), while increases in airway pressure reduce bronchial artery blood flow (Wagner et al, 1987a). However, the same mechanism producing the decreased blood flow (positive end-expiratory pressure) also causes an increase in the clearance of Tc^{99m}-DTPA. Against these findings are the results of two other studies. Dinh Xuan et al (1989) found that prior delivery of inhaled methoxamine (a potent vasoconstrictor) to the airways attenuated exercise-induced asthma, suggesting that changes in mucosal blood flow in the airways may be important in the pathogenesis of exercise-induced asthma. Wagner & Mitzner (1990) have shown in a sheep model that the recovery from methacholine-induced bronchoconstriction can be delayed by a reduction in bronchial mucosal blood flow.

Thus, whether the bronchial circulation plays any role in modulating the action of drugs is not yet clear.

There is evidence to support the view that inhaled drugs, as well as locally released inflammatory mediators may both modulate the bronchial circulation. Laitinen and colleagues (1987) have examined the effects of various agents injected directly into the tracheal circulation of dogs, and have compared the subsequent changes in mucosal vascular resistance to the changes in mucosal thickness. They found that bradykinin, histamine and methacholine all produced vasodilatation with a concomitant increase in tracheal mucosal thickness, that substance P, vasoactive intestinal peptide, prostaglandins $F_{2\alpha}$ and E_1 produced vasodilatation without changes in mucosal thickness, and that salbutamol caused changes that fell in between these two groups. Phenylephrine produced vasoconstriction with a reduction of mucosal thickness. The thickening of the mucosa by these agents is considered to be due to plasma extravasation (Persson & Svensjo, 1983), and this mechanism may be an important factor in increasing airways resistance, especially in airways where the ratio of change in mucosal thickness to the radius of the airway lumen is large.

1.1.2.8.1 Airways microvascular permeability.

Others have confirmed the ability of inflammatory mediators to cause the leakage of plasma from the blood vessels into the interstitium and thence to the airway lumen (Persson & Erjfalt, 1986; McDonald, 1987; O'Donnell & Barnett, 1987). Persson (1986) considers that this plasma leakage may contribute to the development of a vicious circle, as the extravasated plasma may, through pressure effects, cause disruption of the epithelium, which may be further compounded by the action of inflammatory mediators within the plasma. Furthermore, it has been suggested that the disruption of the epithelium and the subsequent appearance of plasma components in the airway lumen may be a protective mechanism designed to allow rapid clearance of the interstitial plasma and resolution of the airway oedema (Erjfalt & Persson, 1989). Thus, it may be that the results of airways inflammation are determined by a complex interplay of factors causing increased permeability of both epithelium and endothelium.

The effects of inhaled drugs on this process may be inferred from work in animals, in which the drugs are given by the intravenous route, rather than as aerosols. Terbutaline attenuates vascular leakage in the cat respiratory tract (Erjfalt & Persson, 1986) and the guinea-pig trachea (Persson, 1987), while adrenaline is also effective in preventing

plasma leakage in the guinea-pig (Boschetto et al, 1989). Corticosteroids are also effective in this regard, although their mechanism of action is unknown (Grega et al, 1982). However, because of the difficulty in establishing a non-invasive model of plasma exudation and subsequent changes in airway wall thickness, the effects of inhaled drugs in human airways is not known.

1.1.2.9 Bronchoactive drugs and other inhaled agents.

Mild asthma is characterised by predominantly large airways constriction (Fairshter & Wilson, 1980), and it may be expected that preferential delivery of bronchodilators to large airways would be more efficacious than delivery to small airways. It is not possible to test this by delivering aerosols solely to the small airways, because any aerosol targeted to this area must traverse the large airways and will therefore deposit at both sites. Unless the site of aerosol deposition is identified and quantified, the effect of different sized aerosols on pulmonary function can be difficult to interpret because it is not clear whether any differences are due to changing central deposition or to the effects of peripheral deposition *per se*. Conclusions regarding the relative importance of the site of deposition can only be made if the dose delivered to the lung when different particle sizes are utilised is matched. Furthermore, any effect of changing deposition pattern may be masked by using doses of bronchodilators that produce supramaximal therapeutic responses (Ruffin et al, 1978a; Barnes & Pride, 1983).

1.1.2.9.1 β_2-adrenoceptor agonists.

Patel and colleagues (1990) reported that the response to an aerosol of inhaled isoprenaline with a MMAD of 2.5 μm was greater than that to an aerosol with a MMAD of 5 μm, especially for indices of small airways function, suggesting that the smaller particles penetrated more peripherally. Rees et al (1982) reported an enhanced response to smaller particles of terbutaline delivered by metered dose inhaler than to larger particles, but it is not clear whether the intra-pulmonary dose was the same for each particle size. Persson & Wirén (1989) found an increased bronchodilator response with increasing amounts of small (< 5 μm) particles of terbutaline when delivered as a dry powder, and Clay (1986) and colleagues reported similar results when delivering nebulised terbutaline of different particle sizes. However, when Dolovich et al (1981a) delivered fenoterol with a MMAD of 0.55 μm, there was no difference in lung function when compared to a larger (2.4 μm MMAD) aerosol, and Mitchell et al (1987) also found no differences in lung deposition or pulmonary function after the delivery of

equal doses of radiolabelled salbutamol aerosol (1.4 vs 5.5 μm MMAD). Conversely, when radiolabelled salbutamol was delivered from different nebuliser systems producing aerosols with MMAD's of 3.3 μm or 7.7 μm, the smaller aerosol produced a higher lung dose and consequently a greater therapeutic response (Johnson et al, 1989).

In clinical terms, none of this matters as long as the inhaled drugs work satisfactorily and safely, and have minimal adverse side-effects. A recent study exemplifies this view, while also suggesting that the need to achieve peripheral deposition is not important for maximum therapeutic response from salbutamol, which depends more on the (central) lung dose. Thus, Zainudin and colleagues (1990) found the greatest bronchodilatation after 9 asthmatic subjects inhaled 400 μg of salbutamol from a metered dose inhaler, compared with the same dose delivered as a dry powder or as a wet aerosol, despite the better peripheral lung penetration of the nebulised drug. The mean dose of salbutamol in the peripheral one-third of the lung was 7.2 μg from the metered dose inhaler and 9.7 μg from the nebuliser; in the central two-thirds of the lung, the doses were 37.6 μg (metered dose inhaler) and 29.9 μg (nebuliser). Others have also found that the particle size of a nebulised aerosol is not important in determining therapeutic response if large enough doses are administered (Douglas et al, 1985; Hadfield et al, 1986).

1.1.2.9.2 Anticholinergics and methacholine.

Only one study has investigated the differential deposition and efficacy of ipratropium bromide (Johnson et al, 1989), and despite differences in lung dose no difference in response was seen. This was interpreted as being due to the central location of the airway cholinergic receptors (Barnes et al, 1982). Gillett et al (1989) have shown that the lung dose of atropine delivered as an aerosol is not enhanced in bronchoconstricted subjects, although lung penetration is reduced, and that the degree of muscarinic antagonism by atropine is positively correlated with the degree of central deposition, supporting the findings of Johnson et al (1989). Similarly, Donna et al (1989) found no difference in the lung dose of inhaled methacholine in normals and asthmatics, although the intersubject variability of response to methacholine inhalation challenge in asthmatics did not correlate with aerosol deposition, suggesting that the enhanced response shown to this agonist by asthmatics is not related to increased central deposition.

1.1.2.9.3 Histamine.

There have been only two studies examining the airway response to histamine based upon differing inhalation techniques or particle sizes. Ruffin and colleagues (1978b) found that by delivering the same dose of 2 aerosols of histamine (3 and 1.5 μm MMAD) at the end of inspiration, different lung deposition patterns could be obtained. The smaller aerosol deposited more peripherally but produced a smaller airway response than the more centrally deposited larger aerosol, suggesting a preponderance of histamine receptors centrally. However, Ryan et al (1981 a & b) found no difference in airways responsiveness to histamine when the aerosol was deposited centrally or peripherally, and it was felt that it was the total dose that determined response rather than the intra-pulmonary distribution of aerosol.

1.1.2.9.4 Sodium cromoglycate and nedocromil sodium.

Only one study has examined the effect of particle size on efficacy of either of these agents. Godfrey et al (1974) found that similar doses of sodium cromoglycate (SCG) when delivered as small particles (2 μm MMAD) were more effective in preventing exercise-induced asthma compared to a larger aerosol (11.7 μm MMAD), and concluded that the drug's site of action was in the small airways. It has also been found that respiratory manoeuvres that stretch epithelial tight junctions increase the plasma levels of both sodium cromoglycate and nedocromil sodium (Richards et al, 1989a; Ghosh et al, 1989), although whether this enhanced clearance affects the efficacy of either drug remains to be seen. Sodium cromoglycate has been delivered to the lungs encapsulated in phospholipid vesicles (liposomes) (Taylor et al, 1989). This method of delivery produces prolonged alveolar retention of the liposome-SCG complex, and plasma levels that are close to those seen after inhalation of therapeutic doses of sodium cromoglycate persist for up to 25 hours after administration. However, whether this prolonged pulmonary retention produces a correspondingly prolonged therapeutic effect is not known.

1.1.2.9.5 Other inhaled drugs.

A number of other therapeutic substances have been delivered to the lungs as aerosols, but the relationship between their particle size, pharmacokinetics and pharmacodynamics has not been examined. These include heparin (Bick & Ross, 1985) for antithrombotic treatment, ergotamine for migraines (Graham et al, 1960), nicotine as an aid to cigarette withdrawal (Burch et al, 1988), and trypsin for pulmonary alveolar proteinosis (Jay, 1979). More recently, pentamidine isethionate has been

administered by nebuliser for the treatment and prophylaxis of *Pneumocystis carinii* pneumonia in immunocompromised patients. The alveolar site of the infection mandates that the drug should be delivered to the lung periphery for maximum effect, and if delivered predominantly to the airways it may cause cough and epithelial bleeding (Van Gundy et al, 1988). Nebulisers that deliver the drug predominantly as small particles produce a greater lung (alveolar) dose with less side-effects (Simonds et al, 1989), and may be more efficacious than nebulisers that produce higher particle sizes (Miller et al, 1989). Antibiotics such as gentamicin have been delivered to the airways of patients with suppurative bronchial diseases such as bronchiectasis (Ilowhite et al, 1987), and there has been recent interest in delivering such compounds encapsulated in liposomes. Legros et al (1990) have shown that in rabbits, peak plasma levels of gentamicin were lower after liposomal gentamicin (administered as an aerosol) than after free gentamicin administration, and that plasma gentamicin levels persisted unchanged for six days after the liposomal preparation, as opposed to 24 hours after free gentamicin, suggesting a possible means of prolonging local drug action whilst reducing systemic toxicity.

1.1.3 Conclusion.

It is clear that despite considerable advances in the understanding of factors that influence the site, activity and absorption of inhaled drugs, there is still much to learn. Indeed, many of the questions posed by Schanker in 1978 remain largely unanswered. What happens to a droplet of drug solution after deposition on respiratory epithelium? What is the influence of the airways and alveolar surface coating on the fate of inhaled drugs? How are drugs absorbed across the epithelium, and what factors modulate this process? What effect do environmental and physiological variables have on inhaled drug activity? To these questions, we should now add the following: where should inhaled drugs be deposited for maximal therapeutic action? Does the bronchial circulation have any role to play in modulating drug activity? Can we make greater use of the large absorptive surface area of the lung for systemic efficacy? Do the pharmacokinetics of inhaled drugs correlate with pharmacodynamics and deposition sites?

From the studies considered above, some of these questions may be partially answered. It is obvious that aerosol therapy should be targeted as accurately as possible to the site of disease, so that, for example, therapy for airspace disease should employ aerosols with a MMAD of about 3.5 μm. The optimal deposition site for

bronchodilators and other bronchoactive drugs is still not known, although the evidence suggests that at least for bronchodilators it is the total lung dose rather than the relative distribution within the lung that determines response. Some of these questions can be answered by very meticulous studies using sub-maximal doses of bronchoactive agents, delivered in equal doses to the lungs by standardised inhalation modes, with accurate measurements of deposition sites and pharmacokinetic parameters.

1.2 Nedocromil sodium.

Nedocromil sodium, a non-bronchodilator anti-inflammatory drug, was introduced as a prophylactic treatment for asthma in 1988. It has similar physico-chemical properties to sodium cromoglycate, although the chemical structure of the drugs is quite different (fig 1.2). Nedocromil sodium is the disodium salt of a pyranoquinolone dicarboxylic acid. It is highly ionized at physiological pH, and consequently is very poorly absorbed from the gastro-intestinal tract.

1.2.1 Development of the compound.

Although sodium cromoglycate is used successfully in the treatment of asthma, it has limitations in the treatment of certain categories of patients, such as the intrinsic asthmatic and those in the older age group. Thus for two decades pharmaceutical companies actively sought compounds with an improved biological profile compared with sodium cromoglycate. A major component of these research programmes was the development of predictive animal screens, work which was largely unsuccessful, probably because of the complex nature of asthma (Stokes & Morley, 1981). This failure to develop an animal model is the reason why so few novel 'anti-asthmatic' compounds have been identified (Eady, 1986). To overcome the lack of a single predictive screen, compounds were examined in both classical and novel test systems developed to reflect the different components of airway disease. Church (1978) discussed a number of putative anti-allergic mast cell-stabilising drugs which had progressed to clinical investigation. These compounds were many times more potent than sodium cromoglycate in the rat passive cutaneous anaphylaxis (PCA) test and *in vitro* chopped human lung studies. A number of these compounds also possessed reasonable activity in antigen challenge studies in asthmatic patients. However, the compounds were without exception significantly inferior to sodium cromoglycate when examined in therapeutic clinical trials in asthmatic patients.

Fig 1.2: The structures of nedocromil sodium and sodium cromoglycate.

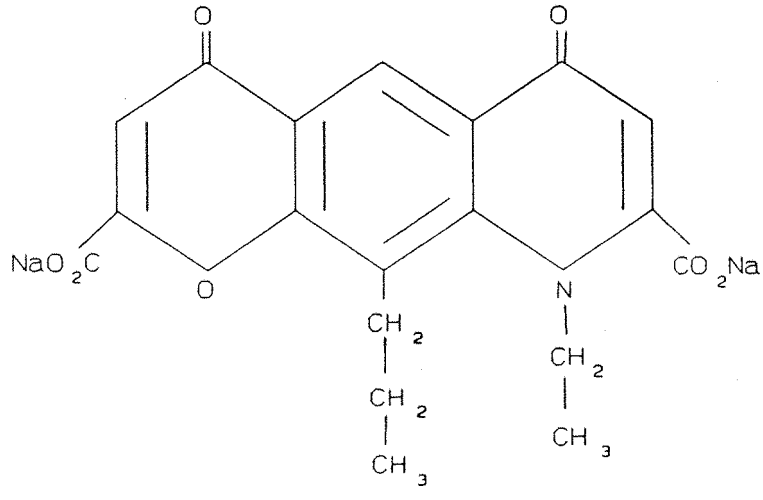

Nedocromil sodium

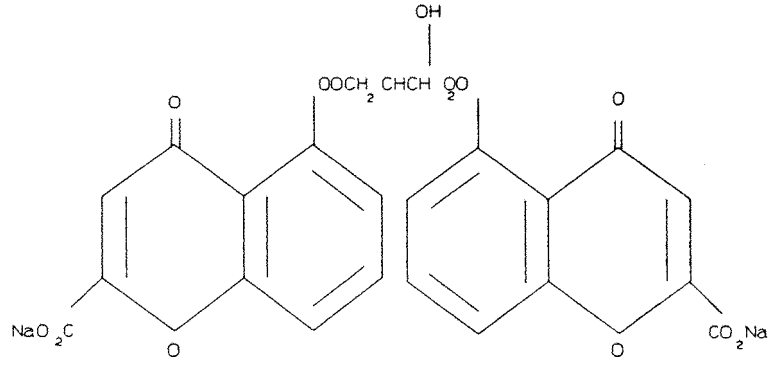

Sodium cromoglycate

It became clear that a new animal model encompassing a multifactorial picture of asthma was required for the identification of new drugs. A new *in vivo* screen in the subhuman primate *Macaca arctoides* was subsequently developed. These monkeys were actively sensitised with the parasite *Ascaris suum* and developed bronchoconstriction and a blood eosinophilia after bronchial challenge with aerosolized *Ascaris suum* antigen (Richards et al, 1983).

Nedocromil sodium was equipotent to sodium cromoglycate when compared by the rat passive cutaneous anaphylaxis test and the rat passive lung anaphylaxis test (Riley et al, 1987), and in its ability to inhibit antigen-induced histamine release from rat peritoneal mast cells (Wells et al, 1986). Additionally, it was significantly more effective than sodium cromoglycate in the *Macaca arctoides in vivo* screen. The clinical development of the drug through a wide range of challenge studies, assessment of the activity of the compound on bronchial hyperreactivity and demonstration of a rapid onset of action in therapeutic studies was subsequently achieved.

1.2.2 Pharmacodynamics of nedocromil sodium.

Nedocromil sodium inhibits the activation of, and mediator release from, mucosal type mast cells (Leung et al, 1988), eosinophils (Moqbel et al, 1989), alveolar macrophages (Damon et al, 1989), platelets (Thorel et al, 1988) and neutrophils (Moqbel et al, 1988). It also inhibits neutrophil and eosinophil chemotaxis (Bruijnzeel et al, 1989). These cells and their activation products are considered to be important in the pathogenesis of the airways mucosal inflammation that underlies the asthmatic state (Djukanović et al, 1990). After allergen inhalation, it inhibits the release of histamine, leukotriene C_4 and prostaglandin D_2 from mucosal mast cells lavaged from the lungs of sensitised monkeys with a potency of at least one hundred times greater than sodium cromoglycate and is more potent than sodium cromoglycate in preventing antigen-induced bronchoconstriction (Wells et al, 1986).

Nedocromil sodium attenuates allergen-induced early- and late-phase asthmatic responses in sheep and guinea pigs (Abraham et al, 1988; Hutson et al, 1988). In sheep, nedocromil sodium blocks the increase in airway responsiveness which develops twenty four hours after allergen challenge (Abraham et al, 1988). In dogs, sulphur dioxide-induced airway hyperreactivity is associated with an increase in lavage epithelial cells and neutrophil numbers, and this cellular influx can be inhibited by nedocromil sodium (Jackson & Eady, 1988). In guinea pigs, nedocromil sodium

treatment reduced antigen-induced microvascular permeability which produces airways oedema and plasma exudation (Evans et al, 1987), and it inhibits the eosinophil influx following allergen-induced late-phase bronchoconstrictor responses in ovalbumin-sensitised guinea pigs (Hutson et al, 1988). The action of nedocromil sodium may depend on its route of delivery, as it has been shown in a hamster cheek-pouch model that the drug can inhibit the allergen-induced increase in microvascular permeability when administered intravenously but not when administered topically (Dahlén et al, 1989). Nedocromil sodium may also act through another mechanism thought to be important in the pathogenesis of asthma, that is by the inhibition of axon reflexes (Barnes, 1986), since it has been found to inhibit bradykinin-induced bronchoconstriction (Dixon & Barnes, 1989).

1.2.3 Clinical studies with nedocromil sodium.

1.2.3.1 Laboratory studies.

In bronchial challenge tests in asthmatic volunteers, nedocromil sodium was more effective than placebo in inhibiting the immediate bronchoconstrictor response produced by challenge with antigen (Nair et al, 1989), adenosine (Crimi et al, 1987), exercise (Shaw & Kay, 1985), sulphur dioxide (Altounyan et al, 1986), cold dry air (Juniper et al, 1987), substance P (Crimi et al, 1988) and neurokinin A (Joos et al, 1988). When compared to sodium cromoglycate, nedocromil sodium was more effective in attenuating the bronchoconstriction induced by adenosine-5'-monophosphate (Phillips et al, 1989; Richards et al, 1989b), sulphur dioxide (Altounyan et al, 1986), cold air challenge (Juniper et al, 1987), bradykinin (Dixon & Barnes, 1989).

1.2.3.2 Studies in asthma.

Non-comparative and placebo-controlled studies of between four and fifty two weeks duration have demonstrated the tolerability and efficacy of inhaled nedocromil sodium in adults with all types of asthma (Gonzalez & Brogden, 1987). Nedocromil sodium has produced improvements in peak expiratory flow rate recorded by patients, symptom scores and other uses of medication recorded on diary cards, patient and physician assessments and lung function tests performed at clinic visits (Lal et al, 1986; Carrasco & Sepulveda, 1986). In placebo-controlled studies, where patients were maintained on bronchodilator therapy, nedocromil sodium produced significant reductions in concomitant day- and night-time bronchodilator use compared to placebo (Van et al, 1986).

Nedocromil sodium was not able to totally substitute for inhaled corticosteroid therapy (Paananen et al, 1986) but enabled maintenance corticosteroid doses to be reduced by half without loss of symptomatic control in many patients (Lal et al, 1986; Boulet et al, 1990). However, in patients with chronic steroid-dependent asthma, nedocromil sodium does not have an oral corticosteroid sparing effect (Goldin & Bateman, 1986). Nedocromil sodium can reduce bronchial hyperreactivity to methacholine to the same degree as beclomethasone dipropionate in nonatopic asthmatics (Bel et al, 1990), and has also been found to reduce airway hyperresponsiveness in atopic asthmatics when given through the pollen season (Gonzalez & Brogden, 1987). It appears to be as effective as inhaled beclomethasone dipropionate in double-blind, placebo-controlled crossover trials in the control of asthma symptoms and pulmonary function (Svendsen et al, 1989; Bergmann et al, 1990).

1.2.4 Pharmacokinetics of nedocromil sodium.

The pharmacokinetic properties of nedocromil sodium have been studied in animals, healthy volunteers and patients with asthma (Neale et al, 1987). High performance liquid chromatography and radioimmunoassay have been used in these studies with the latter technique allowing concentrations of nedocromil sodium as low as 0.25 ng/L to be detected in plasma and urine (Gardner et al, 1988). The pharmacokinetic results obtained for nedocromil sodium are similar to those for sodium cromoglycate (Neale et al, 1986).

After inhalation of 4 mg of nedocromil sodium from a metered dose inhaler, the plasma concentration rose rapidly to a peak within fifteen minutes (Neale et al, 1987), remained steady for approximately one hour and fell monoexponentially with a terminal half life of 2.3 hours. By contrast, intravenous nedocromil sodium has a significantly shorter terminal half-life (1.5 hours). The terminal half-life of inhaled nedocromil sodium therefore represents the absorption half-life (Neale et al, 1987), and thus the plasma pharmacokinetics of inhaled nedocromil sodium are termed absorption rate-limited. The rate-limiting factor is the absorption of the drug across the pulmonary epithelium. Inhalation of sodium cromoglycate from a Spinhaler results in a rapidly rising plasma concentration which peaks within fifteen minutes after inhalation (Pauwels, 1986), and has a terminal half-life of 1.4 hours. When administered intravenously the plasma half-life is about 40 minutes (Fuller & Collier, 1983), and thus absorption limited kinetics also apply to sodium cromoglycate.

The studies by Neale and colleagues with both sodium cromoglycate (1986) and nedocromil sodium (1987) suggested that the drugs are absorbed more rapidly from the alveolar epithelium than from the airways epithelium because the pharmacokinetic profile of both drugs was better fitted to a two absorption rate model. However, the kinetic profile of sodium cromoglycate is similar whether the drug is delivered as an aerosol or is instilled directly into the proximal bronchial tree (Richards et al, 1988b), which does not support Neale's contention of two separate absorption sites.

The extent of absorption or bioavailability of nedocromil sodium after inhalation in volunteers is around 7 - 9% of the administered dose. This figure includes an element of oral absorption and if allowance is made for this (2 - 3%) the extent of absorption from the respiratory tract is approximately 5 - 6% of the dose (Neale et al, 1987). The extent of absorption of sodium cromoglycate is similar (Richards et al, 1987). Whilst this may appear low it is not unusual for the inhalation route which at best yields up to 10% bioavailability (Newman et al, 1981b). Nedocromil sodium is not metabolised and does not accumulate with repeated dosing. Following intravenous administration plasma clearance of nedocromil sodium is rapid via excretion in urine and bile. Sodium cromoglycate is not metabolised and its elimination from plasma into urine and bile is also rapid (Neale et al, 1986). The pharmacokinetic profile of nedocromil sodium in patients with asthma is similar to that observed in healthy volunteers, although the dose absorbed in patients is slightly lower.

Richards et al (1989a) investigated the effect of inspiratory and expiratory manoeuvres on the absorption of sodium cromoglycate. Immediately after both consecutive FEV_1 manoeuvres and after a full inspiration followed by a thirty second breath-hold, the plasma concentration increased and then declined rapidly to reach the baseline concentration from which it departed. It was concluded that deep inspiration was the major determinant of this apparent increase in the absorption of sodium cromoglycate from the airways into the systemic circulation. Neale et al (1988) demonstrated a similar phenomenon for nedocromil sodium after vigorous exercise by normal and asthmatic subjects. In an attempt to identify which component of the exercise challenge is responsible for this phenomenon, Ghosh and colleagues (1989) studied the effects of various manoeuvres on plasma nedocromil sodium concentration. These manoeuvres were steady state exercise for eight minutes, a series of FEV_1 manoeuvres, exercise plus FEV_1 manoeuvres, three valsalva manoeuvres and hyperventilation. Because plasma nedocromil sodium concentrations rose with after all

the manoeuvres except valsalva and hyperventilation, it was suggested that the increase in nedocromil sodium concentration may be due to inflation and/or deflation of the lung rather than circulatory changes. The possibility exists that mechanical changes in epithelial structure can occur with lung inflation and deflation to alter the permeability of the lung to nedocromil sodium and sodium cromoglycate and thus allow increased absorption. Other possible mechanisms are an increase in lung surface area, a thinning of the surfactant layer or a change in blood flow. Whether these alterations in drug clearance from the lung can affect drug efficacy has not been studied.

1.3 Aims of the studies carried out in this thesis.

1.3.1 To assess the possibility that part of the action of an inhaled drug may be due to its absorption into the bronchial circulation and subsequent redistribution to other sites of activity, a comparison was made of the efficacy of the drug when given by inhalation, by mouth or as an intravenous infusion against bronchial provocation by adenosine-5'-monophosphate. After baseline tests of lung function and airways responsiveness to inhaled histamine and adenosine-5'-monophosphate, asthmatic subjects were given, in a single blind fashion, either inhaled, oral or intravenous nedocromil. Blood samples were taken for four hours after each dose, and at an appropriate time point after the dose, AMP challenge was repeated. In this way, a comparison of the relative efficacy of the drug when given by different routes was obtained, as well as information relating the degree of protection afforded by the drug to plasma levels and baseline airway reactivity.

1.3.2 To further study the phenomenon of the increase in plasma drug levels after respiratory manoeuvres, and to attempt to assess whether such increases can be modulated through alterations in mucosal blood flow or by attempting to influence drug absorption across the respiratory mucosa. Normal volunteers inhaled nedocromil sodium under controlled conditions, after which a plasma concentration-time curve was constructed by taking blood at intervals over a four hour period. At certain time-points after inhalation, the volunteers performed each of three separate manoeuvres, being a deep inspiration followed by a breath-hold, nine consecutive FEV_1 manoeuvres or one separate FEV_1 manoeuvre to show which, if any, of these manoeuvres produced a change in the plasma level of nedocromil sodium. On two more occasions, subjects repeated the test, but on one occasion they were premedicated with probenecid and penecillin to determine if this drug affected either the whole plasma-concentration time curve or the expected increases in plasma levels after the respiratory manoeuvres, and on the other occasion they inhaled nebulised methoxamine to assess if changes in the bronchial mucosal circulation are responsible for the increases in plasma drug levels.

1.3.3 To develop a technique of radiolabelling nedocromil sodium for pulmonary deposition studies so that when expelled from a metered dose inhaler the label and drug distribute together, without altering the size characteristics of the original aerosol. This technique was then used to assess whether the site of deposition of inhaled nedocromil sodium within the lungs of normal subjects influences the subsequent pharmacokinetic profile. Two different particle size formulations of nedocromil sodium

were used, fine and coarse. The volunteers inhaled nedocromil sodium from metered-dose inhalers under controlled conditions in order to minimise differences in inspiration. After inhalation, a tomographic gamma-emission image of the chest (SPECT image) was obtained, and blood taken at regular intervals for plasma nedocromil levels and to assess the level of radioactivity in the blood. This study was undertaken on two occasions so that each subject inhaled both aerosols. To enhance the precision of the SPECT images, a limited CT scan of the thorax was obtained for each subject. The opportunity provided by the acquisition of 3-dimensional data was used to develop novel methods of image analysis.

This work, when taken as a whole, aims to yield information on the pharmacokinetics of nedocromil sodium, with particular reference to the importance of the site of deposition within the lung, information that is not available for any inhaled drug. Further, it is hoped to yield information regarding the contribution of the bronchial circulation to the action of inhaled drug, and to shed some light on the mechanisms of absorption of the drug.

Chapter 2. Methods and statistical analyses.

2.1 Assessment of atopic status.

Subjects were assessed for atopic status by skin-prick testing (Pepys, 1975) to six common aeroallergens: house dust, *Dermatophagoides pteronyssinus*, mixed grass pollens, mixed feathers and cat and dog dander (Bencard, Middlesex, UK). Both positive (histamine 100 μg/ml) and negative (normal saline) control skin-prick tests were also carried out. Twenty-five gauge needles were used for testing, and the weal responses were measured as the maximal weal diameter, at ten minutes for histamine and fifteen minutes for the allergens (Voorhorst, 1980). Subjects were considered atopic if any allergen weal diameter exceeded that of the positive control by 2 mm or more.

2.2 Measurements of airway calibre.

Asthma is characterised by episodes of airflow obstruction due to narrowing of the airways, which may be reversible spontaneously or as a result of drug treatment. The propensity to develop airways narrowing is associated with increased bronchial responsiveness, which is the exaggerated response of the airways to a variety of specific and non-specific stimuli (Boushey et al, 1980). In this thesis, airways calibre was assessed by measurement of the forced expiratory volume in one second (FEV_1) and specific airways conductance (sGaw).

2.2.1 FEV_1.

During forced expiration, intrathoracic pressure is increased and air flow results. After about the first third of the vital capacity has been expired, maximum expiratory flow reaches a plateau due to the formation of flow-limiting segments caused by progressive dynamic narrowing of the central intrathoracic airways (West, 1979). Any further increase in intrathoracic pressure results in further narrowing of the flow-limiting segments, thereby preventing any increase in expiratory flow by increasing airflow resistance. This phase of forced expiration is therefore effort-independent, in contrast to the earlier phase where expiratory flow is dependent on the driving pressure.

Expiratory flow is also dependent on the elastic recoil pressure of the lungs, and therefore the final flow rate achieved depends upon the elastic recoil pressure of the lungs, the calibre of the conducting airways and dynamic airway narrowing (Mead et al, 1967; Pride et al, 1971). The FEV_1 encompasses both effort-dependent and effort-

independent parts of the flow volume curve, and its magnitude is directly proportional to the lung elastic recoil pressure and inversely proportional to airways resistance. As long as full inspiration is achieved, it is relatively independent of effort. Because acute changes in lung elasticity are uncommon, sequential changes in FEV_1 will reflect variations in airways calibre.

Normal values for FEV_1 were calculated by the method of Cotes (1979). The apparatus used to measure the FEV_1 was the Vitalograph dry wedge-bellows spirometer (Vitalograph Ltd, Bucks, UK). Subjects were seated in front of the Vitalograph, asked to put on a nose-clip, instructed first to take a full inspiration and then, having placed their mouth around the mouthpiece so as to achieve an airtight seal, to expel the air forcibly.

2.2.2 Specific airways conductance.

As air flows in and out of the tracheobronchial tree, the resistance at any specific point depends on the total cross-sectional area of the airways at that point (Tattersfield & Keeping, 1979). Because the total cross-sectional area is greatest at the lung periphery, the major site of resistance in the lungs is in the proximal airways, and as a result, any measured changes in airways resistance reflects changes in large airways calibre.

Airways resistance measurements (Raw) depend on the number and size of patent airways. A reduction in the number of parallel airways decreases the total cross-sectional area leading to increased airways resistance. Airway size depends on both intrinsic airway factors, such as smooth muscle tone, mucosal oedema and secretions, and the airway distending pressure which is related to static lung recoil pressure (Butler et al, 1960). The rapid changes in Raw that are observed with inhalation bronchial challenge are assumed to be due to changes in intrinsic airway factors as marked direct effects on lung recoil pressure are unlikely. Although these changes are generally considered to be due to bronchial smooth muscle contraction, both mucosal oedema and bronchial secretions may also play a role.

Airway resistance decreases with increases in lung volume and thus Raw will depend on the lung volume at which it is measured. In addition, lung volume increases with increasing airways obstruction. For these reasons, it is necessary to measure lung volume if measurements of Raw are to be made during bronchial challenge

experiments. The relationship between resistance and lung volume is curvilinear, whereas the reciprocal of airway resistance, airway conductance (Gaw), shows an approximately linear relationship to lung volume (Briscoe & DuBois, 1958). Specific airway conductance (sGaw) is derived by converting Raw to Gaw, and then dividing by the thoracic gas volume (TGV) to correct for changes in lung volume at which the measurements are made.

$$Gaw = \frac{1}{Raw} \quad ; \quad sGaw = \frac{Gaw}{TGV}$$

In this thesis, Raw and TGV were measured in a pressure-compensated volume-displacement body plethysmograph (Fenyves & Gut, Basle, Switzerland) based on the principle first described by Dubois and colleagues in 1956. This technique has the advantage of measuring both Raw and TGV simultaneously. The plethysmograph is a 690 litre container with a magnetically sealed perspex door on one side. When the door is closed, the only communication with the external atmosphere is through a heated pneumotachograph. The subjects breathe through another pneumotachograph, with a remote controlled solenoid-operated shutter between the pneumotachograph and the mouthpiece. On activation, the shutter closes at end-expiration. The air passing through the shutter and the pneumotachograph is derived from within the cabinet.

Inside each pneumotachograph is a resistance to airflow consisting of a series of small parallel tubes which maintain laminar flow in the air passing through the pneumotachograph. This creates a differential pressure proportional to air flow rate, and two pressure transducers on either side of the resistance record the pressure differential across it. The pressure difference is amplified and fed into an integrator to produce the box volume signal. Signals from the pressure transducer in the mouthpiece are treated similarly to yield mouth pressure and mouth flow. These signals are then passed to an Amstrad 1640 computer using a purpose-written software program (Hiscock, 1980) to compute Raw, TGV and sGaw.

The subject pants at two breaths per second which helps to keep the glottis open and ensures a small tidal volume which reduces any drift in box pressure (Pb) due to differences in temperature or water vapour saturation between inspired and expired air. When panting with the shutter open, changes in alveolar pressure (Palv) produce reciprocal changes in Pb which are measured and displayed on the horizontal axis of an oscilloscope. Simultaneously, changes in airflow at the mouth (Fm) are displayed

on the vertical axis, and by relating the changes in Fm to the changes in Pb, airways resistance can be calculated. By closing the shutter the airway is occluded at the mouth while the subject continues to make panting efforts. Pressure at the mouth (Pm) is then traced on the vertical axis while the horizontal axis records Pb with the signal reversed. The slope of the line Pm/Pb is measured. It is assumed that under conditions of zero flow, which occur when the airway is occluded, Pm equals Palv. Airway resistance is then the ratio of alveolar pressure to flow, thus:

$$Raw = \frac{\Delta\ Palv}{\Delta\ Fm} = \frac{Palv/Pb}{Fm/Pb}$$

Using this information, and by the application of Boyle's law, TGV is computed, thus allowing the correction of airways resistance for the lung volume at which they were made.

Subjects pant for about ten breaths with the shutter open, and a further five breaths with the shutter closed. The computer programme analyses repeated slopes from which mean values were derived. Because such measurements are very sensitive, to reduce variability this cycle of events was repeated four times, and a mean value for each cycle computed. The sensitivity of these measurements is particularly important for studies undertaken in normal subjects as it allows for small changes in airway calibre to be detected, and is also valuable for determining changes in the calibre of large intrathoracic airways.

2.3 Measurement of inspiratory parameters and delivery of pressurised aerosols.

For the purposes of the studies described in this thesis, it was necessary to control inspiration in order to standardise the inhalation of nedocromil sodium, and to have the facility for the remote actuation of radioactive metered dose inhalers. Respectively, these were necessary because the lung deposition of aerosols depends partly on inspiratory parameters (Newman et al, 1982), and to limit exposure to radioactive sources. This was achieved using an electronic spirometer (Vitalograph Compact, Vitalograph, Bucks, UK) which detects instantaneous expired and inspired air with a pneumotachograph. The differential pressure across the pneumotachograph is monitored by a differential pressure transducer inside the Vitalograph enclosure. Signals from this are integrated by a microprocessor, and displayed on a liquid crystal display.

The Vitalograph Compact displays inspiratory flow rate on-screen during inhalation, and

is coupled with a solenoid-actuated piston which, when activated remotely, depresses the metered dose inhaler canister to deliver the aerosol to the subject. The pneumotachograph of the Vitalograph was connected to the housing within which the metered dose inhaler was contained, so that inspiration through the metered dose inhaler mouthpiece produced a signal on the Vitalograph screen (figs 2.3.1). By use of inbuilt menu-driven software, the desired inspiratory flow rates and the time from the start of inspiration at which the aerosol is to be fired may be stipulated, and displayed on-screen as a 'target' (fig 2.3.2). In this thesis, these parameters were set as follows: upper flow rate, 45 l/min; lower flow rate, 30 l/min; upper time limit, 2.0 sec; lower time limit, 0.5 sec. A cross was displayed on the inspiratory flow trace when the aerosol was fired (fig 2.3.2).

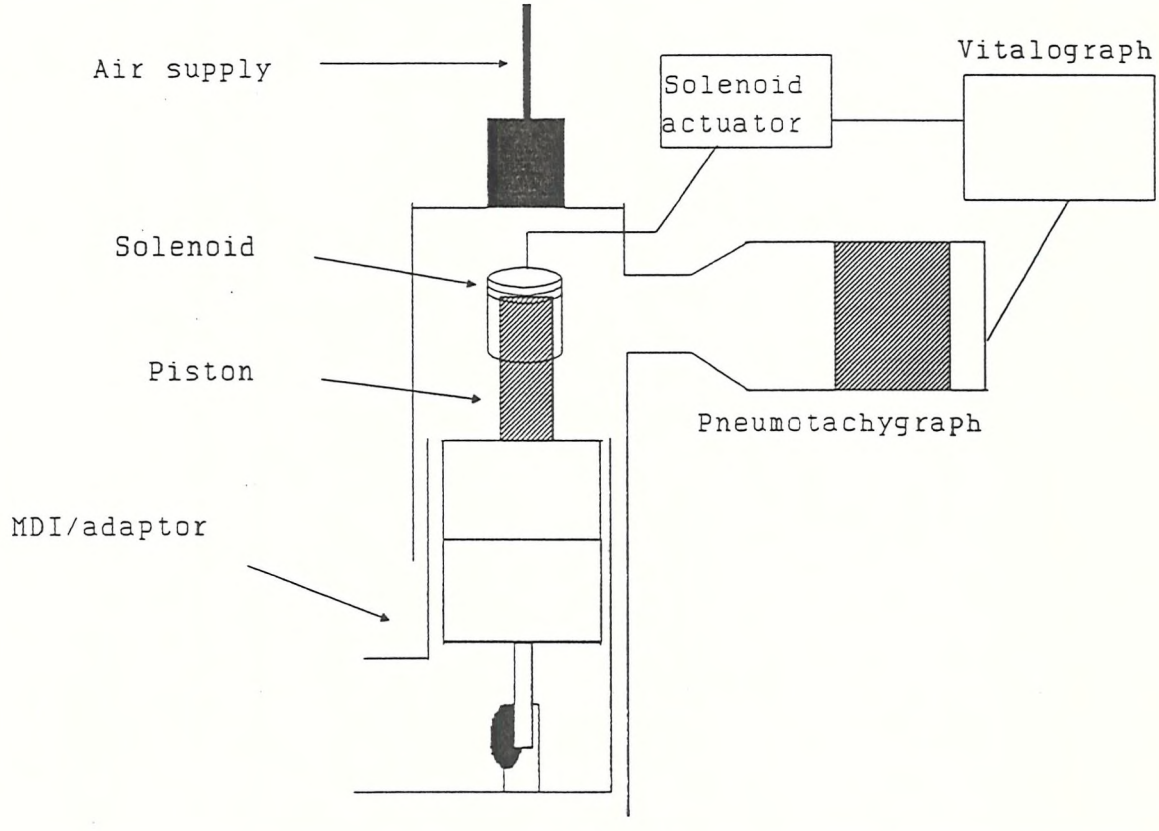

Fig 2.3.1: diagram of inhalation apparatus.

Subjects were taught to inhale slowly from residual volume to total lung capacity at a flow rate of thirty to forty five l/min, and to breath-hold for ten seconds at the end of inspiration (fig 2.3.2). The metered dose inhaler was actuated remotely when inspiratory flow had reached the required rate. Subjects were taught to achieve this

within two seconds of the start of inspiration. By this means, it was intended to deliver the inhaled aerosol at approximately 20% of the inspired volume. Inspiratory training and aerosol actuation were performed by myself on every occasion. After each inhalation, the Vitalograph printed out the following parameters: breath-holding time (BHT), the elapsed time between the subject holding the breath at the end of inspiration and the subsequent expiration; peak inspiratory flow (PF), the highest instantaneous flow rate recorded between the start of inspiration and the onset of breath-holding; time of firing (TF), the time at which the aerosol was fired; instantaneous flow rate at the time of aerosol firing (FF); inspiratory vital capacity (IV), the volume inspired from the onset of inspiration to the onset of breath-holding; total inspired volume from the start of inhalation to the time of aerosol firing (VF); and the ratio of VF to IV expressed as a percentage (VF%) (fig 2.3.2).

Figure 2.3.2 (overleaf). The Vitalograph Compact display.

The top panel shows the Vitalograph screen prior to inhalation. Time (sec) is shown on the x-axis, and inspiratory flow (l/min) on the y-axis. The dotted lines outline the target area for MDI actuation, set as follows: upper flow rate, 45 l/min; lower flow rate, 30 l/min; upper time limit, 2.0 sec; lower time limit, 0.5 sec.

The second panel shows a tracing of inspiratory flow rate, and the third panel shows the screen after a full inspiration during which the MDI was actuated. The cross denotes the time and inspiratory flow at actuation. The final panel shows an example display of the parameters measured during inspiration.

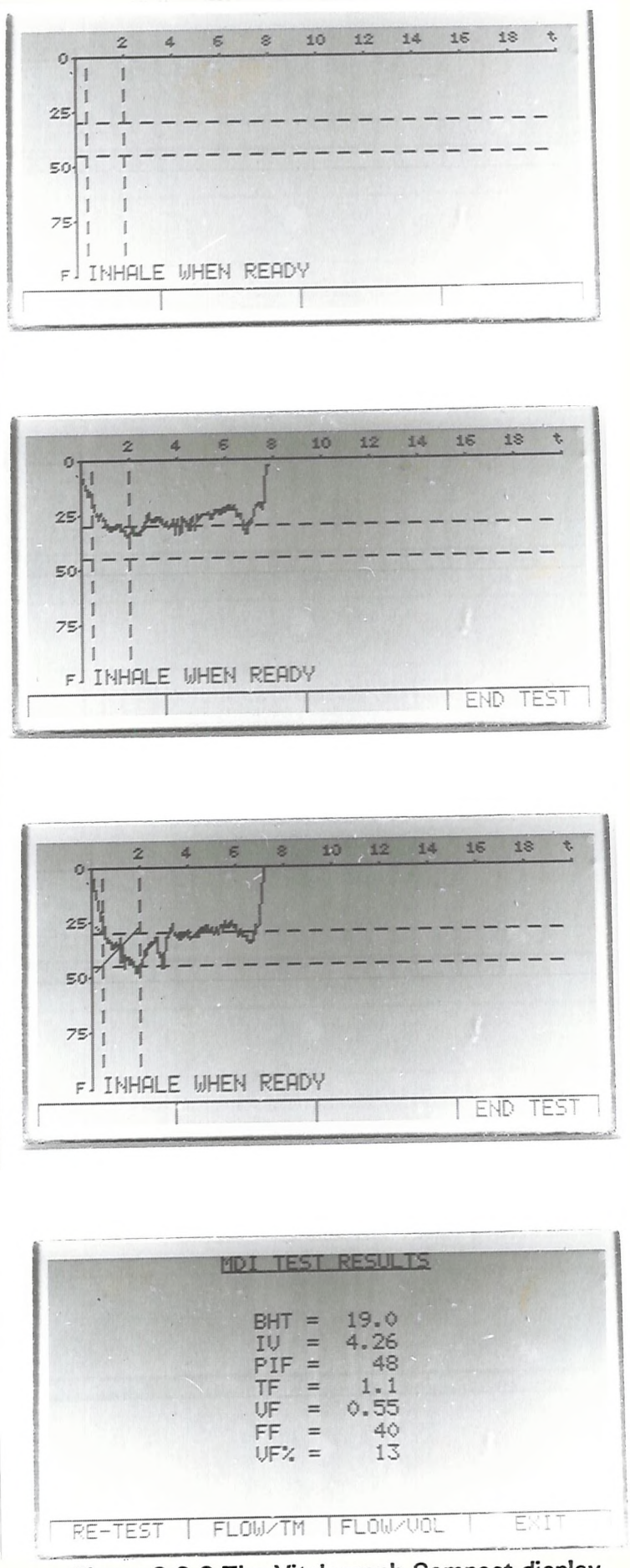

Figure 2.3.2 The Vitalograph Compact display.

2.4 Bronchial reactivity testing.

2.4.1 The generation and delivery of nebulised aerosols.

An Inspiron Mini-neb jet nebuliser (CR Bard International, Sunderland, UK) was used in this thesis. This was attached to a mouthpiece with an integral one-way valve. A standardised starting volume of four millilitres in the nebuliser chamber was used throughout, as was a gas flow rate of eight l/min. Under these conditions, the nebulizer produces an aerosol with a mass median aerodynamic diameter of 6.3 μm and a geometric standard deviation of 1.73 (Newman et al, 1986). In all inhalation challenges, each dose of aerosol was delivered by instructing the subjects to take five consecutive breaths from functional residual capacity (FRC) to total lung capacity (TLC) via a mouthpiece (Chai et al, 1975).

2.4.2 Preparation of solutions.

On each study day, histamine as histamine acid phosphate (BDH Chemicals, Poole, Dorset, UK) and AMP (Sigma Chemical Co., Poole, Dorset, UK) were made up in 0.9% sodium chloride to produce a range of doubling concentrations of 0.03 - 64 mg/ml (0.2 - 327 mmol/l) and 0.04 - 400 mg/ml (1.1 - 1151.4 mmol/l), respectively. Histamine (mol wt 307.14) is a naturally occurring amine present in a wide variety of tissues (Best 1927), and is one of the mediators released on activation of mast cells (Bartosch et al, 1932). It causes bronchoconstriction in man partly by stimulation of the H_1 receptor (Nogrady & Beven, 1981; Rafferty et al, 1987a), and partly by a reflex (neurological) mechanism (Holtzman et al, 1980).

Mast cell activation and histamine release is also a feature of the bronchial response to inhaled adenosine and AMP (mol wt 347.2). Both atopic and non-atopic asthmatics react to inhaled AMP, and the resultant bronchoconstriction can be almost totally inhibited by H_1-antagonists (Rafferty et al, 1987b; Phillips et al, 1987), and also by inhaled theophylline, a histamine purinoceptor antagonist (Cushley et al, 1984). Cushley's work suggests that the mechanism of action of adenosine is via cell surface purinoceptors, as the concentration of inhaled theophylline was lower than that needed to inhibit phosphodiesterase. Further evidence for involvement of the mast cell and release of histamine is the lack of a late-phase response or the development of bronchial hyperresponsiveness after AMP inhalation (Phillips & Holgate, 1988). Adenosine is released following allergen challenge, both rising in concert with the initial bronchoconstriction followed by a later peak, and this sequence of events is also seen after methacholine provocation (Mann et al, 1986). Another possible mechanism of

action of this substance is by the stimulation of adenosine receptors on postganglionic vagal nerve endings (Drazen et al, 1989). The role of adenosine in the pathogenesis of asthma is not certain, but it appears to be a secondary mediator in causing release of histamine and other mediators via purinoceptor activation of mast cells. As it can be released following certain bronchoconstrictor stimuli, it may be a mediator that can augment a bronchoconstrictor response rather than being primarily causative (Polosa et al, 1989). Because AMP-induced bronchoconstriction can be inhibited by nedocromil sodium and sodium cromoglycate, it was chosen as a tool in this thesis to examine the airways effects of nedocromil sodium (Phillips et al, 1989).

2.4.3 Inhalation challenge.

Changes in airway calibre during AMP challenge tests were followed as sGaw rather than FEV_1 since the forced expiratory manoeuvre can transiently increase the plasma concentration of drugs exhibiting absorption-limited pharmacokinetics (Richards et al, 1989a; Ghosh et al, 1989).

The AMP bronchial challenge tests were carried out as follows. After measuring baseline sGaw, subjects inhaled 0.9% saline from the nebuliser as five breaths from FRC to TLC, and sGaw was measured after three minutes. Provided it did not fall by > 20% of the starting baseline value, the AMP provocation was undertaken. Increasing doubling concentrations of AMP were inhaled at five minute intervals with sGaw being measured at three minutes after each inhalation. The challenge was terminated when the sGaw fell by > 50% of the post-saline value or until the highest dose of AMP had been inhaled. The fall in sGaw expressed as a percentage of the post-saline baseline was plotted against the concentration of AMP, and the provocative concentration that produced a 50% fall in sGaw (the PC_{50} sGaw AMP) was derived by linear interpolation.

Histamine challenge was undertaken at least one hour after AMP challenges, or when the FEV_1 had returned to within 10% of its starting value. This challenge was used to define the degree of "non-specific" airways responsiveness. The procedure was carried out in an identical fashion to that used for AMP, giving histamine in increasing concentrations from 0.03 - 8 mg/ml, and following changes in airway calibre as FEV_1 rather than sGaw. The test proceeded until FEV_1 fell by > 20% of the post-saline value. A PC_{20} FEV_1 histamine value was derived by linear interpolation of the last two points of the concentration response curve.

2.4.4 Delivery of nebulised methoxamine using a dosimeter.

The apparatus was built by the Medical Engineering Department of Southampton General Hospital. It consists of a solenoid-operated valve which controls the air supply to the nebuliser. The solenoid is activated for a set period of time when a temperature drop is detected in the thermistor attached to the mouthpiece. Therefore, when the subject begins to inhale, air passes over the thermistor and causes the valve to open, thus allowing compressed air to pass into the nebuliser, generating the aerosol (fig 2.4).

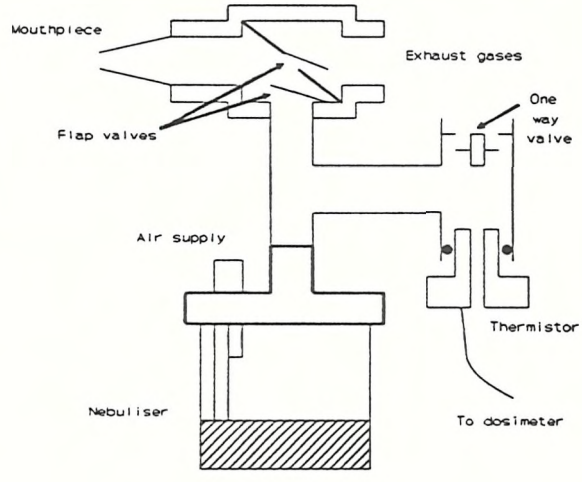

Fig 2.4: apparatus used to deliver nebulised methoxamine.

The air supply requires a pressure of twenty lb/in^2 which develops an air flow rate of eight l/min through the nebuliser. The dosimeter allows the delivery of precise quantities of aerosol during inspiration, and prevents aerosol being lost to atmosphere except that which is exhaled. A nebulisation period of 3.5 seconds was used, and by gravimetric analysis it was determined that this delivered 1.46 mg of methoxamine with each inspiration when the nebuliser pot was filled with two millilitres of methoxamine solution (20 mg/ml). The delivered dose of methoxamine was calculated as a function of body weight, and subjects inhaled the appropriate number of breaths consecutively, inhaling slowly from FRC to TLC.

2.5 Plasma nedocromil sodium pharmacokinetics.

2.5.1 Blood sampling.

Blood samples were taken from an indwelling Teflon catheter inserted into a forearm vein before and at various times after drug administration. The cannula was kept patent by the use of saline. Thirty ml of blood was withdrawn prior to dosing, and plasma from this was taken to construct the standard curve used to analyse the post dose samples. After dosing, blood samples were taken and transferred to glass lithium heparin tubes (Beckton Dickinson Vacutainer, Cowley, Oxford, UK). The samples were then centrifuged at 3000g for ten minutes and the plasma separated and stored at -20°C for subsequent drug assay.

2.5.2 Nedocromil sodium radioimmunoassay.

Plasma concentrations of nedocromil sodium were assayed by a double antibody radioimmunoassay (Gardner et al, 1988). The radioimmunoassay is specific, and does not interact with other drugs, including closely related compounds. All materials were supplied by Fisons plc for use in Southampton. The method was as follows:

(1) Preparation of the radiolabel by iodination of nedocromil sodium monotyramide. Potassium iodide (40 μl of a 10 μg/ml solution) was added to a vial containing 37 megabecquerels (MBq; 1 millicurie) sodium (^{125}I) iodide (Amersham International, Amersham, Bucks), and mixed with nedocromil sodium monotyramide (50 μl of a 100 μg/ml solution). After mixing with 40 μl of Chloramine T (50 μg/ml) to oxidise the iodide to iodine, the solution was left for forty five minutes to allow aromatic ring substitution of the monotyramide. Sodium metabisulphite (40 μl of a 150 μg/ml solution), a reducing agent, was added to stop the reaction, and the contents transferred to a scintillation vial, using 10 ml sodium phosphate buffer (0.1M, pH 7.2).

(2). Primary antibody production. Antibody to nedocromil sodium (NS) had been raised in Suffolk-cross sheep (AB-sh) by the repeated intramuscular injection of 0.5 ml emulsion of aqueous BCG and nedocromil sodium-bovine serum albumin in Freund's incomplete adjuvant. Boosting immunisations were given on days 31, 59, 107 and 192, with antiserum collection taking place on days 40, 69, 118 and 207. The antiserum was mixed with control sheep serum (10 μl) and diluted with 0.1M phosphate buffer, pH 6.0 (100 ml) (solution A). The antibody solution (0.5 ml) was added to the plasma sample (100 μl) containing an unknown amount of nedocromil sodium and a complex was formed:

$$NS + AB\text{-}sh \text{ -----> } NS.AB\text{-}sh$$

(3). Nedocromil sodium monotyramide, iodinated with ^{125}I (20 μl of the stock solution) was mixed with 2.5 ml of donkey antisheep serum (RAST Allergy Unit, Benendon Chest Hospital, Cranbrook, UK) and diluted to 100 ml with 0.1M phosphate buffer, pH 6.0. An aliquot of this solution (0.5 ml) was added to each tube containing plasma and anti-nedocromil sodium antibody. The radiolabelled nedocromil derivative (NS*) competes with plasma nedocromil sodium for the AB-sh and an equilibrium is established in which the extent of binding of NS* is inversely proportional to the concentration of NS:

$$NS.AB\text{-}sh + NS^* \text{ ----> } NS + NS^*.AB\text{-}sh + NS.AB\text{-}sh$$

The second antibody (AB-d), raised in donkeys to the sheep serum was then added, and the tube left in a cool room for twelve hours after which it was centrifuged at 4000 rpm for 30 min. A complex consisting of nedocromil sodium and both antibodies was formed and precipitated out of solution. Following centrifugation a pellet was formed, which, after the removal of the supernatant was counted by a gamma-emission counter:

$$NS.AB\text{-}sh + NS^*.AB\text{-}sh + AB\text{-}d \text{ ----> } NS.AB\text{-}sh.AB\text{-}d + NS^*.AB\text{-}sh.AB\text{-}d$$

The amount of radiolabelled nedocromil sodium in the pellet is inversely proportional to the amount of nedocromil sodium in the blood since the radiolabelled drug has to compete with the plasma drug for AB-sh and therefore more radiolabelled nedocromil sodium will bind if plasma nedocromil sodium is low.

A standard curve (fig 2.5.2) was generated using known concentrations of nedocromil sodium added to the predose plasma, and this was used to convert gamma-emission counts to nedocromil sodium concentration. Non-specific binding was measured by incubating the pre-dose plasma with control sheep serum (30 μl/100 ml) in place of solution A, and was always $<5\%$. The standard curve was run with each batch of samples as the radiolabel decays with time. All samples were analysed in quadruplicate, with a quadruplicate standard curve containing 0, 0.25, 0.5, 1.0, 1.5, 2, 3, 4, 6, and 8 ng/ml of nedocromil sodium prepared in the predose plasma from that subject. The 0.25 ng/ml standard was measurable in most analyses, but for some the

limit of measurement was 0.5 ng/ml. The mean intra-assay coefficient of variation for samples was ± 9.6% at ≈ 0.8 ng/ml (n = 48) or ± 4.9% at ≈ 5.3 ng/ml. Because differences were found in the slope and sensitivity of the standard curve constructed from the predose plasma samples from different subjects, plasma concentrations of nedocromil sodium for each subject were always derived from a standard curve prepared from the predose plasma in that subject. Therefore data on inter-assay coefficients of variation are not available. For each quadruplicate sample, a mean and standard deviation (SD) was calculated. To eliminate outlying values, samples with values greater than one standard deviation from the mean were deleted, and a new mean and SD calculated to give the final result.

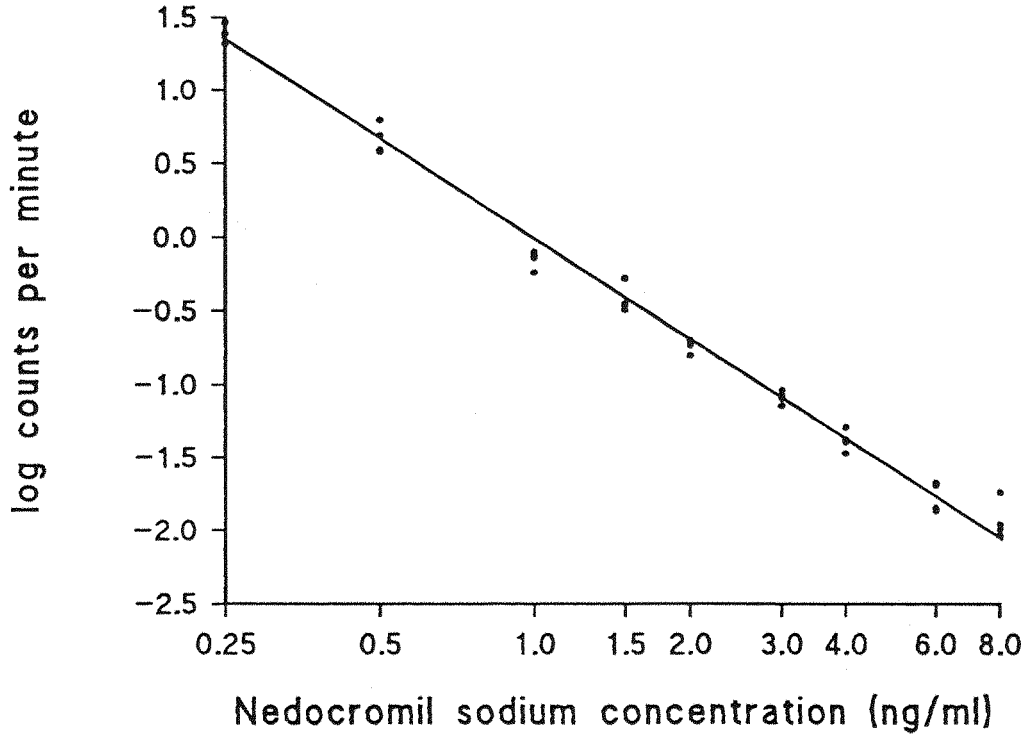

Fig 2.5.2: an example standard curve redrawn from the nedocromil sodium radioimmunoassay. Each concentration is represented by 4 points.

2.5.3 Pharmacokinetic assessment.

The time course of plasma concentrations of nedocromil sodium after drug administration were analysed by a program which uses linear least-squares regression analysis to determine the slope (k) of the terminal log-linear part of the concentration-time data. The half-life was calculated as:

$$t_{1/2} = \frac{0.693}{k}$$

The area under the plasma concentration-time curve (AUC) was calculated using the linear trapezoidal rule. The mean residence time (MRT) was calculated by plotting the product of plasma concentration and time against time, and then by trapezoidal integration to derive the area under the curve, known as the first moment curve (AUMC). The AUMC was then divided by the AUC. Both the AUC and the AUMC were extrapolated to infinity using standard formulae for the calculation of MRT (Gibaldi & Perrier, 1982). If a terminal slope could not be obtained, then the AUC was calculated as the observed value, rather than being extrapolated to infinity, and MRT could not be calculated.

For intravenous infusion, MRT was calculated by:

$$MRT_{infusion} = MRT + \frac{T}{2}$$

where T is the infusion time.

The maximum plasma drug concentration (Cmax) and the time at which it occurred (Tmax) are given as the observed values. The concentration of nedocromil sodium at the time of AMP challenge when sGaw fell by > 50% (Cchall) was derived by log-linear interpolation (chapter 3). The dose absorbed (F) after inhalation and oral administration was calculated from the $AUC_{0-\infty}$ and the $AUC_{0-240min}$ respectively and the $AUC_{0-\infty}$ for the infusion study in the same subject. For example, the dose absorbed after drug inhalation is calculated by:

$$F = \frac{AUC_{inhaled}}{AUCiv} \times \frac{dose_{iv}}{dose_{inhaled}}$$

A terminal half-life could not be calculated for the oral data and therefore the value of

F calculated was not the absolute bioavailability but the fraction of the dose absorbed during the study period.

The clearance (Cl) of drug from the body after intravenous administration, defined as the capacity of the organs of elimination to remove drug from the plasma, was calculated by dividing the administered dose by the subsequent $AUC_{0-\infty}$. The apparent volume of distribution (Vss) was calculated thus (Gibaldi & Perrier, 1982):

$$Vss = \frac{infused\ dose \times AUMC}{AUC^2} - \frac{infused\ dose \times T}{2 \times AUC}$$

2.6 Measurement of aerosol particle size distribution.

In this thesis, the size distribution of particles within the aerosols generated by metered dose inhalers was measured using a modified multi-stage liquid impinger (Fisons Scientific Instruments, Loughborough, UK) (fig 2.6). The original three stage liquid impinger described by May (1966) was adapted to incorporate four stages together with a pre-impinger device or "throat" which was used to simulate the oropharynx. The multi-stage liquid impinger was used with dry sintered glass stage plates since the surfactant in the formulation serves to prevent the phenomena of particle bounce and re-entrainment (Rao & Whitby, 1978; Marple & Willeke, 1979).

The basic operation of the multi-stage liquid impinger is as follows. A jet of aerosol from a nozzle is directed at an impaction surface plate. Particles with high inertia strike the plate, whilst smaller particles remain airborne and pass onto another nozzle-impactor plate arrangement. The second nozzle has a smaller diameter which increases the velocity and inertia of the remaining particles. The larger particles are collected by the second plate, and the process allowed to continue through two further stages of impaction followed by a filter which collects the remaining particles. The most important characteristic of the impinger stage is its collection efficiency, defined as the fraction of particles collected from the airstream as a function of particle size. Under ideal conditions, the impinger would collect all particles above a certain size and none of the smaller ones (Marple & Willeke, 1979). However, in practice collection efficiencies vary around a mean value, above which collection increases in efficiency and below which collection efficiency decreases. The diameter at which the collection efficiency is equal to 50% is usually termed the "cut-off" diameter. Thus, if the size of particle cut-off for each stage is known then it is possible to derive the size

distribution of the aerosol by plotting the amount of particles impacting at each stage against the cut-off size for each stage.

The particle size distribution of nedocromil sodium aerosols was assessed by firing ten doses from a metered dose inhaler into the throat of the multi-stage liquid impinger, each shot being separated by sixty seconds. The aerosol was drawn through the multi-stage liquid impinger by a vaccuum pump operating at a flow rate of sixty l/min. Each stage of the impinger, the throat, the filter and the metered-dose inhaler adaptor were then washed in trichlorofluoromethane to dissolve the surface active agent. The washings were individually filtered through 0.45 μm membrane filters to trap any suspended drug particles. After drying, the membranes and impinger components were washed quantitatively with distilled water. The quantity of compound in each solution, and hence at each location, was then determined by spectrophotochemical assay. In this way, the quantity of compound at each location could be determined to an accuracy of better than 0.01 mg.

The amount of drug measured on each stage of the multi-stage liquid impinger was expressed as the cumulative percentage undersize by weight, and was plotted against the known aerodynamic "cut-off" diameters of each stage on logarithmic-probability paper (Smith & Jordan, 1964). The cumulative percentage undersize by weight was used because it reflects the mass of particles considered likely to penetrate into the lung. From these plots, the particle size distribution of each aerosol was further characterised by determining the mass median aerodynamic diameter (μm) and the geometric standard deviation. The percentage of the aerosol mass contained in droplets of < 10 μm, designated P_{10}, and < 4 μm diameter, designated P_4, being the optimal particle sizes for penetration into the respiratory tract as a whole and the alveoli were also derived from the graphs.

The particle size distribution of the nedocromil sodium powder used to formulate different aerosols was measured by centrifugal sedimentation, an in-house method developed at Fisons. Briefly, this classifies particle size by the rate of particle sedimentation when suspended in a fluid subjected to a centrifugal force in a device called the Joyce-Loebl Disc Centrifuge.

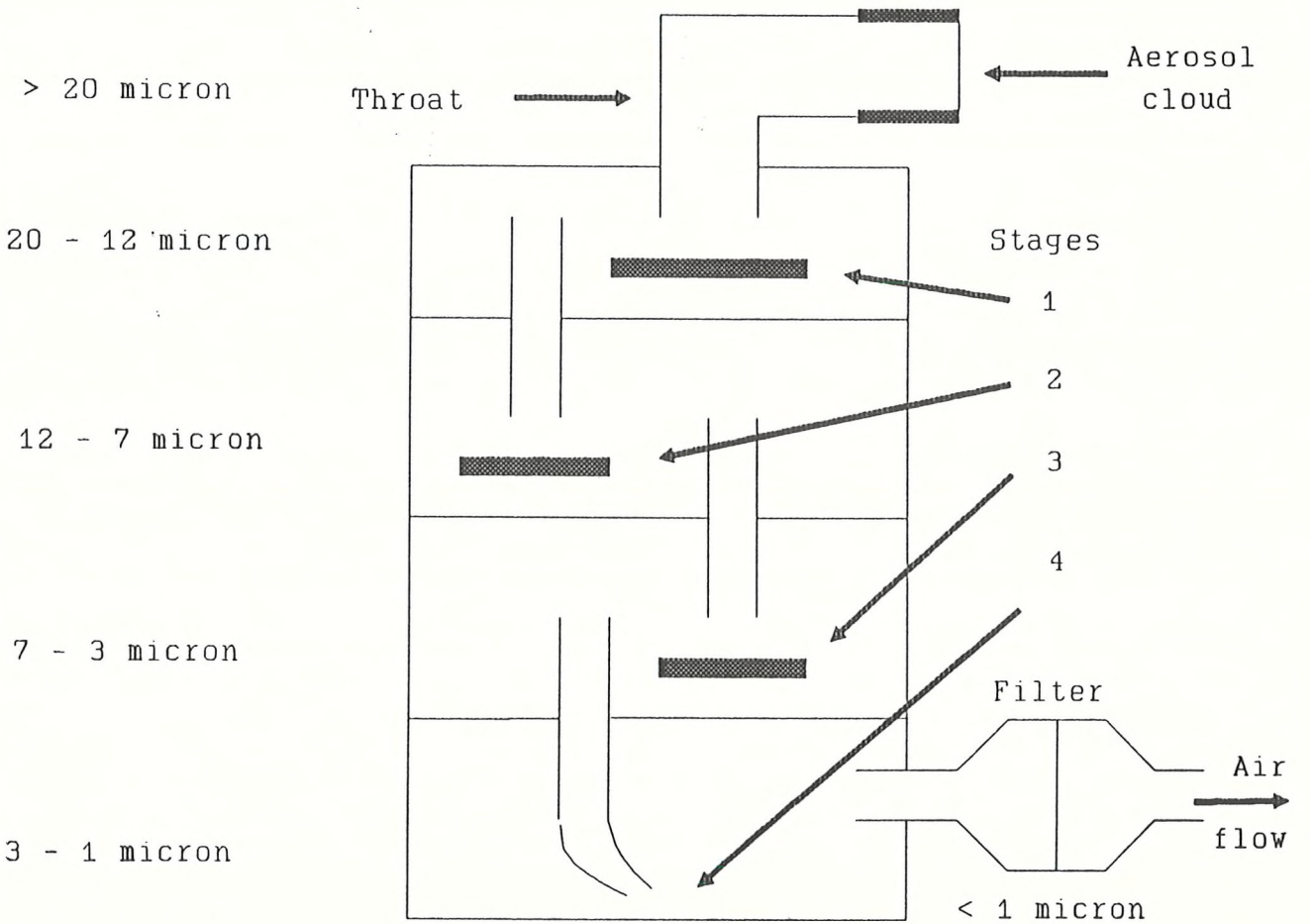

Fig 2.6: the multi-stage liquid impinger.

2.7 Acquisition of images.

2.7.1 Gamma scintigraphy.

A gamma-camera consists of a large detector which can be positioned at various orientations to a source of gamma-ray emissions. Placed in front of the detector is a collimator, a plate with a large number of holes in it which serves to focus incident gamma-rays. The collimator ensures that there is a predictable relationship between the position at which the gamma-rays hit the underlying detector and that from which they were emitted by the source. The detector is a large scintillation crystal of sodium iodide with trace quantities of thallium which, when struck by gamma-rays, is able to emit light. The light is transmitted to an array of photomultiplier tubes and processed to give three signals, two of which give the spatial location of the scintillation and the third represents the energy deposited in the crystal by the gamma-ray. This enables a flash to be produced on a cathode ray tube, and an image, which may be stored on film or computer, results from the integration of multiple flashes (Sharp, 1989).

In this thesis, both planar and tomographic gamma-scintigraphy were used. Planar scintigraphy is performed simply by taking one view of a radioactive source, or alternatively by taking two images at 180° to each other and then combining the images to produce a geometric mean image (Fleming, 1979). Planar imaging portrays a three-dimensional distribution of radioactivity as a two-dimensional image, so that there is no depth information and structures lying at different depths are superimposed. This results in a loss of contrast in the plane of interest due to the presence of underlying and overlying structures. In an attempt to overcome this, single photon emission computed tomography (SPECT) has been developed. SPECT also involves the collection of multiple planar views, typically sixty four, although each view usually has fewer counts than would be acceptable in a conventional image. These views can be reconstructed to give a set of sections through the subject or source. The sections are usually viewed in transaxial and coronal planes. Transaxial images are obtained directly from SPECT data, while coronal images are derived from a stack of transaxial sections.

To obtain transaxial sections, projections of the distribution of radioactivity within a subject must be collected at a series of points around the subject. On each image, the appearance of a source of gamma-emission will differ according to its position and depth in the subject relative to the position of the camera. To reconstruct an image of the original distribution of activity, a process known as back-projection is utilised. For each element of each source of gamma-emission, this involves back-projecting its

image from each view onto an image array in a computer, so building up a final, numerical image. Such an image is generally blurred and there is a high, structured background noise, although sources of high activity will show up well. The high background activity can be partially overcome by the use of filters and attenuation correction prior to the reconstruction. A filter is a mathematical tool employed by the computer to smooth the image by reducing signal at higher spatial frequencies, which has the effect of causing a reduction in fine detail as well as a reduction in background noise (Gemmell, 1989).

If the image is not corrected for the attenuation of photons by overlying tissue, superficial structures are emphasised at the expense of deeper ones, and there is a general decrease in count density from the edge to the centre of an image. Attenuation correction is carried out before reconstruction by multiplying each element in each view by a factor which will depend on the thickness of tissue at the appropriate angle of the subject being imaged. Because the attenuation of radiation by a specific tissue is proportional to the radiological density of that tissue (Fleming, 1989), a map of the density of tissues can be obtained from an x-ray computed axial tomographic image (CT), and then manipulated to give attenuation coefficient values for each tissue. A further problem is the ability of different tissues to scatter photons depending on their density. This can also be partially corrected for prior to the reconstruction by use an appropriate factor (Axelsson et al, 1984).

In this thesis, all images were obtained using a large-field-of-view gamma camera fitted with a parallel, low energy, general purpose collimator (International General Electric Company, New York) and interfaced to a Link MAPS computer (Link Systems, High Wycombe, Bucks, UK). Subsequently, the images were transferred to a DEC Vax 11/730 computer (Digital Equipment Corp, Massachusetts, USA) with a Sigmex A7000 display processor (Sigmex, Horsham, Surrey, UK) for processing using PICS medical image processing sofware (Fleming et al, 1987).

Immediately following inhalation of radioactive aerosols, thirty second timed planar images of the oropharynx, anterior thorax and anterior stomach were taken with the subject lying supine, followed by posterior images of the thorax and stomach. These images were followed immediately by the SPECT study, which consisted of 64-angle tomographic views of thirty second/angle, lasting approximately 34 minutes. The subjects lay supine with their arms above their heads. Radioactive markers (^{57}Co) were

then placed on each nipple, the suprasternal notch and the xiphisternum, and anterior images obtained to allow alignment of the SPECT and subsequent CT images in the axial direction. The extremities of the chest wall were also outlined by the markers in both anterior and lateral planes for alignment in the transaxial plane. All images were acquired in a 64 × 64 matrix.

2.7.2 CT imaging.

Subjects underwent a limited CT study of the thorax to obtain anatomical information to delineate the lung fields and intrathoracic structures, and to provide information to enable attenuation correction to be made for the SPECT images. This study was performed only once, on a Siemens Somatom DR2 CT scanner (Siemens, Ehrlangen, Germany). Images were acquired during tidal breathing, at sixteen millimetre intervals with a slice width of eight millimetres, and included the whole body outline. Radio-opaque markers were placed on the nipples, suprasternal notch and xiphisternum. The images were stored on computer media, and were thus transferred to the Vax 11/730 computer.

2.8 Statistical analysis of data.

2.8.1 Hypothesis testing.

Statistical analysis of data is done in order to test a hypothesis and help draw conclusions regarding the population based on the data obtained from a sample. The procedure involves formulating two hypotheses, one of no difference between the groups being tested (called the null hypothesis) and the other being its alternative. A statistical test is chosen to evaluate the null hypothesis, and a test statistic is computed. If the observed significance level of the statistical test is judged low enough, the null hypothesis is rejected. In this thesis, the null hypothesis was rejected if the observed significance level (p) was less than 0.05, and all test statistics were computed using two-tailed tests. All statistical analyses were carried out by the SPSS/PC+ V3.0 computer program (Norušis, 1988) using an IBM 55SX personal computer.

2.8.2 Determination of distribution.

Before a test statistic can be chosen, it is necessary to determine the spread of data in the sample being measured. CF Gauss (1777-1855) described a mathematical formula to represent certain distributions of data in the population. Lambert Quietelet (1796-1874) found that many natural frequency distributions such as height closely

approximated to the Gaussian formula. In time, this Gaussian distribution became known as the 'normal' distribution, and data that conformed to this distribution as 'parametric'. To assess the distribution of data in this thesis, the Kolmogorov-Smirnov one-sample test was used. This test is based on a comparison of the sample cumulative distribution function to a hypothesised normal distribution function, and the significance of any deviation from the normal distribution is computed. Some data are known to be distributed in a logarithmic fashion, and it is possible to manipulate such data by logarithmic transformation to produce a normal distribution in order to perform statistical analysis. The values for PC_{20} FEV_1 and PC_{50} sGaw are treated in this manner.

The distribution of data can be described by the mean, standard deviation, skew and kurtosis. Skew is an index of the symmetry of distribution about the mean or the degree to which the tail of the distribution extends to the left or right; a negative value indicates a long left tail. Kurtosis is an index of the extent to which observations are clustered around the mean value; a negative value indicates that values are clustered around the mean to a greater extent than in the normal distribution, while a positive result indicates that cases are clustered in the tail.

2.8.3 Statistical tests.

Comparisons of parametric data were made using Student's t-test for paired or unpaired data as appropriate. For multiple tests, an analysis of variance was performed, and if a significant difference was observed between variables, the Student-Newman-Keuls test was used to determine where the difference lay. When data depart from the normal distribution, or if they are 'borderline' normal, or if their likely distribution is not known, they were analysed by non-parametric statistics (Siegel, 1956). Because non-parametric tests make no assumptions about the distribution of underlying data, they allow exact probability statements to be made regarding the data. These tests are only slightly less efficient than parametric tests when applied to normally distributed data, but are considerably more powerful if the underlying population is not evenly distributed. Comparisons of paired data were made by the Wilcoxon signed-rank test, and of unpaired data by the Mann-Whitney U-test. In the Mann-Whitney U test, the observations from both samples are first combined and then ranked from smallest to largest. For each group, the mean rank is then calculated, and a test statistic calculated for the difference; if the two groups do not differ, then the sums of the ranks (and therefore their means) will not differ. The Wilcoxon signed-ranks test is similar, but in this case the differences between paired data are ranked ignoring their signs. The

means of the ranks for positive and negative differences are then calculated, and if the groups do not differ significantly, the mean ranks will be similar.

To assess the degree of correlation between different sets of data, Pearson's correlation coefficient (r) was calculated. The absolute value of r indicates the strength of the linear relationship, and its sign indicates the direction of slope of the relationship. A value of zero indicates no linear relationship. It should be noted that two variables may be strongly associated but have a small correlation coefficient if the relationship is not linear. If there is a linear relationship between two variables, a straight line can be used to summarise the data. The linear regression line can be fitted to the data using the least squares method which minimises the sum of the squared vertical distances from the data points to the line. This also allows the derivation of the Pearson's correlation coefficient, and the number of observations can be used to determine the significance of the relationship. For non-parametric data, Kendall's coefficient of concordance was calculated. In order to compare specific points on dose-response curves, e.g. for PC_{50} sGaw AMP, the slopes of the terminal part of the curves were determined by linear regression and then compared.

2.9 Ethical approval.

All studies were approved by the Southampton Hospitals and University Joint Ethical Committee, and where appropriate, by the Administration of Radioactive Substances Advisory Committee. All subjects gave informed written consent.

Chapter 3. The protective efficacy of inhaled, oral and intravenous nedocromil sodium against adenosine-5'-monophosphate-induced bronchoconstriction in asthmatic volunteers.

3.1 Introduction.

In this study, the ability of nedocromil sodium to protect against AMP-induced bronchoconstriction after administration by inhalation, by mouth or by intravenous infusion was determined in a group of atopic and non-atopic asthmatic volunteers. The relationship between the plasma pharmacokinetic profile of the drug and its protective efficacy was also studied.

3.2 Methods.

3.2.1 Subjects.

Nine subjects, (6 male), mean (SD) age 38.4 (12.98) yrs, participated in this study. All were non-smokers, and six were atopic on the basis of either a clinical history of allergic rhinitis or eczema, and/or positive skin prick tests to six aeroallergens (mixed grass pollen, *Dermatophagoides pteronyssinus*, house dust, cat hair, dog hair and mixed feathers. All patients had baseline FEV_1 values $\geq$ 69% of their predicted maximum, and none was receiving oral corticosteroids for regular treatment. All were taking inhaled salbutamol and beclomethasone dipropionate, and three were taking slow-release theophylline preparations. Inhaled medication was continued throughout the period of the study, but was omitted for at least six hours for inhaled salbutamol and twenty four hours for slow release theophylline prior to each visit to the laboratory. Patients were not studied within four weeks of an upper respiratory tract infection or an exacerbation of their asthma. The demographic data and baseline pulmonary function of the subjects is shown in table 3.1.

3.2.2 Formulation and administration of nedocromil sodium.

Inhaled nedocromil sodium was supplied by Fisons Pharmaceuticals plc (Loughborough, UK) as the standard commercially available preparation (Tilade®). Each actuation of the metered-dose inhaler delivers a nominal dose of 2 mg of nedocromil sodium. After using a placebo canister to ensure that inhalation technique was adequate, the subjects were asked to inhale two actuations separated by 1 min. The inhaler was placed in the mouth, the subjects' lips were closed around the mouthpiece and the dose was delivered at the onset of a slow, full inspiration, followed by a breath hold for 10 s. Note that the apparatus used elsewhere in this thesis for monitoring and controlling

inspiration was not available at this time.

Nedocromil sodium for oral and intravenous use were prepared from milled powder supplied by Fisons plc. The oral dose consisted of one capsule containing 80 mg of nedocromil sodium. The intravenous formulation was administered as a sterile solution of nedocromil sodium (25 μg/ml) made up to a volume of 100 ml in 0.9% sodium chloride, and infused at 0.2 μg/kg/min for a period of 30 min to give a total dose of 6 μg/kg. These doses were chosen to correspond with those used by Neale and colleagues (1987).

3.2.3 Drug analysis and blood sampling.

Blood samples were taken from an indwelling Teflon catheter inserted into a forearm vein before and at various times after drug administration. The cannula was kept patent by the use of saline. Thirty ml of blood was withdrawn prior to dosing, and plasma from this taken to construct the standard curve used to analyse the post dose samples. After dosing, blood samples were taken, centrifuged at 3000g for ten minutes, and the plasma separated and stored at -20°C for subsequent drug assay. Plasma concentrations of nedocromil sodium were assayed as described (chapter 2.5.2).

After inhaled nedocromil sodium, blood samples were taken at 2, 5, 10, 15, 30, 45, 60, 90, 120, 180 and 240 minutes. After oral nedocromil sodium, blood sampling was at 15, 30, 45, 60, 75, 90, 120, 150, 180 and 240 minutes. With intravenous drug administration, blood samples were taken at 5 minute intervals for 60 minutes from the start of the infusion, then at 75 and 90 minutes, and then every 30 minutes until 4.5 hours after the start of the infusion.

3.3 Protocol.

The study involved four phases; on the first visit the subjects' clinical condition and airways responsiveness were assessed, and the effects of nedocromil sodium investigated on subsequent visits. On the first visit, baseline FEV_1 was measured, the best of 3 measurements being recorded. Skin prick tests with allergen extracts were also performed. Each subject then underwent an AMP bronchial provocation test, and histamine inhalation challenge was undertaken at least 1 hr after the AMP challenge, or when the FEV_1 had returned to within 10% of its starting value.

Visits 2 - 4 comprised the major part of the study in which the effect of nedocromil

sodium administered by each of the 3 routes was observed against AMP-induced bronchoconstriction. The AMP bronchial challenge data after nedocromil sodium were compared with the AMP bronchial challenge results obtained during the first visit. The 3 routes of administration were randomised, and in order to ensure adequate blood levels at the time of challenge, each challenge procedure was timed to occur after the predicted peak plasma concentration of nedocromil sodium (Neale et al, 1987). Thus, AMP challenge was undertaken 60 min after inhalation, 120 min after drug ingestion and 75 min after the start of the infusion.

3.4 Data Analyses.

Values for FEV_1 are presented as the mean (SEM). The results of the bronchial challenges were logarithmically-transformed, and the group data are presented as the geometric mean (GM) with the range in parentheses. For each subject, concentration ratios (CR) were calculated for the effect of each method of administration of nedocromil sodium compared to placebo [CR = $\log_2$ (PC_{50} sGaw post-drug) - $\log_2$ (PC_{50} sGaw baseline)], which determines the displacement of the PC_{50} value in doubling dilutions of AMP. The CR is distinct from a dose ratio which is derived from the geometric mean PC value after drug divided by that before drug. The slopes of the AMP dose-response curves were determined by linear regression analysis and compared by using 2-factor analysis of variance. Comparisons of drug-induced changes in the PC_{50} values were by Student's t-test for paired data, and relationships between the pharmacokinetic data, pulmonary function and bronchial challenges were calculated by Pearson's correlation coefficent.

The time course of plasma concentrations of nedocromil sodium after inhaled, oral and intravenous administration were analysed to derive the terminal (elimination) half-life (t½), the mean residence time of nedocromil sodium in the circulation (MRT), and the area under the plasma concentration-time curve (AUC). These data are presented as the mean (SEM). The Cmax and Tmax are given as the observed values, and the concentration of nedocromil sodium at the time of AMP challenge (Cchall) was derived by log-linear interpolation. Comparisons between t½ and MRT for the inhaled and intravenous routes of drug administration were made by one-factor analysis of variance. The doses absorbed after inhalation and oral administration were calculated as described (chapter 2.5.3).

3.5 Results.

The provocative concentration values for histamine and AMP inhalation challenges are shown in table 3.1. There was a significant correlation between baseline values for PC_{20} histamine and for PC_{50} AMP ($r = 0.724$, $p = 0.014$). The GM for PC_{20} FEV_1 histamine was 0.33 mg/ml (0.03 - 4.0). There was no significant difference found for the slopes of the AMP dose-response curves at baseline or after the different routes of administration of nedocromil sodium.

The GM for the baseline (visit 1) PC_{50} sGaw AMP was 4.37 mg/ml (0.158 - 26.38), 28.84 mg/ml (12.39 - 44.94) after inhaled nedocromil sodium, 7.24 mg/ml (2.19 - 39.49) after oral drug, and 7.94 mg/ml (1.15 - 36.25) after intravenous nedocromil sodium. Thus, inhaled nedocromil sodium produced a geometric mean 6.6-fold displacement of the AMP dose-response curves to the right. There was also an increase in the geometric mean PC values for AMP of 1.66- and 1.82-fold for oral and intravenous drug. The concentration ratios after inhaled, oral and intravenous nedocromil sodium increased by 2.71, 0.75 and 0.88 doubling dilutions respectively. There was no significant difference between PC_{50} AMP values measured at baseline and those after oral or intravenous nedocromil sodium. However, after inhaled nedocromil sodium the PC_{50} sGaw AMP was significantly different when compared with either that measured at baseline ($p = 0.019$), or after oral drug ($p = 0.002$) or intravenous drug ($p = 0.005$). There was no difference between the PC_{50} sGaw AMP after oral and intravenous nedocromil sodium ($p = 0.767$). Two subjects, both of whom were atopic and highly reactive to inhaled histamine, obtained marked protection against AMP-induced bronchoconstriction by nedocromil sodium administered by all three routes (subjects 3 and 4, table 3.1). The AMP dose-response curves for all subjects are shown in figures 3.5.1.a to 3.5.1.i (subjects 1 and 4 respectively).

There were significant correlations between the baseline indices of histamine and AMP responsiveness and the degree of protection conferred by nedocromil sodium administered by all three routes against the airway effects of AMP when described as the concentration ratios. Thus, PC_{20} FEV_1 histamine correlated significantly with the concentration ratio for inhaled drug ($r = -0.79$, $p = 0.011$), for oral drug ($r = -0.80$, $p = 0.01$), and for intravenous nedocromil sodium ($r = -0.76$, $p = 0.019$). The corresponding relationships of PC_{50} sGaw AMP with the drug concentration ratios were: inhaled, $r = -0.96$ ($p < 0.001$), oral, $r = -0.82$ ($p = 0.007$), and intravenous nedocromil sodium, $r = -0.85$ ($p = 0.004$). These data indicate the more reactive the

airways the greater any protection afforded by nedocromil sodium for all three modes of administration.

The mean plasma concentration-time curves for each route of administration are shown in fig 3.5.2 (a-c). The mean pharmacokinetic data are shown in table 3.2. The t½ for inhaled nedocromil sodium, 85 (9) min, was not significantly longer than that of intravenous drug, 65 (8) min, $p > 0.05$, but the MRT for the inhaled drug, 129 (12) min, was significantly longer than that of the intravenous dose, 48 (6) min, $p < 0.001$, indicating a prolonged and slow absorption phase. No relationship could be found between Cmax, Cchall or AUC and the protective efficacy of nedocromil sodium against AMP challenge or baseline values of FEV_1. However, the relationship between the concentration ratio and AUC or Cchall for intravenous nedocromil sodium approached statistical significance ($p = 0.053$, $p = 0.068$ respectively).

3.6 Discussion

This study has demonstrated the bronchoconstrictor activity of inhaled AMP in asthma and established a positive but weak relationship between responsiveness to this stimulus and to inhaled histamine, a more widely used index of airways responsiveness. This finding is similar to that reported by others for both histamine and methacholine (Phillips et al, 1989; Mann et al, 1986), and serves to reinforce the view that the mechanism of bronchoconstriction induced by AMP is not by direct stimulation of airways smooth muscle but by stimulation of cell surface purinoceptors leading to the enhanced release of mast cell mediators (Polosa et al, 1989). Following inhalation, AMP is rapidly hydrolysed by 5'-nucleotidase to adenosine, the agonist thought responsible for the purinoceptor-mediated effects of this nucleotide. An additional mechanism of action is the stimulation of adenosine receptors on postganglionic vagal nerve endings (Drazen et al, 1989).

The opportunity that AMP provides in provoking dose-dependent bronchoconstriction without a late response or an increase in airways hyperresponsiveness has enabled its use to quantify the protective action of nedocromil sodium. Because the drug did not influence the slopes of the dose-response curves, it was possible to describe their position as a single point, the PC_{50} value. Although the degree of displacement of the AMP dose-response curve by inhaled nedocromil sodium was less than that described by others in similar studies in which the FEV_1 was used to follow airway calibre (Phillips et al, 1989; Richards et al, 1989b), this study has confirmed that nedocromil

sodium is a potent inhibitor of this stimulus to the airways. By contrast, the degree of displacement of the dose-response curves by oral and intravenous nedocromil sodium was smaller and failed to reach statistical significance.

The study was designed in such a way that the bronchial challenge procedure was undertaken after the peak plasma concentrations of nedocromil sodium had been achieved (Neale et al, 1987) at a time when the plasma concentrations of the drug should have been similar. After inhaled and oral nedocromil sodium the plasma drug concentrations at the time of the AMP challenges were similar, 1.86 (0.3) and 1.94 (0.4) ng/ml respectively, whilst after intravenous administration plasma concentration of the drug was slightly more than half of these values.

The rationale for using an infusion of nedocromil sodium which did not reach steady state was to compare this route of administration with the inhaled route, which is effective in preventing AMP-induced bronchoconstriction after a single dose, and the oral route, where steady state can only be achieved by prolonged dosing for which there is no safety data available. It should be emphasised that the relationship between the concentrations in the plasma and those at the site of action in the airways may vary for different routes of administration and different times after administration. The only way to establish the plasma concentration-effect relationship unequivocally would be by constant infusion or inhalation until steady-state had been reached. Thus the results of this study do not preclude the possibility of an effect under different conditions of intravenous or oral dosing.

The measured plasma concentration-time profiles were very similar to those reported by Neale and colleagues (1987) in healthy volunteers, with one major difference. In the present study, the terminal half-life of inhaled nedocromil sodium was not significantly longer than that of intravenous nedocromil sodium. However, the MRT for inhaled drug, 129 (12) min was significantly longer than for intravenous nedocromil sodium, 48 (6) min. The difference between inhaled and intravenous MRT values is termed the mean absorption time (MAT) (Gibaldi, 1984), and the high value obtained (81 min; 129 - 48 min) indicates that nedocromil sodium is absorbed slowly from the lungs. Thus, any difference between inhaled nedocromil sodium and oral or intravenous drug in attenuating the response to AMP is likely to be a reflection of absorption-limited kinetics.

The greatly reduced protective action of the drug against AMP for intravenous and oral administration compared with the inhaled route confirms the "topical" activity of this drug. However, if perfusion of the bronchial tree contributes to the efficacy of this drug, then the concentration of nedocromil sodium in the bronchial circulation after inhalation is likely to be far higher than after oral administration and therefore does not discount local systemic perfusion being an important aspect of this drug's efficacy. The overall finding that intravenous nedocromil sodium was no less active in protecting some of the subjects against AMP when compared to the oral route whilst achieving half the plasma concentration suggests that circulating drug levels per se are a poor reflection of efficacy for these non-inhaled routes. This interpretation is supported by the lack of correlation between pharmacokinetic indices of nedocromil sodium and its protective efficacy by any of the three routes of administration. The closest link between efficacy and plasma concentration of drug was observed with the intravenous preparation, but with the number of subjects studied statistical significance was not achieved.

Against these overall observations, 2 subjects (nos 3 and 4) were identified as responding differently to the various nedocromil sodium formulations than the others, in that all three forms of drug administration produced marked protection against bronchoconstriction provoked by AMP. It is of particular interest that these two subjects were the most reactive to inhaled histamine and AMP. It has been suggested that the degree of non-specific bronchial responsiveness correlates well with indices of airways inflammation (Wardlaw et al, 1988), and that the more hyperreactive the airways, the greater the likelihood of increased microvascular permeability, epithelial damage and exposure of afferent nerve endings (Laitinen et al, 1985). Since nedocromil sodium has a range of actions directed against many of the components of the asthmatic inflammatory response, the demonstration of a relationship between the degree of protection afforded by each route and the baseline bronchial reactivity to both histamine and AMP indicates that the more reactive (and possibly the more inflamed) the airways, the greater the benefit likely to be derived from nedocromil sodium, regardless of the route of drug administration. The work of Dahlén et al (1989) in experimental animals would suggest that nedocromil sodium reaching the airways by vascular perfusion might be partially efficacious against any inflammatory response that increased post capillary venule permeability and oedema formation, although these workers used doses that were an order of magnitude greater than those used in this study. By contrast, the doses of inhaled and intravenous nedocromil sodium used by

Jackson et al (1989) to influence bronchial C-fibre discharge in the dog lung were almost exactly the same as the doses used in this study, and it is therefore possible that the drug may be exerting some of its effects through the modulation of neural transmission.

In conclusion, the relationship between the pharmacodynamics and pharmacokinetics of nedocromil sodium given by 3 different routes has been examined. The findings have confirmed that when given by inhalation it is a potent inhibitor of AMP-induced bronchoconstriction, and that it displays absorption-limited pharmacokinetics. Overall, oral and intravenous nedocromil sodium produce limited protection against this airway stimulus. However, in subjects with highly responsive airways, nedocromil sodium reaching the airways via the circulation may be protective. The data supports the view that the preferred route of administration of this drug in asthma is by inhalation, although following its absorption into the bronchial circulation, it is not possible to dismiss an important effect of local systemic perfusion.

Table 3.1: Demographic, pulmonary function and bronchial challenge data.

Subject	Sex	Age	Atopy	Baseline FEV_1,	PC_{20} histamine	PC_{50} sGaw AMP			
						Baseline	Inhaled	Oral	Intravenous
1	M	48	-	2.40 (70)	0.17	3.06	43.41	4.18	1.15
2	F	31	+	2.60 (75)	0.22	5.97	12.39	2.39	5.89
3	F	35	+	2.45 (82)	0.07	0.78	62.19	8.32	36.25
4	F	20	+	2.90 (90)	0.03	0.16	44.94	7.32	13.31
5	M	59	+	2.70 (96)	4.00	8.30	16.49	2.19	2.45
6	M	23	+	4.12 (92)	0.16	22.83	41.79	39.49	18.83
7	M	59	-	2.48 (89)	0.65	5.35	18.17	23.57	10.04
8	M	21	+	3.65 (91)	1.35	26.38	40.35	15.73	19.77
9	M	50	-	3.62 (69)	1.15	9.49	16.95	3.13	4.64
Mean (SEM)		38.4		83.8 (3.4)	0.33*	4.37*	28.84*	7.24*	7.97*

* - geometric means.

Table 3.2: Pharmacokinetic parameters of nedocromil sodium after inhalation, oral and intravenous dosing.

	Inhaled	Oral	Intravenous
Dose administered (mg)	4	80	0.405 (0.019)
Dose absorbed (mg)	0.39 (0.09)	0.37 (0.07)	-
Cmax (ng.ml)	3.27 (0.48)	2.78 (0.48)	9.55 (0.62)
Cchall (ng/ml)	1.86 (0.30)	1.94 (0.40)	0.93 (0.17)
AUC (ng.min/ml)	439 (98)[a]	408 (72)[b]	463 (36)[a]
Tmax (min)	19 (5)	137 (25)	22 (1)
t½ (min)	85 (9)	-	65 (8)
MRT (min)	129 (12)	-	48 (6)
Clearance (ml/min)	-	-	901 (52)
Volume of distribution (l)	-	-	44 (6)

Results are shown as the mean (SEM)

a - extrapolated to infinity.

b - calculated from time 0 to time 240 minutes only (because no terminal slope was obtained for most subjects).

Legend to figures.

Figures 3.5.1.a to i. The effect of nedocromil sodium on AMP-provoked falls in sGaw after administration by inhalation (■), by mouth (♦) and by intravenous infusion (●) in each of 9 subjects; ▲ represents the AMP response at baseline.

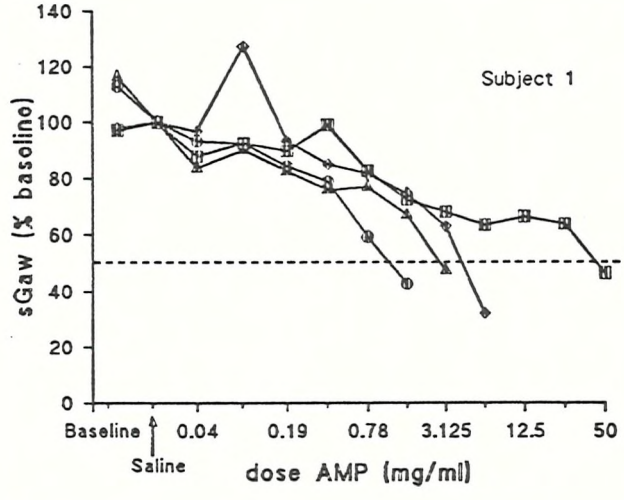

Fig 3.5.1.a

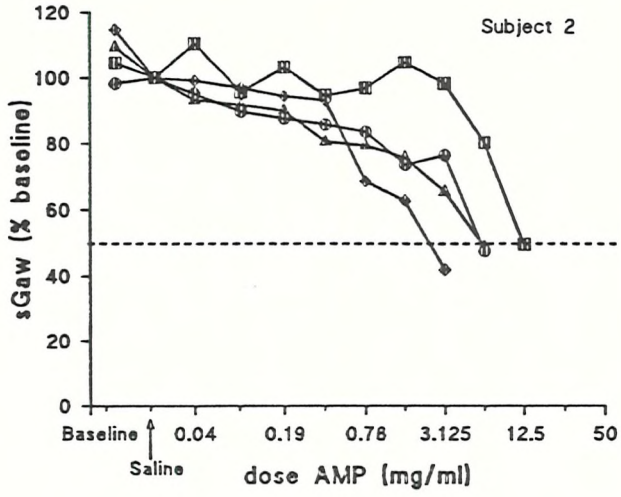

Fig 3.5.1.b

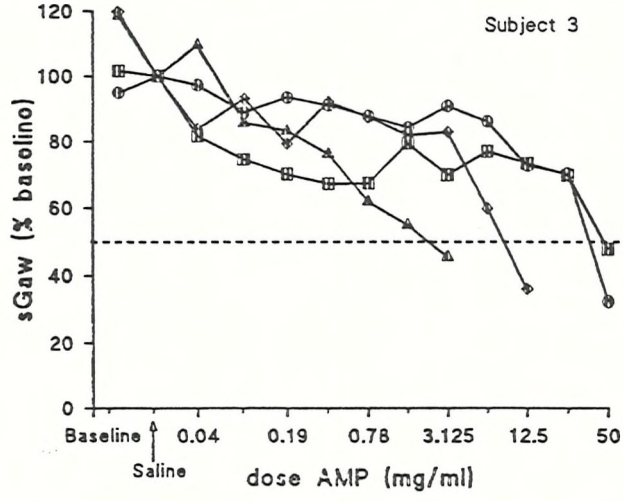

Fig 3.5.1.c

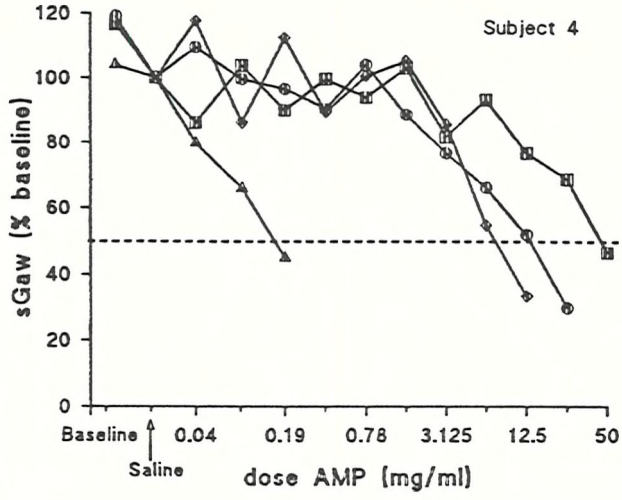

Fig 3.5.1.d

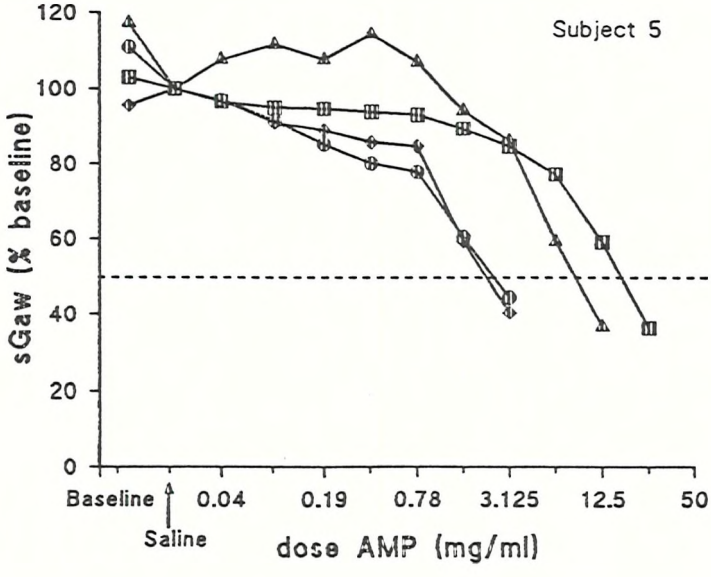

Fig 3.5.1.e

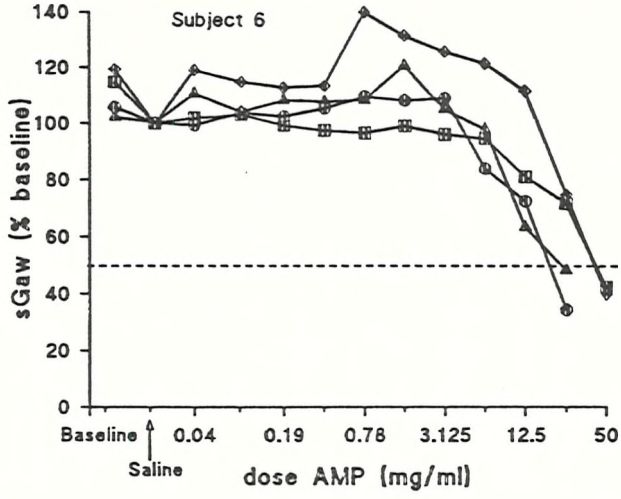

Fig 3.5.1.f.

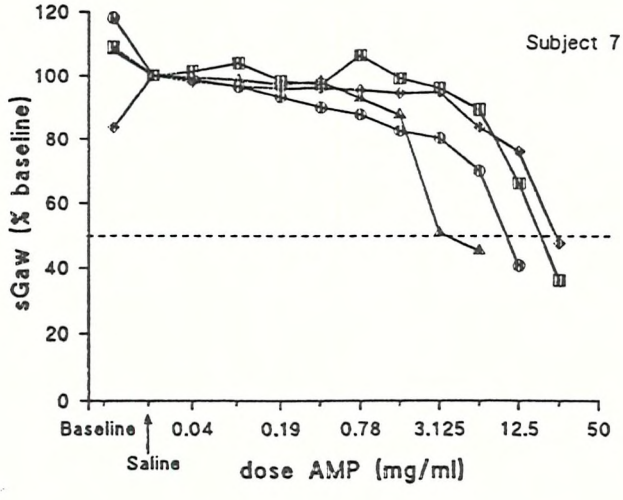

Fig 3.5.1.g.

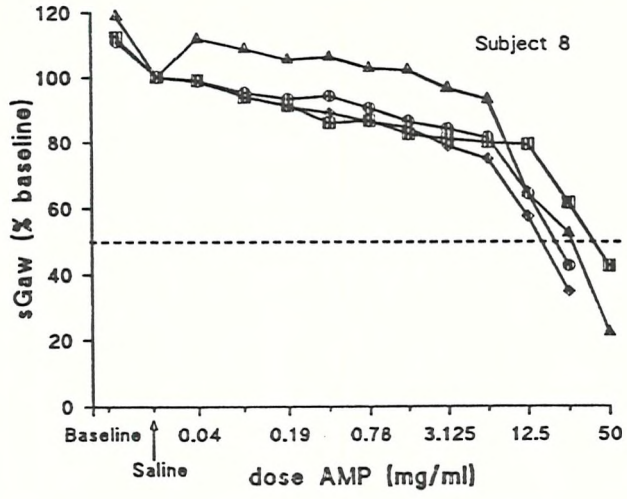

Fig 3.5.1.h.

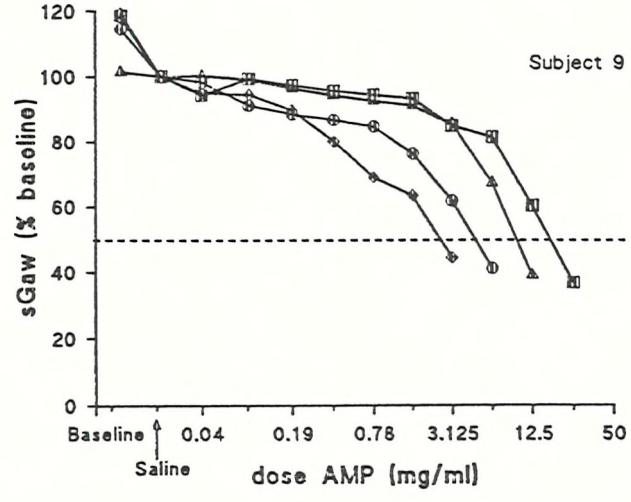

Fig 3.5.1.i.

Figures 3.5.2 (overleaf) show the mean (SEM) plasma nedocromil sodium concentrations with time after each method of drug administration for all 9 subjects. The top panel depicts the nedocromil sodium time course after inhalation (4 mg), the middle panel shows that after intravenous administration (6 μg/kg; note that the first 30 minutes represents the duration of infusion) and the lower panel depicts the time course after oral administration (80 mg).

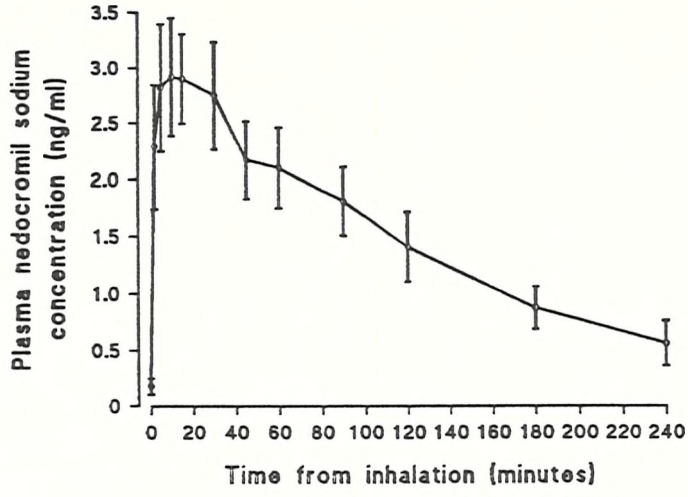
Plasma nedocromil sodium concentration (ng/ml)
3.5
3.0
2.5
2.0
1.5
1.0
0.5
0
0 20 40 60 80 100 120 140 160 180 200 220 240
Time from inhalation (minutes)

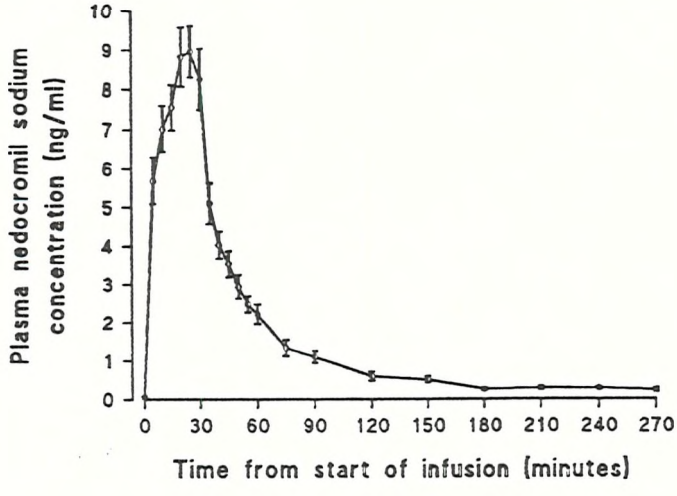
Plasma nedocromil sodium concentration (ng/ml)
10
9
8
7
6
5
4
3
2
1
0
0 30 60 90 120 150 180 210 240 270
Time from start of infusion (minutes)

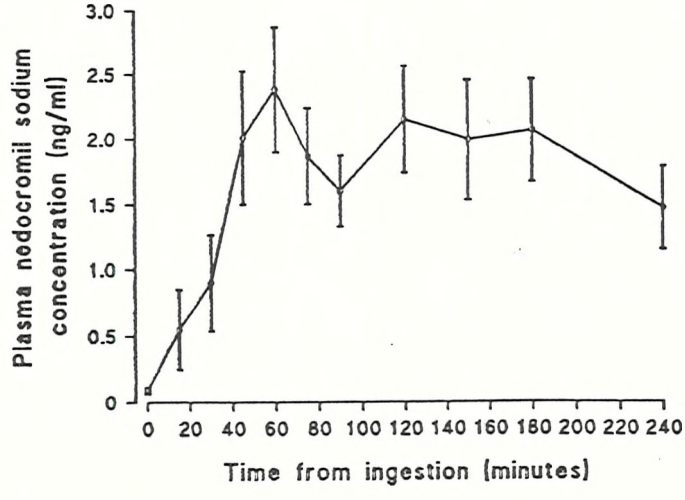
Plasma nedocromil sodium concentration (ng/ml)
3.0
2.5
2.0
1.5
1.0
0.5
0
0 20 40 60 80 100 120 140 160 180 200 220 240
Time from ingestion (minutes)

Chapter 4. The effect of respiratory and pharmacological manoeuvres on the pharmacokinetic profile of inhaled nedocromil sodium.

4.1 Introduction

Richards et al (1989a) showed that, during the terminal absorption rate-limited phase of SCG kinetics, plasma concentrations of the drug rapidly increased immediately following a forced expiratory manoeuvre, and then declined to reach the baseline value from which they departed. The inspiratory limb of this manoeuvre was shown to be responsible for this increase in drug absorption. After inhalation of nedocromil sodium, a period of vigorous exercise performed by normal and asthmatic subjects has also been shown to increase plasma concentrations of nedocromil sodium (Neale et al, 1988). On the basis that circulating drug levels also increase after both exercise and forced expirations, but not after Valsalva manoeuvres, Ghosh et al (1989) have suggested that the rapid absorption of nedocromil sodium may be due to lung inflation and/or deflation rather than any change in the bronchial or pulmonary circulations.

Both SCG and nedocromil sodium are hydrophilic anions with molecular weights of 512 and 415 daltons respectively. The absorption of SCG across rat tracheal epithelium has been shown to occur in part by a saturable carrier-mediated transport, and can be inhibited by other anionic compounds such as probenecid and penicillin, indicating some specificity for the transport process (Gardiner & Schanker, 1974). On the basis of the similar pharmacokinetic profile of SCG and nedocromil sodium, it is possible that a similar carrier-mediated transport system across the respiratory epithelium also exists in the human lung for nedocromil sodium.

To investigate these phenomenona, the effects of respiratory manoeuvres on the absorption of nedocromil sodium from the airways have been studied. Since changes in lung volume and intrathoracic pressure may change bronchial blood flow (Modell et al, 1981; Wagner et al, 1987a), the effect of reducing bronchial mucosal blood on the absorption of the drug flow using the vasoconstrictor agent, methoxamine, has also been investigated. Finally, to investigate the possibility of competition for the transport of nedocromil sodium across the bronchial epithelium, the effect of oral probenecid and penicillin on the plasma pharmacokinetics of nedocromil sodium has been studied.

4.2 Methods

4.2.1 Subjects

Eight healthy non-smoking volunteers (6 male, 2 female) aged 18-25 took part in the study (table 4.1). No subject had a past history of respiratory disease or an upper respiratory tract infection within 4 weeks prior to the study, and none were taking any medication. The subjects' mean (SD) baseline pulmonary function was 104.8 (5.63) percent of the predicted value and all were able to inhale nedocromil sodium from a metered-dose inhaler correctly.

4.2.2 Drug administration

Nedocromil sodium was supplied by Fisons plc, Pharmaceuticals Division (Loughborough, UK) as the standard commercially available preparation (Tilade®). It was administered from a pressurised metered-dose inhaler (MDI) which delivered a nominal dose of 2 mg of nedocromil sodium per actuation. Subjects inhaled 2 actuations of the drug, using the standardised technique described in chapter 2.3.

4.2.3 Blood sampling and drug analysis.

Blood sampling and plasma nedocromil sodium radioimmunoassay were described in chapters 2.5.1 and 2.5.2.

4.2.4 Study design

The study involved 3 visits to the department. Subjects were rested throughout the study. On a preliminary occasion, they were trained to inhale nedocromil sodium from an MDI using the technique described.

The first study day was conducted to investigate the effect of respiratory manoeuvres on the absorption of nedocromil sodium, and was also a control day for comparison with subsequent visits. Nedocromil sodium was inhaled, and blood samples were taken at 5 min intervals for 20 min, and then at 10 min intervals until 70 min after inhalation. Subjects then performed 9 consecutive forced expiratory volume in one second (FEV_1) manoeuvres over a 3 minute period using a dry wedge-bellows spirometer (Vitalograph), and blood sampling continued at 73, 76, 80, 90, 100, and 110 min. At 110 min, subjects took one deep inspiration from functional residual capacity (FRC) to total lung capacity (TLC), and held their breath for 30 sec with the glottis and larynx open. Blood sampling continued at 113, 116, 120, 130, 140, and 150 min. At 150 min a single FEV_1 was performed and blood samples were taken at 153, 156, 160,

165, 170, 180, 200, 220, 240 and 270 min.

On the second visit this sequence of events was repeated. However, at 60 min after drug inhalation volunteers were given methoxamine, a potent bronchial vasoconstrictor (Dinh Xuan et al, 1989). A solution of methoxamine in 0.9% sodium chloride at a concentration of 20 mg/ml was nebulised as described in chapter 2.4.4; the delivered dose was 0.15 mg/kg body weight. The methoxamine aerosol was generated by a disposable Inspiron Mini-nebulizer (CR Bard International, Sunderland, UK) driven by compressed air at a pressure of 20 lb/in^2 and at a flow rate of 8 l/min. Under these conditions, the nebulizer produces an aerosol with a mass median aerodynamic diameter of 6.3μm and a geometric standard deviation of 1.73 (Newman et al, 1986). The subjects were instructed to take the appropriate number of breaths consecutively from FRC to TLC via a mouthpiece. The study was then conducted as for the second visit. After the 9 FEV_1 manoeuvres, the best value for each subject was recorded for comparison with the value recorded before methoxamine inhalation.

Prior to the third visit, subjects were orally premedicated for two days with probenecid (500 mg 8 hourly) and penicillin (500 mg 6 hourly). Six hours after the last dose, nedocromil sodium was administered. Blood samples were taken and respiratory manoeuvres were again performed at the appropriate times, as in visit 2. Prior to the beginning of this study, blood was taken for probenecid and penicillin assay (Rumble & Roberts, 1985).

4.3 Data analyses.

Differences between paired data were analysed using Student's t-test except where indicated, and the null hypothesis rejected if $p < 0.05$. To ensure that drug inhalation on the different study days was similar, the mean values for the various inspiratory parameters were compared. FEV_1 values before and after methoxamine inhalation were compared to assess the effect of this drug on airway calibre.

The time course of plasma concentrations of nedocromil sodium after drug administration were analysed by deriving the area under the plasma concentration-time curve (AUC) for the study period (0-270 min) using the linear trapezoidal rule. The initial maximal plasma concentration (Cmax) and the time taken to achieve this (Tmax) are given as the observed values, and compared between study days.

To assess the effect of each manoeuvre the AUC for the whole plasma concentration-time curve was first calculated. The curve was then manipulated to delete the 3 points immediately following the manoeuvre which encompassed any increase in area resulting from the rise in plasma nedocromil, and the AUC recalculated. The difference between the 2 AUC values was compared by Wilcoxon's matched-pairs signed rank test. The change in AUC produced by each manoeuvre was also expressed as a percentage of the total AUC. For example, to assess the effect of the 9 FEV_1 manoeuvres the total AUC was calculated, the 3 points following the 9 FEV_1s were deleted and the AUC recalculated. The same procedure was followed for the other two manoeuvres. The effect of probenecid on the pharmacokinetics of nedocromil sodium was assessed by comparing the AUC for the whole curve with that from the control visit. The change in AUC after each manoeuvre was also compared across study days.

4.4 Results.

All subjects completed the study. There were no differences in the inhalation of nedocromil sodium between the study days (table 4.2). Methoxamine inhalation did not change airway calibre, the mean (SEM) FEV_1 before and after methoxamine being 4.74 (0.19) and 4.78 (0.22) l respectively. All subjects had measurable levels of probenecid in their plasma (39, 42, 54, 39, 56, 60, 49 and 72 mg/l respectively for subjects 1-8); howver, penicillin concentrations were below the limit of detection of the assay.

Figure 4.1 shows the plasma concentration-time curves for each subject on the first study day. Plasma nedocromil sodium concentrations rose rapidly to a peak in all subjects, and no differences were found between study days when Cmax and Tmax were compared. The peak value was always achieved within 20 min and usually within 10 min of inhalation. Thus, Cmax was 4.12 (0.76) ng/ml on the first day, 3.77 (0.59) ng/ml on the methoxamine day, and 5.26 (1.34) ng/ml on the probenecid day, and Tmax was 8.75 (2.06), 10.63 (2.20) and 8.75 (1.83) min respectively. Plasma nedocromil sodium concentrations rose rapidly after all respiratory manoeuvres in all subjects, except in one subject (no 5 at 150 min), and returned to the value from which it departed within 3 or 4 time points after the manoeuvre. It was also apparent that plasma nedocromil sodium concentrations rose spontaneously at times not associated with a respiratory manoeuvre, and most usually toward the end of the study period (e.g. subjects 3 and 6, fig 4.1). In some cases, individual plasma concentrations were grossly and spuriously elevated with no obvious cause at isolated time points. For example, the plasma nedocromil concentration at 165 min in subject 3 on day 1 was

> 11 ng/ml, whereas the values immediately before and after this were 0.305 and 0.265. Such gross elevations were infrequent, occurring at 11 single time points out of a total 768 samples, and could be due to contamination. Such values were deleted before analysis.

The median (range) total AUC on the first study day was 365.1 (51.5-774.1) ng.min/ml (table 4.3). The changes produced by the respiratory manoeuvres reached statistical significance for both the multiple forced expirations and the breath-hold, but not for the single forced expiration. Thus, on the control day, the median total AUC was 365.1 as compared to 355.1 ng.min/ml after deletion of the rise due to the multiple forced expirations ($p = 0.05$) and 363.1 ng.min/ml after deletion of the rise due to the breath-hold ($p = 0.037$).

Neither methoxamine nor probenecid significantly altered the total AUC for nedocromil sodium. On the methoxamine study day, the AUC values were 387.1 ng.min/ml for the total AUC, 380.8 after the forced expirations ($p = 0.0357$) and 382.6 after the breath-hold ($p = 0.0117$); on the probenecid day they were 388.4 for the total AUC, and 377.4 and 382.9 respectively ($p = 0.0117$ for both).

When the change in AUC produced by each manoeuvre was expressed as a percentage of the total AUC, and compared across study days, significant differences were found (table 4.3). The median change after the multiple manoeuvres on the third (probenecid) day was 2.86%, as compared with 1.74% on the first day ($p = 0.0173$) and 1.495% on the methoxamine day ($p = 0.0357$).

4.5 Discussion.

This study has confirmed that both multiple forced expirations and a single deep inspiration with a breath-hold can produce significant rises in plasma nedocromil sodium concentrations. A single forced expiration produced small changes in plasma nedocromil sodium levels in some but not all subjects and which did not reach significance. The prior inhalation of methoxamine had no effect on the subsequent rise in plasma nedocromil sodium after multiple forced expirations, and did not alter airway calibre. However, while premedication with oral probenecid did not alter the total AUC, Tmax or Cmax, a larger rise was seen in plasma nedocromil sodium after multiple forced expirations when compared to the same manoeuvre on the other 2 study days. The failure to measure penicillin in any of the subjects' plasma is due to the time delay

between dosing and blood collection. These data confirm that absorption from the airways is the rate limiting step in determining the plasma kinetics of this drug and that the facilitated transport mechanism contributes at least to some of this absorption.

These findings confirm those of Richards et al (1989a) for SCG and those of Ghosh et al (1988) for nedocromil sodium, in that both studies found significant rises in plasma drug concentrations with multiple forced expirations, although only Richards et al (1989) reported the effects of a deep inspiration and breath-hold. The current findings also indicate that it is the inspiratory limb of the manoeuvre which is responsible for the rapid increases in plasma drug concentration. This most likely produces a widening of epithelial intercellular junctions, and hence a more rapid paracellular egress of the drug into the bronchial vasculature. Other possible explanations include a thinning of airways or alveolar lining fluid with deep inspiration facilitating more rapid absorption of drug, movement of drug to more peripheral sites with a greater surface area and/or different absorption characteristics, and changes induced in the bronchial or pulmonary circulation.

There is abundant evidence that lung stretching can give rise to increased absorption of substances across the lung. Egan (1980) showed that alveolar pore radii increased with lung inflation in dogs, and that there was a concomitant increased passage of solutes across the lung. Both Nolop et al (1986) and Marks et al (1985) reported that increases in lung volume accelerated the clearance of Tc^{99m}-DTPA from the lung, and Dusser et al (1986) reported increased clearance of Tc^{99m}-DTPA from the upper lobes compared to the lower lobes in the upright posture, a situation in which the upper lobes are stretched because of gravity. Lorino et al (1989) provided further evidence that lung stretch is the most likely cause of this phenomenon by documenting an increase in lung permeability 30 minutes after maximal exercise, at a time when any possible exercise-induced changes in blood flow or thickness of the airways or alveolar lining fluid would have resolved.

The finding that premedication with probenecid did not alter the plasma kinetic profile of nedocromil sodium or overall total absorption of the drug but did result in considerably larger peaks of absorption with multiple forced expirations adds support to the view that these peaks relate to an airway or alveolar surface phenomenon. Probenecid will inhibit only that part of SCG absorption that is dependent upon active carrier-type transport (Gardiner & Schanker, 1974), and because nedocromil sodium

has an almost identical pharmacokinetic profile it is likely that a similar mechanism exists for this drug. Both SCG and nedocromil sodium are hydrophilic anions, and thus are likely to cross the respiratory mucosa through the paracellular pathway (Gumbiner, 1987), the absorptive pathway likely to be affected by stretch-induced disruption of epithelial tight junctions. The greater increase in plasma nedocromil after the multiple forced expirations following probenecid may be a consequence of that fraction of drug absorption through the transcellular route being retarded, resulting in more drug being available at the mucosal surface for paracellular transport. This is the first time that a probenecid-sensitive facilitated transport mechanism has been shown for a drug in the human lung.

The selective α-agonist, methoxamine, when inhaled prior to the multiple forced expirations did not affect the subsequent increases in plasma nedocromil sodium. Methoxamine was used because of its potent vasoconstrictor effect on the bronchial vasculature. The dose selected (0.15 mg/kg) was chosen because it had been shown to attenuate exercise-induced asthma, a response in asthmatic airways thought in part to be due to post-exertional airway rewarming and rebound vasodilatation (Dinh Xuan et al, 1989). However, methoxamine may have a direct effect on airway calibre in asthma in causing bronchoconstriction (Snashall et al, 1978), although like others (Snashall et al, 1978; Black et al, 1982) no such effect was seen in the normal subjects used in this study. By contrast, Anthracite et al (1971) did report methoxamine-induced changes in airway calibre in normal subjects, but the responses, measured as changes in specific airways conductance, were small and may not have been detected by FEV_1 measurements.

Since methoxamine had no effect on the absorption of nedocromil sodium, it is likely that the mucosal circulation contributes little to the absorption characteristics of nedocromil sodium, the rate limiting step being epithelial transport. Although the dose of inhaled methoxamine was selcted to produce mucosal vasoconstriction, it is not possible to exclude any effect on the bronchial circulation being at least partially responsible for these changes. Wagner & Mitzner (1990) have shown that dramatic reductions in the bronchial blood flow in sheep has the effect of delaying recovery from methacholine-induced bronchoconstriction, suggesting that the bronchial circulation does play an important role in clearing the agonist from the airways, and it was anticipated that methoxamine might have produced a similar effect. However, the respiratory manoeuvres may have other effects on the bronchial circulation which

would obviate the influence of methoxamine. Thus, Baile et al (1984) have shown that high levels of positive end-expiratory pressure induced an increase in broncho-pulmonary anastamotic blood flow, and Wagner et al (1987a) have shown that increases in airway pressure not only reduce mucosal blood flow but increase flow into the pulmonary circulation. The same group has further (Wagner et al, 1987b) studied the 'paralysed' bronchial circulation in order to exclude neural- or mediator-induced changes in vessel calibre after lung inflation, and found that blood flow changes occurred irrespective of the presence of the paralysing agent. This work suggests that inflation-induced bronchovascular changes are due to mechanical factors. This may be due to stretching of vessels, with narrowing and lengthening, or to compression of vessels, or to both, as changes in blood flow can occur both with increases in lung volume at constant transpulmonary pressure and increases in transpulmonary pressure at constant lung volume (Modell et al, 1981). Thus the manoeuvres performed in this study may have diverted blood flow away from the mucosa to the pulmonary circulation, but if so it is difficult to see how this diversion of blood flow should be followed by rises in nedocromil sodium in the peripheral circulation unless the drug was simultaneously drawn into the alveolar compartment.

Finally, the results for Cmax are similar to those reported elsewhere (Neale et al, 1987; chapter 3), although the Tmax in this study (8.75 ± 2.059, 10.625 ± 2.203 and 8.75 ± 1.83 min for the 3 study days) is faster than that found in those studies (20 ± 6 and 19 ± 5 min respectively). The most likely explanation for this difference is natural variation.

In conclusion, this study has shown that multiple forced expirations and deep inspiration with a prolonged breath-hold produce a rapid increase in plasma concentrations of nedocromil sodium, a phenomenon which is enhanced by therapeutic concentrations of probenecid. These findings can be best explained by nedocromil sodium being rate-limited in its absorption from the lung, involving both para- and transcellular pathways. It is possible that similar environmental influences such as exercise can occur during daily life, and will therefore influence the rate of absorption of the drug. What is now clearly needed is a careful evaluation of whether such manoeuvres influence the drug's protective efficacy as indicated by at least one study (Schoeffel et al, 1981).

Table 4.1 Subject details and FEV_1 before and after inhaled methoxamine.

Subject	Age	Sex	Weight (kg)	Baseline FEV_1 (% predicted)	FEV_1 with methoxamine	
					Before	After
1	23	M	75	4.6 (105)	4.6	4.85
2	23	F	73	4.3 (110)	4.75	4.75
3	38	M	82	3.87 (106)	4.1	4.05
4	32	M	70	3.92 (102)	4.1	4.0
5	29	M	98	5.55 (110)	5.75	5.85
6	29	M	82	4.51 (101)	4.7	4.75
7	33	M	75	4.2 (94)	4.8	4.7
8	22	M	78	5.15 (110)	5.15	5.35
Mean	28.6		79.1	4.56 (104.8)	4.74	4.78
SD	5.68		8.7	0.58 (5.63)	0.54	0.61
SEM					0.19	0.22

Table 4.2 Inhalation of nedocromil sodium on the 3 study days.

	No treatment	Methoxamine	Probenecid
Breath holding time (s)*	10.83 (0.275)	10.73 (0.152)	10.81 (0.208)
Inspired volume (l)	4.6 (0.168)	4.6 (0.177)	4.51 (0.172)
Peak inspiratory flow (l/min)	50.69 (1.886)	47.69 (1.457)	49.0 (1.960)
Time of actuation (s)	1.49 (0.073)	1.51 (0.047)	1.51 (0.071)
Inspired volume at actuation (l)	0.93 (0.054)	0.92 (0.05)	0.89 (0.036)
Flow rate at actuation (l/min)	41.13 (1.828)	37.81 (1.484)	38.25 (1.567)
Inspired volume at actuation (%)	20.31 (1.024)	20.44 (1.231)	20.06 (0.897)

* - mean (SEM) for 8 subjects.

Table 4.3. Plasma nedocromil sodium pharmacokinetics on the 3 study days.

	No treatment	Methoxamine	Probenecid
AUC whole study (ng.min/ml)	365.1*	387.1	388.4
	51.5-774.1#	165.8-747.6	88.6-1888.7
AUC whole study minus the	355.1	380.8	377.5
increase after 9 FEV_1	49.9-769.1	163.4-752.8	86.3-1794.3
AUC whole study minus the	363.1	382.6	382.9
increase after deep inspiration	49.7-764.4	165.6-740.4	86.7-1865.6
AUC whole study minus the	365.9	385.5	386.2
increase after 1 FEV_1	51.1-774.3	165.5-747.9	89.7-1879.6
Change in AUC after 9 FEV_1	1.74	1.50	2.86
(% of total AUC)	-2.58-3.37	-0.69-3.36	0.73-5.65
Change in AUC after breath-hold	1.3	0.95	1.195
(% of total AUC)	-0.68-4.43	0.12-3.17	0.1-2.19
Change in AUC after 1 FEV_1	0.12	0.235	0.29
(% of total AUC)	-0.35-1.10	-0.05-0.78	-1.22-0.98

Median* and range# for 8 subjects.

Figure 4.1. The figures on the next 2 pages depict plasma nedocromil sodium concentration-time curves for the individual subjects on the first study day. The 3 arrows indicate the times at which the inspiratory manoeuvres were performed. The first arrow (70 min) indicates 9 FEV_1 manoeuvres, the second arrow (110 min) indicates a full inspiration with a 30 second breath-hold, and the third arrow (150 min) indicates a single FEV_1.

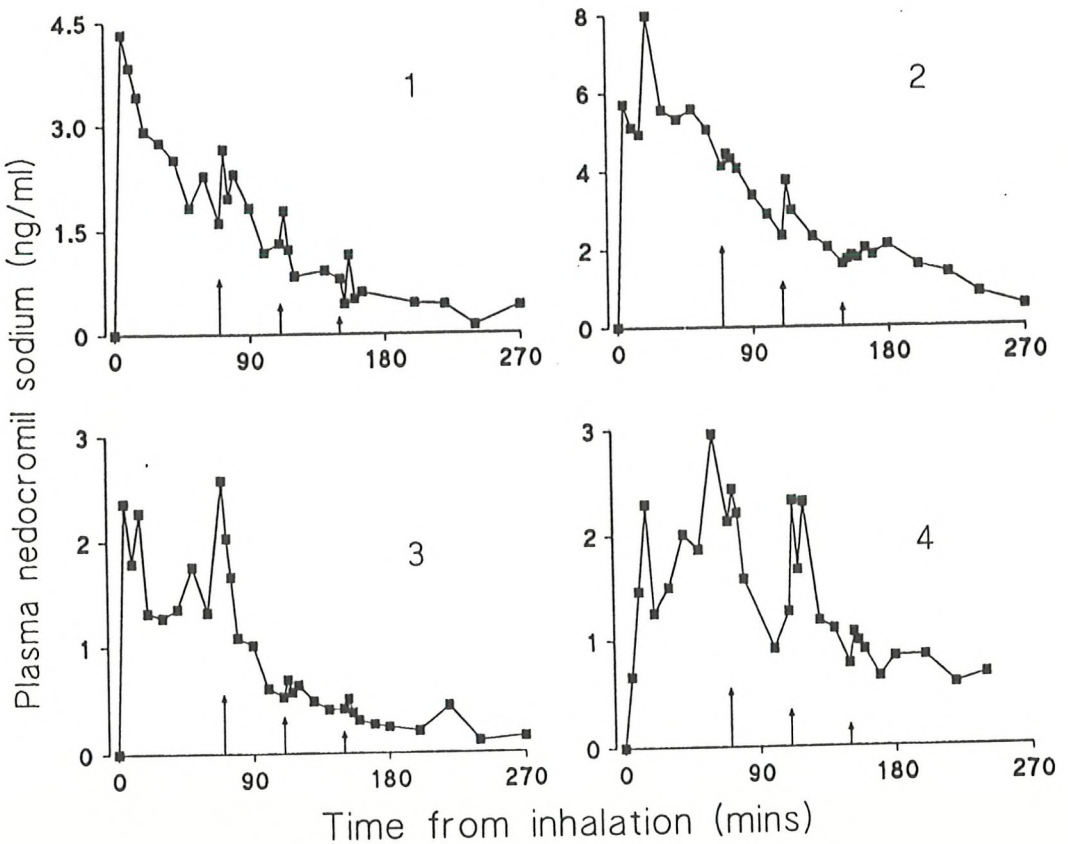
Plasma nedocromil sodium (ng/ml)
1
2
3
4
4.5
3.0
1.5
0
8
6
4
2
0
90
180
270
Time from inhalation (mins)

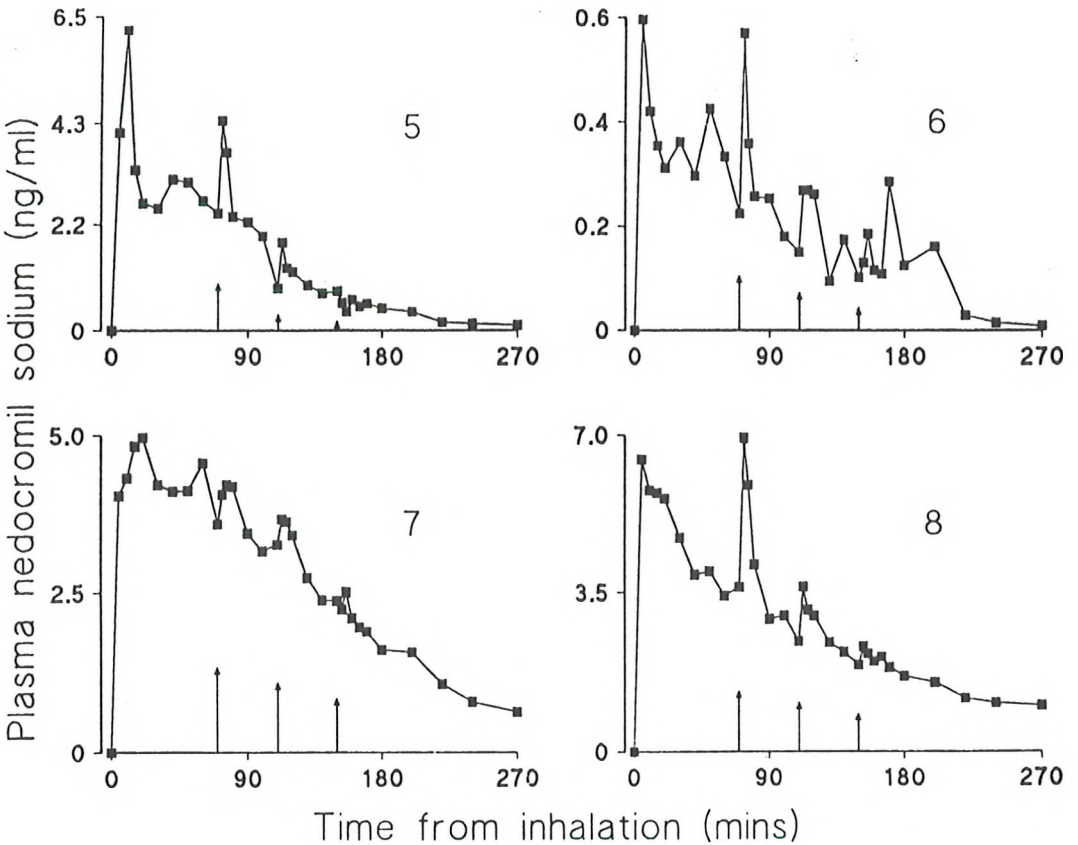
Plasma nedocromil sodium (ng/ml)
6.5
4.3
2.2
0
5
0.6
0.4
0.2
0
6
5.0
2.5
0
7
7.0
3.5
0
8
0
90
180
270
Time from inhalation (mins)

Chapter 5. The preparation of a radio-labelled aerosol of nedocromil sodium for administration by metered dose inhaler.

5.1 Introduction.

To obtain information on the sites of deposition of inhaled drugs used to treat diseases of the airways, non-invasive methods have been developed involving radionuclide imaging. For this technique to provide useful information, it is essential that any gamma-emitting radionuclide added to an aerosol is deposited within the lung at the same sites as the drug. In an attempt to circumvent the difficulties associated with radiolabelling drugs, others have employed radiolabelled inert particles which are substituted for the active drug. The most suitable radionuclide for this purpose is technetium-99m (Tc^{99m}) since it has a half-life of 6 h, and an acceptable emission energy for gamma-camera imaging. This nuclide has been used to label Teflon particles which were added to a metered dose inhaler in order to assess pulmonary deposition following inhalation (Newman et al, 1981b), and has also been incorporated in the solvent of metered dose inhalers containing $ß_2$-adrenoceptor agonists to study the intrapulmonary distribution of the gases and particles delivered by metered dose inhaler (Dolovich et al, 1981b). Use of labelled Teflon particles and solvents provides information regarding the site of aerosol delivery in the lung, but the physical and chemical properties of these systems are almost certainly different from those containing active drugs, making it inappropriate to draw conclusions regarding the intrapulmonary distribution of inhaled drugs.

Recently, 2 methods of labelling bronchoactive drugs for delivery by metered dose inhaler have been developed. Vidgren and co-workers (1987) have described a method in which a solution of sodium cromoglycate and Tc^{99m} is spray-dried prior to its incorporation into a metered dose inhaler canister containing sorbitan trioleate as a surfactant, and a chlorofluorocarbon propellant gas. Using this labelled aerosol, approximately 10% of the dose delivered from the metered dose inhaler was deposited in the lung, a value similar to that reported previously (Newman et al, 1981b; Dolovich et al, 1981b). In a second method, Köhler and colleagues (1988) have described a procedure to label the particles of the $ß_2$-agonist, fenoterol, generated by a metered dose inhaler. The method involves transferring Tc^{99m} from an aqueous solution into ethyl methyl ketone, followed by evaporation of the solvent to dryness. Surfactant and propellant gases were added to the dry radioactive container, and after stirring to reduce the volume, the resultant radioactive mixture was transferred to a metered dose

inhaler canister through a hole made in its base, which was subsequently sealed.

In this study, a comparison of Köhler's labelling technique is made with a technique modified from one described by Newman and colleagues (1989a) to prepare a radiolabelled aerosol suitable for studying the deposition characteristics of 2 aerosol formulations of nedocromil sodium. In assessing the 2 procedures particular attention was focussed on the particle size distribution of both formulations before and after the labelling procedure.

5.2 Methods.

The study was designed to compare the particle size distribution of 2 formulations of nedocromil sodium, and to compare these aerosols before and after the addition of Tc^{99m} using two different methods. The formulations of nedocromil sodium contained drug powders of differing particle sizes. The MMAD of the powders, as measured by centrifugal sedimentation (Joyce Loebl Disc Centrifuge) was 2 μm ("fine") and 8 μm ("coarse"), with a GSD of 2 and 2.7 respectively. Consistency of particle size was ensured by using 1 batch of each material for particle manufacture. Both were prepared for administration from metered dose inhalers by adding surfactant and a mixture of chlorofluorocarbons. These agents were placed in a standard aluminium canister which was sealed by crimping a 100 μl metering valve on to the open end thereby forming the metered dose inhaler. The metered dose inhalers each contained 112 doses of nedocromil sodium with each actuation intended to deliver 2 mg of the active drug. In order to limit the radioactivity needed in the labelling procedure, prior to their use in the study, the canisters were fired repeatedly so that, when determined gravimetrically, approximately 30 metered doses remained.

Two methods for radio-labelling the contents of the metered dose inhalers with Tc^{99m} were assessed. The first method (method 1) was adapted from that of Köhler et al (1988). Five to 10 ml of Tc^{99m} was eluted from a commercial technetium generator (Amersham, Aylesbury, UK), and shaken with the same volume of ethyl methyl ketone. The 2 phases were allowed to separate, the supernatant removed and the process repeated on 2 further occasions. This resulted in approximately 90% of the initial Tc^{99m} partitioning into the solvent, which was then slowly evaporated to dryness at 130°C in a siliconised glass container over which a steady stream of nitrogen was blown. After cooling, 10 ml Freon 11 and 10 μl surfactant (sorbitan trioleate) were added and the mixture stirred until its volume had reduced to 0.5 ml. The residual liquid was

aspirated into a pre-cooled syringe, and transferred to a canister containing 1 of the 2 formulations of nedocromil sodium which had been pre-cooled in a mixture of dry ice and propan-2-ol. The liquid was introduced into the canister through a perforation in its base and was sealed with a latex ring and self-tapping screw. After protecting the valve assembly, the canister was immersed in a water bath to assess the patency of the seal and shaken vigorously. On a further occasion, the same procedure was undertaken in the absence of adding surfactant to assess the effect on subsequent particle size distribution.

The second method (method 2) involved drying the Tc^{99m} directly onto the wall of the canister prior to adding the drug formulation and the other metered dose inhaler constituents. Ethyl methyl ketone containing Tc^{99m} was transferred to an empty metered dose inhaler canister, and evaporated at room temperature to dryness in a stream of nitrogen. After cooling in a dry ice/propan-2-ol mixture a second canister containing 1 of the 2 drug formulations had its valve assembly removed, and the liquid contents transferred immediately into the canister containing the internal coating of Tc^{99m}. A new valve assembly unit was attached to the canister by use of a crimping tool. The patency of the seal was assessed by immersion in a water bath. The canisters were then agitated for 5 min in an ultrasonic water bath to fully disperse the drug and label. This procedure was not done on 1 occasion to assess the effect of sonication on the resultant aerosol.

The initial activity of Tc^{99m} eluted from the technetium generator was measured by γ-counting in a radio-isotope calibrator (CRC-10, Delariese Enterprises, Reading, Berks, UK). Once prepared, the activity incorporated into the metered dose inhaler was measured by counting in a radio-isotope calibrator.

5.3 Protocol.

After the labelling techniques were evaluated fully, the 2 procedures were compared. Prior to the addition of Tc^{99m}, the particle size distribution of each formulation of nedocromil sodium aerosol was assessed using the multi-stage liquid impinger. Following the labelling procedure, the radioactive canister was fired into the multi-stage liquid impinger, and the impinger subjected to γ-emission imaging using a Siemens large-field-of-view gamma-camera and a parallel, high resolution, low energy collimator (International General Electric Company, New York). The multi-stage liquid impinger was imaged before and after rotation through 180°. In addition, the throat, filter and

metered dose inhaler adaptor were imaged to determine the fraction of the total activity delivered to each site. The results were stored on a computer (Vax 11/730, Digital Equipment Corp, Massachusetts, USA). On retrieving the data, regions of interest were drawn around each part of the multi-stage liquid impinger and metered dose inhaler adaptor to allow calculation of the proportions of activity at each site. For each of the stages of the multi-stage liquid impinger, because attenuation of γ-emission measured in this manner is exponential (Fleming, 1979), the geometric mean of two readings at 180° was taken to represent the value of γ-emission except for stage 4, where the highest reading obtained was used to compensate for attenuation of radiation by the glass of the multi-stage liquid impinger. The multi-stage liquid impinger was stored for 4 days until the γ-emmission of the Tc^{99m} activity had decayed completely, following which the concentration of nedocromil sodium collected at each site was measured.

5.4 Analyses of Results.

Data relating the amount of nedocromil sodium deposited on each stage of the multi-stage liquid impinger before and after each of the radiolabelling procedures and the relationship between the distribution of drug and label was obtained. The amount of nedocromil sodium and Tc^{99m} measured on each stage of the multi-stage liquid impinger was expressed as the cumulative percentage undersize by weight, and was plotted against the known aerodynamic "cut-off" diameters of each stage on logarithmic-probability paper to allow derivation of the MMAD, the GSD, and the percentage of particles less than 10 and 4 μm in diameter (P_{10} and P_4 respectively).

The yield of Tc^{99m} at the end of each labelling procedure was calculated as the amount of γ-emitting radioactivity within the metered dose inhaler expressed as a percentage of the initial activity used. The variability of each procedure was expressed as the coefficient of variation (CV). The mean dose of nedocromil sodium delivered by each actuation was measured before and after each labelling procedure, and the results compared by Student's paired t-test. The differences in P_{10} and P_4 before and after labelling were compared by the Mann-Whitney U test.

5.5 Results.

The two methods of labelling the nedocromil sodium aerosols differed widely in the efficiency and variability of the labelling procedure. Using method 1, only 28.45% of the initial Tc^{99m} label was incorporated into the metered dose inhaler with marked

variability between individual procedures (CV 38.5%, n = 15). Method 2 provided a more efficient final yield of label (mean 62.05%) with substantially less variability (CV 14.68%, n = 8) (tables 5.1, 5.2).

Prior to labelling with method 1 the mean (SEM) yield of nedocromil sodium per actuation was 1.84 (0.087) mg, which was not significantly different to that after labelling, 1.589 (0.043) mg ($p = 0.064$). Before labelling with method 2, the mean amount of drug delivered per actuation was 1.892 (0.071) mg, which was not significantly different to that after labelling, 2.153 (0.196) mg ($p = 0.095$) (table 5.3).

Figures 5.1 and 5.2 show the particle size distribution for a single aerosol of the fine nedocromil sodium formulation before and after labelling by the two methods described. Figures 5.3 and 5.4 show a similar plot for the coarse formulation. By using the labelling procedure of method 1, a close association of the radiolabel with the drug was observed for both preparations of nedocromil sodium, but the size distribution of the particles was displaced to the left indicating a coarser aerosol. Before labelling, the MMAD of the fine nedocromil sodium preparation was 16.5 μm, GSD 5.32. However, after labelling it was not possible to determine the MMAD because < 50% of the aerosol entered the impinger. The P_{10} and P_4 values for this single aerosol was 44% and 24% respectively, and after labelling 28% and 9%.

Method 2 also produced an aerosol in which the radiolabel travelled closely with the drug. However, in contrast to method 1, this method produced an aerosol with physical characteristics that varied little from that of the unlabelled drug preparations. Figs 5.2 and 5.4 show that the particle size distribution of this aerosol for both nedocromil sodium preparations was virtually unchanged by the labelling procedure. Thus, P_{10} and P_4 values for the unlabelled fine aerosol were 36% and 17%, and for the labelled aerosol 32% and 14%, while for the coarse formulation the decrease in P_{10} was 4% and for P_4 was 0.8%.

For the whole group of aerosols, the mean decrease of P_{10} after labelling with method 1 was 8.54% (n = 5), and after labelling with method 2 was 5.2% (n = 5), which are not significantly different ($p < 0.075$). The mean decrease of P_4 after labelling with method 1 was 6.8%, and 2.44% after method 2, which are not significantly different ($p < 0.055$) (table 5.4).

The effect of using method 1 to label the fine nedocromil sodium formulation without adding surfactant is shown in fig 5.5. The resultant size distribution was shifted to the left indicating a coarser aerosol than was observed before adding the label, however the change was not great in that P_{10} was decreased by only 6%, and the P_4 by 6.5%. The effect of ultrasonic dispersion on the particle size characteristics is depicted in fig 5.6. This procedure maintained the size distribution characteristics of the nonlabelled aerosol (P_{10} decreased by 3.5%, P_4 by 1%). Without the procedure the aerosol was coarser as shown by P_{10} decreasing by 10% and P_4 by 5%.

5.6 Discussion.

This study has shown that the two methods of adding radiolabel to metered-dose inhalers containing nedocromil sodium are effective in that an aerosol is produced in which the radioactive marker is closely associated with the drug, and that these methods can be used for aerosols of different particle size. The method that was developed in Southampton conserves the particle size distribution of the original aerosol (method 2), whereas the method described by Köhler et al displaced the particle size distribution to the left, resulting in a coarser aerosol. The change of particle size distribution produced by adding the radiolabel in method 1 just failed to reach statistical significance when compared to the change produced by method 2 for the percentage of particles $< 4\mu m$ diameter, and was not significantly different for particles $< 10\ \mu m$ diameter. This suggests that after labelling with method 1 less aerosol is likely to be available for penetration to the lung periphery although the amount of aerosol deposited in the lung may be unaltered. Employing method 2 to label the aerosol had negligable effect in changing the particle size distribution of the unlabelled drug. However, although the decrease in P_{10} and P_4 after labelling with method 1 did not achieve statistical significance, reference to figures 5.1 and 5.3 shows that this change is appreciable, and it is therefore not possible to exclude a reduction of total lung deposition, and peripheral lung penetration.

Once labelled, these aerosols may subsequently be used to assess drug delivery in the lung with nuclear imaging techniques as Köhler and colleagues (1988) have described. However, since Köhler's method changes the particle size distribution of the aerosol, it is clear that it is not suitable for its intended application. The reason(s) for the change of particle size distribution is not clear, although it appears that the use of Freon 11 may be implicated as the change occurred whether or not surfactant was used in the labelling procedure. Moreover, this method of labelling has an unacceptably low yield

and high variability. The method requires a number of passages of the radioactive marker from one container to another before being transferred to the metered dose inhaler. The high number of manipulations probably contribute to the variable and low yield, together with the propensity of technetium to adhere to surfaces, irrespective of whether the surfaces are silicon-treated or glass substituted for by polycarbonate vessels. It was also found that the use of heat to evaporate the solvent often left a solid residue after the solvent had evaporated, and the solid residue was subsequently difficult to dissolve after the addition of chlorofluorocarbon and surfactant. The appearance of the solid residue was a variable phenomenon, and seemed to be related to the heating process, as it was less prominent when nitrogen gas was used in conjunction with heat. A further problem with this method was the difficulty experienced in obtaining a perfect seal with the self-tapping screw and latex O-ring. The potential risk of leakage occurring and the high number of manipulations both increase the radiation hazard of the procedure.

The alternative method of adding label to the metered dose inhaler does not alter the particle size distribution of the resultant aerosol, so that any investigation of pulmonary deposition after its inhalation could be attributed to the original aerosol. Moreover, this method produces a much higher yield and had less variation than that described by Köhler et al, thought to be due to the minimal use of glassware and fewer passages of radioactive material. In addition, the use of a crimping tool was a more secure way of sealing the canister. The importance of ultrasonic agitation is demonstrated by the preservation of the aerosol particle size distribution after labelling, and the production of a coarser aerosol if the labelled nedocromil sodium is not subjected to ultrasonic agitation. It is important to note that in these procedures, the nedocromil sodium itself has not been radiolabelled, but the radioactive marker travels with the drug in such a way that an image of its distribution can be assumed to represent the distribution of drug.

There are several methods available for particle size measurement of aerosols, and include direct microscopy (Hallworth & Hamilton, 1976), light scattering (Allen et al, 1979) and laser holography (Swithenbank et al, 1977). The advantages of using inertial impaction are that the other methods are time consuming, expensive and are unable to distinguish drug particles from foreign or excipient particles. However, most importantly, they are unable to assess the effects of oropharyngeal deposition (Yu et al, 1984; Hallworth & Andrews, 1976; Hallworth & Westmorland, 1987). Unlike the

other sizing methods, the multi-stage liquid impinger is able to assess the whole of an emitted aerosol cloud and therefore allows information to be obtained on the total delivered dose, which can be used to predict pulmonary deposition. A further advantage of the inertial impaction method is that it is able to assess the aerosol cloud as a dynamic entity, whereas the other methods of sizing are more appropriate for more static aerosols, such as those produced by nebulisation. Thus, an aerosol that is produced from a pressurised canister has been reported to have a MMAD of 36 μm at the actuator, reducing with distance from the adaptor to 12 μm at 10 cm, with only marginal reduction in size at a distance of 25 cm (Morén & Anderssen, 1980). This size change is due to evaporation of the propellants.

The aerosols have been described in terms of their particle size distribution because of this dynamic behaviour. To characterise the aerosol solely in terms of its MMAD and GSD would be misleading, as it implies a static aerosol. Furthermore, it was not always possible to derive the MMAD if less than 50% of the aerosol was deposited in the impinger. The MMAD may be derived by extrapolation if the particle size distribution of the aerosol is log-normally distributed, in which case it will be represented by a straight line on the graph, but if the particle size distribution is non-linear, it is not possible to extrapolate in this manner.

The MMAD obtained for the fine nedocromil sodium aerosol (16.5 μm) is considerably larger than the description of the MMAD of similar pressurised aerosols of different drugs reported in the literature. This is partly due to the different drug formulations measured, but it is considered that the predominant reason for this difference is due to the way in which the aerosols were sized. In all of the studies discussed below, the propellants were allowed to evaporate partially or wholly before particle size analysis. The method of particle size analysis utilised in this study yields information that is more clinically relevant than the sizing methods used in the studies to be discussed.

Bouchiki and co-workers (1988) have assessed a number of different metered dose inhalers by measuring particle size using an aerodynamic particle sizer and firing the aerosol into a 5 l glass cylinder from which it was drawn into the apparatus. They found MMAD's ranging from 2.3 to 8.3 μm, a result quite different to the findings of this study. A further reason for this difference is because the method used for calibration may have lead to an underestimation of particle size (Griffiths et al, 1986). Most of the other published studies of particle size distribution of aerosols delivered

from pressurised canisters were carried out in this manner, and therefore their results do not predict the behaviour of these aerosols when used in life (Kim et al, 1985; Hiller et al, 1978, 1980 a & b, 1983; Dolovich et al, 1981b; Polli et al, 1969; Hallworth & Andrews, 1976). A further problem with many of these studies is the use of the single-particle, aerodynamic relaxation time (SPART) analyzer, which is most accurate in the size range 0.3 μm to 6 μm, and can only measure particles up to 10 μm (Hiller et al, 1980 a & b; 1978; 1983). All of these studies reported MMAD's no greater than 4.3 μm with the exception of Polli et al (1969), who reported a figure of up to 5.6 μm for drug particles (i.e. particles measured after the propellant had evaporated completely), and 9.0 μm for aerosol particles, although their aerosols were also fired into a glass chamber before sizing. These authors also observed a direct relationship between drug and aerosol particle size.

Other authors have used inertial impaction techniques to obtain an estimate of the deposition characteristics for inhaled aerosols (Kirk, 1972; Meakin & Stroud, 1983; Padfield et al, 1983; Hallworth & Westmoreland, 1987). In these studies an impactor system was used to simulate drug deposition in the lung. Thus, if the impactor system showed that a larger amount of one drug formulation was able to penetrate further than a different formulation of the same drug, the clinical efficacy of the formulation penetrating further was found to be greater as assessed by changes in lung function after inhalation.

Studies of drug deposition in the lung have shown that only 10% of an aerosol inhaled from a pressurised metered-dose device passes the larynx (Newman et al, 1981b; Vidgren et al, 1987; Spiro et al, 1984). However, the lung models proposed by Heyder et al (1986) predict that a far greater percentage of the aerosol would be deposited in the lung if the MMAD was in the order of 4.3 μm. Approximately 30% of aerosol nedocromil sodium had an aerodynamic diameter of less than 10 μm, and only particles smaller than this would be expected to enter the lung. Moreover, to draw the aerosol into the multi-stage liquid impinger a flow rate of 60 l/min was used, while the inspiratory flow rate used by Newman et al (1981b) varied from this figure up to 120 l/min. Higher inspiratory flows would be expected to decrease aerosol deposition in the peripheral lung region due to more inertial impaction in the mouth. In the study reported by Vidgren et al (1987), lower inspiratory flow rates of 55-70 l/min were used. Similar preparations delivered by pressurised metered dose inhaler would be unlikely to have a significantly different size distribution as the propellant gases are the major

determinants of size distribution when the aerosol is sampled in this way. However, it is possible that by using different propellant gases or by altering other physical properties of the inhalers, a finer aerosol could be achieved (Morén, 1978; Newman et al, 1982a).

In conclusion, two methods for radiolabelling two galenic formulations of nedocromil sodium have been described. Of the two methods, one, originally described by Köhler et al (1988), was shown to alter the particle size characteristics of the aerosol such that it was coarser than before labelling, and therefore its behaviour would no longer be expected to represent that of the unlabelled drug. By contrast, the method developed here does not change the particle size distribution of the aerosol, enabling studies of pulmonary deposition to be performed. In addition, the MMAD of the aerosol particles of fine nedocromil sodium is much greater than commonly quoted for metered dose aerosols of this type, and the larger MMAD provides a more accurate estimate of lung deposition. It is anticipated that this method of aerosol labelling could be applied to any drug formulation delivered from pressurised metered dose inhaler. However, for any drug delivered by metered dose inhaler for which particle size and lung deposition characteristics are required it is desirable to measure the particle size distribution before and after any manipulation to ensure that it has not been altered.

Figure 5.1 (top panel overleaf). The particle size distribution of fine nedocromil sodium before (○) and after (●) the addition of Tc^{99m} (◇) (Method 1 - Köhler et al, 1988).

Figure 5.2 (lower panel overleaf). The particle size distribution of fine nedocromil sodium before (○) and after (●) the addition of Tc^{99m} (◇) (Method 2).

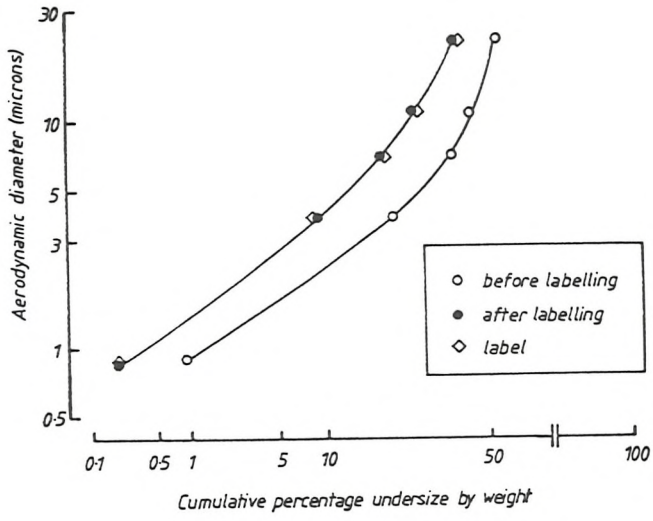
Aerodynamic diameter (microns)
30
10
5
3
1
0·5
0·1
0·5
1
5
10
50
100
Cumulative percentage undersize by weight
before labelling
after labelling
label

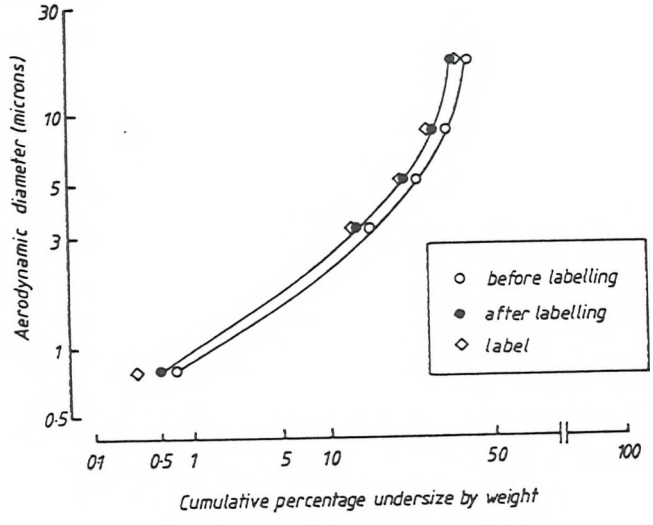
Aerodynamic diameter (microns)
30
10
5
3
1
0·5
01
0·5
1
5
10
50
100
Cumulative percentage undersize by weight
before labelling
after labelling
label

Figure 5.3 (top panel overleaf). The particle size distribution of coarse nedocromil sodium before (○) and after (●) the addition of Tc^{99m} (◇) (Method 1 - Köhler et al, 1988).

Figure 5.4 (lower panel overleaf). The particle size distribution of coarse nedocromil sodium before (○) and after (●) the addition of Tc^{99m} (◇) (Method 2).

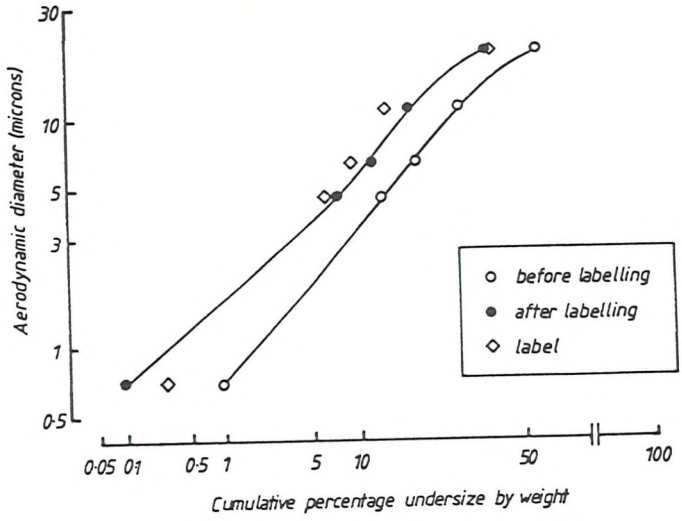
30
10
5
3
1
0·5
Aerodynamic diameter (microns)
before labelling
after labelling
label
0·05 0·1 0·5 1 5 10 50 100
Cumulative percentage undersize by weight

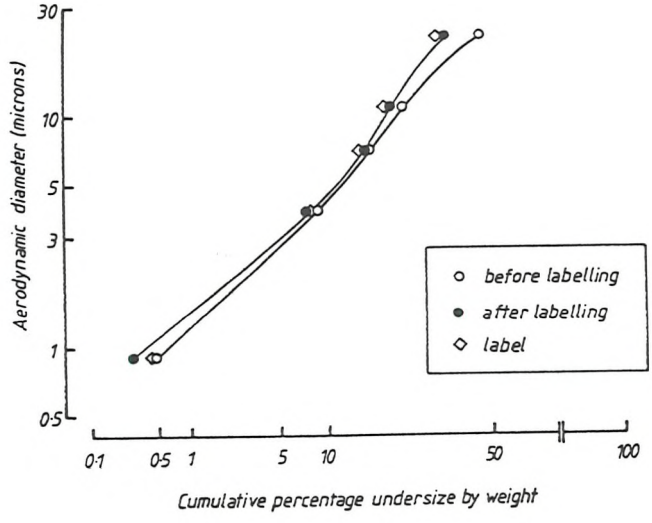
30
10
5
3
1
0·5
Aerodynamic diameter (microns)
before labelling
after labelling
label
0·1 0·5 1 5 10 50 100
Cumulative percentage undersize by weight

Figure 5.5 (top panel overleaf). The particle size distribution of fine nedocromil sodium before (○) and after (●) the addition of Tc^{99m} (Method 1 - Köhler et al, 1988). No surfactant was used in this procedure.

Figure 5.6 (lower panel overleaf). The effect of ultrasonic agitation on the particle size distribution of fine nedocromil sodium before (solid lines) and after (dashed lines) the addition of Tc^{99m} (Method 2). ● - with sonication; ○ - no sonication.

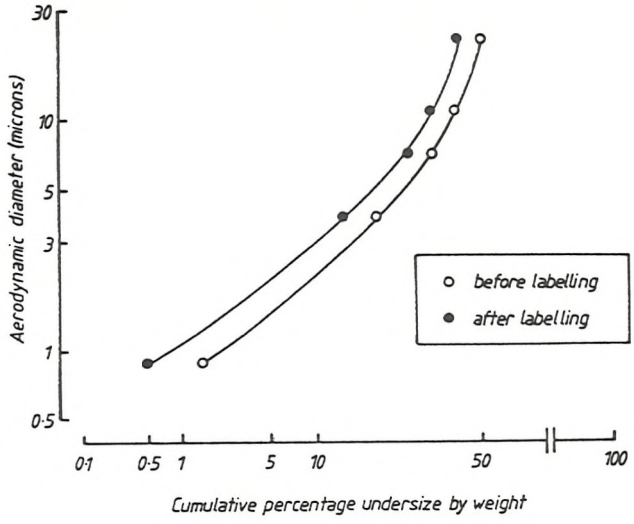
30
10
5
3
1
0·5
Aerodynamic diameter (microns)
0·1
0·5
1
5
10
50
100
Cumulative percentage undersize by weight
before labelling
after labelling

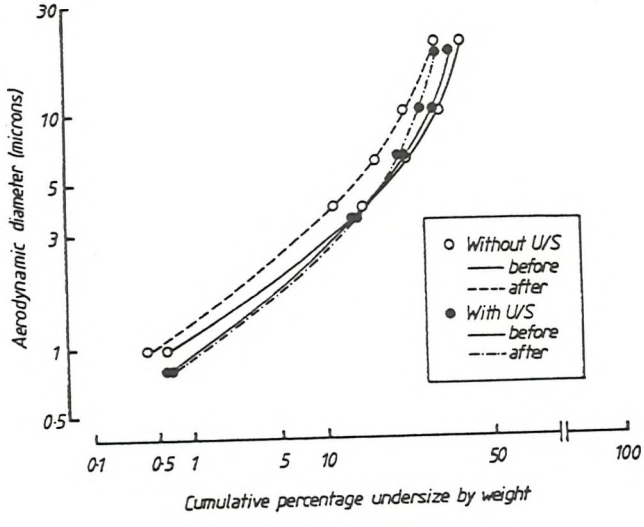
30
10
5
3
1
0·5
Aerodynamic diameter (microns)
0·1
0·5
1
5
10
50
100
Cumulative percentage undersize by weight
Without U/S
before
after
With U/S
before
after

Table 5.1: Yield and variability of labelling method 1.

Run	Initial activity (MBq)	Activity within inhaler (MBq)	% yield
1	164.5	15	9.1
2	300	44	14.7
3	228	78	34.2
4	816	280	34.3
5	711	320	45.0
6	968	250	25.8
7	880	160	18.2
8	937	377	40.2
9	715	222	31.0
10	1450	533	36.7
11	1645	554	33.7
12	1726	720	41.7
13	1240	351	28.3
14	853	146	17.1
15	896	203	22.6
Mean			28.84
SD			10.668
CV			36.99

Table 5.2: Yield and variability of labelling method 2.

Run	Initial activity (MBq)	Activity within inhaler (MBq)	% Yield
1	960	417	43.4
2	558	385	68.9
3	460	280	60.9
4	450	320	71.1
5	455	317	69.7
6	351	215	61.3
7	280	157	56.1
8	1180	767	65
Mean			62.05
SD			9.112
CV			14.684

Table 5.3: Nedocromil sodium dose delivered (mg) before and after labelling.

	Method 1		Method 2	
	Before	After	Before	After
	1.763	1.489	1.773	2.077
	1.557	1.582	1.762	1.890
	1.658	1.765	1.777	1.696
	1.957	1.475	2.182	3.060
	2.000	1.620	1.833	1.965
	2.105	1.602	2.025	2.233
Mean	1.840	1.589	1.892	2.153
SD	0.214	0.105	0.173	0.479
SEM	0.087	0.043	0.071	0.196

Table 5.4: Change in percentage of particles less than 10 μm (P_{10}) and less than 4 μm (P_4) in diameter produced by the two labelling methods.

	P_{10}		P_4	
	Method 1	Method 2	Method 1	Method 2
	16	5	17	3.5
	6.1	3	4.5	2.4
	5.9	11	2	4
	6.7	4	4	1.5
	8	3	6.5	0.8
Mean	8.54	5.2	6.8	2.44
Median	6.7	4	4.5	2.44
SD	4.25	3.347	5.922	1.335
SEM	1.90	1.497	2.649	0.597

Chapter 6. Pulmonary deposition of two aerosols of nedocromil sodium delivered by MDI assessed by single photon emission computed tomography and computed axial tomography.

6.1 Introduction.

Once inhaled, the distribution of radioaerosols within the lungs has conventionally been assessed using two-dimensional (2D) gamma scintigraphy to obtain planar views of the chest. Regions of interest can be drawn to represent separate areas that contain predominantly large, conducting airways ('central' zone) or alveoli ('peripheral' zone), and a value can then be derived to represent the ratio of counts in the two zones. This is termed the penetration index, and does not take into account the volume of the lung in which the aerosol is contained, but reflects the count density in the regions of interest. It is not possible to assess the dose of an aerosol delivered to discrete areas of the lungs from such measurements. Moreover, because of the three-dimensional (3D) structure of the lung, the central zones invariably contain both large airways and alveoli, thus reducing the accuracy of such measurements. A further inherent disadvantage of this technique is that it fails to make full use of all the acquired data. Logus and colleagues (1984) have described a 3D technique for the acquisition of more detailed information using single photon emission computed tomography (SPECT), and more recently Phipps et al (1990) have shown that SPECT is a better discriminator than planar gamma scintigraphy for demonstrating differences in radioaerosol deposition in central and peripheral lung regions.

In this study, SPECT was used to assess the deposition of radiolabelled nedocromil sodium delivered by MDI. Inhalation was standardised by use of a controlled inspiratory technique. The deposition of two different particle size formulations of the drug was studied to assess the sensitivity of the imaging system, and to investigate whether the pharmacokinetics of both the drug and the radioisotope correlate with the site of drug deposition. In the process, some novel methods of lung image processing and analysis were developed, the results of which are presented here.

6.2 Methods.

6.2.1 Subjects.

Ten healthy male subjects, mean age (SD) 26.8 (4.7) yr, were recruited. All subjects had normal baseline pulmonary function (FEV_1 101.8% (5.9%) of predicted), were non-smokers, had no past history of respiratory disease, and had had no clinically

significant illness within the 6 weeks prior to the study.

6.2.2 Preparation of radiolabelled nedocromil sodium.

The labelling method is described in chapter 5.1. The amount of Tc^{99m} incorporated into the MDI was determined by counting the activity eluted from the Tc^{99m} generator in a radioisotope calibrator (CRC-10, Delariese Enterprises, Reading, Berks, UK), and then counting the MDI after the labelling procedure.

6.2.3 Inhalation technique.

Subjects inhaled 2 breaths of radioaerosol (chapter 2.3). Each actuation of the nedocromil sodium MDI was intended to deliver approximately 200 MBq of Tc^{99m} along with 2.0 mg of drug. After each inhalation, subjects exhaled into a filter (Heat and Moisture Exchanging filter, no BB50T, Pall Biomedical Ltd, Portsmouth, UK) to collect any expired radioactivity. After the two inhalations, subjects twice rinsed the oropharynx with 50 ml of water, collected the mouthwashes and then drank 100 ml of water to flush the oesophagus. Radioaerosol inhalation was carried out with either the fine or coarse aerosol on 2 separate occasions on a double-blind randomised basis. The study days were separated by at least 1 week.

The amount of radioactivity delivered by the two actuations was determined by re-counting the MDI in the radioisotope calibrator. To assess dose repeatability, on each occasion 2 test shots were fired into a filter attached to a vacuum pump, and the MDI re-counted in the radioisotope calibrator.

6.2.4 Acquisition of images.

6.2.4.1 Gamma scintigraphy and computerised tomographic imaging.

Immediately after inhalation of the aerosols, planar views of the oropharynx, thorax and stomach were obtained, followed by the SPECT study (chapter 2.7). The planar views of the oropharynx, thorax and stomach were repeated after the SPECT procedure. Separate images were then obtained for the mouthwashes, the expiratory filter, the MDI adaptor, a Tc^{99m} standard of known activity and the MDI adaptor and filter used to collect the test shots. Such images allowed an assessment of the delivered activity to be made. Computed tomographic images were acquired on one further occasion (chapter 2.7.2).

6.2.5 Blood sampling and drug analysis.

Blood sampling and plasma nedocromil sodium radioimmunoassay were described in chapter 2.5.1 & 2.5.2. The blood samples were stored and the radioimmunoassay done after allowing 4 days for γ-emission from the Tc^{99m} to decay. 1 ml of plasma from each sample was used to determine the time course of Tc^{99m} absorption by γ-counting. After inhaling the radiolabelled aerosol, blood samples were taken at 2.5, 5, 7.5, 10, 15, 30, 45, 60, 90, 120, 180, 240, 300 and 360 min.

6.3 Data treatment.

6.3.1 Aerosol labelling and inspiration of aerosols.

The efficiency of the labelling procedure was expressed as the percentage of the initial radioactivity eluted from the Tc^{99m} generator that was incorporated into the MDI canister, and the mean efficiency was compared between the two formulations. The variability of each labelling process was expressed as the coefficient of variation. To assess the repeatability of the aerosol dose, the mean activity delivered to the subjects and as test shots, both determined from the radioisotope calibrator data, were compared. In order to ensure the aerosols were inhaled in similar fashion, the following inspiratory parameters were compared for both formulations: BHT, PF, TF, FF and VF%.

6.3.2 Derivation and analyses of the planar and SPECT images.

The images obtained by the γ-camera were displayed on-screen. The anterior and posterior images were combined to yield geometric mean planar views, enabling each lung, the central thoracic regions (trachea, upper oesophagus and larynx) and the stomach to be outlined. The activity within each region of interest was first corrected back to the time of inhalation to allow for radioactive decay using the formula:

$$N_t = N_0 \, e^{-0.693 \, t/T}$$

where N_t is the measured activity, N_0 is the initial activity, t is the elapsed time between N_0 and N_t in hours, and T is the half-life of the isotope (Goodwin & Rao, 1977). To correct for attenuation of γ-rays, mean attenuation thicknesses (Fleming 1979a) were defined for the lung, stomach and oropharynx from an anatomical atlas and scaled according to the actual size of the subject. These, together with a practical value of attenuation coefficient, were used to correct the geometric mean count from the chest, stomach and oropharynx respectively (Fleming 1979b). After dividing these

counts by the counting efficiency of the gamma camera, which was determined from the count rate of the known standard, a figure for the γ-emission activity at each site in MBq was derived. The scanned images of the mouthwashes, expiratory filter and MDI adaptor were treated in a similar manner.

Thus, for each subject, the γ-emission at each site could be assessed, and a figure derived for the total activity delivered by the MDI. To assess the accuracy of this estimate, the total activity was compared with that measured by the radioisotope calibrator. The γ-activity deposited in the lungs, on the expiratory filter, the gastro-intestinal tract (representing the sum of activities in the mouthwashes, oropharynx and stomach) and that remaining on the adaptor was expressed as a percentage of the delivered dose, and compared between the fine and coarse formulations.

By dividing the total delivered activity by the delivered dose of nedocromil sodium (4 mg), it was possible to derive an index representing specific activity of the drug, and, therefore, to assess the amount of drug deposited both in the chest as a whole and in the right lung. The mean specific activity in the whole chest and in the right lung were compared for the two aerosols.

The CT images were modified to represent an attenuation coefficient map of the various tissues (Fleming, 1989). The SPECT images were reconstructed employing an iterative convolution back-projection algorithm incorporating scatter and attenuation correction using the attenuation map derived from the CT images (Fleming, 1989). Coronal and transverse slices of the thorax were then constructed from the corrected SPECT data. Anatomical boundaries of the intrathoracic structures were identified from the CT data after correct alignment of the respective scans.

The SPECT images were manipulated to isolate the whole right lung. The count rates were converted to activity using the measured planar sensitivity of the gamma camera and a previously determined calibration factor relating planar count sensitivity to SPECT image sensitivity for the reconstruction algorithm (Fleming, 1989). These data were corrected back to the time of inhalation to give the total activity in MBq in the right lung, from which specific drug activity could be calculated and compared for each formulation. The specific activity in the right lung derived from the planar scans was compared with that from the SPECT images.

Five transverse SPECT slices, taken from the level of the tracheal bifurcation extending down one-quarter of the lung height (i.e. from a point where the lungs had their greatest width), were summed, as were the same number of coronal slices taken from the point of greatest lung height. The lung boundary was outlined on these summed images, and regions of interest drawn to delineate 'central' and 'peripheral' regions. Using the dimensions described by Phipps et al (1989), the central region was defined as a box drawn along the medial edge of the right lung, centred on a point mid-way along the medial edge, and having the dimensions of half the lung height and half the lung width and the peripheral region defined by a line starting from a point mid-way on the medial border of the right lung, and describing a strip equal to one-third of the lung height inside the outer lung boundary. Only the right lung was used for this analysis because of possible corruption of data in the left lung by scatter of radiation from the stomach.

The activities in the delineated regions were then determined to produce a ratio of central to peripheral counts, the C/P ratio or penetration index (PI). For the different aerosols the PI in both coronal and transverse planes could be compared. By transferring the regions of interest onto the planar images, differences between the PI derived from the different scans could be compared by Wilcoxon's matched-pairs signed rank test.

6.3.3 Correction for pulmonary intravascular Tc^{99m}.

It was expected that some of the inhaled radioactivity would be absorbed into the circulation during the course of the SPECT imaging, and that this absorbed activity might contribute to the measured lung activity. To assess this, an estimate of the ratio of the volume of blood contained within a unit volume of the lung to the volume of blood contained within a unit volume of the heart was made in two patients undergoing cardiac function studies using intravenous injections of Tc^{99m}-labelled erythrocytes, in whom SPECT images of the thorax were obtained. The maximum activity per voxel (a pixel is the basic element of a planar image; the voxel is the volumetric equivalent) was found in the heart and was compared with the mean activity per voxel in the peripheral lung. Values obtained in the 2 volunteers for the heart maximum voxel intensity was 454 and 441 counts and 44.8 and 46.9 counts for the lung periphery respectively. These measurements indicated a peripheral lung circulatory activity amounting to 10% of that in the left ventricle. Since the peripheral aerosol deposition concentration is low and therefore most sensitive to blood correction, a blood correction factor of 10% of

the γ-emission in the left ventricle was applied to all voxels in the right lung. Penetration indices were corrected for blood background activity, and compared to the uncorrected data.

6.3.4 Three-dimensional analyses.

To make full use of the whole 3D data set for analysis, the right lung image was analysed by three novel methods. The first comprised plotting the natural logarithm of voxel activity against the number of voxels containing that activity. The shape of each curve was then described by its standard deviation, skewness and kurtosis, and compared for the two aerosols. The second method comprised drawing a line through each voxel from the hilum to the lung periphery. Because the length of each line from hilum to periphery varied depending on its position, its length was normalised to 100%. Each voxel could then be characterised in terms of its normalised percentage position from the hilum and its activity. The median voxel activity at each position was determined, and this figure was corrected for blood background activity. When the average corrected voxel activity was plotted against position from the lung hilum, it was found that the most intense activity was located centrally, and that there was approximately an exponential fall of activity density from hilum to periphery. Therefore the natural logarithm of each voxel's activity was plotted against its position, and a linear regression line was fitted to the data. The slope of the line was determined, and a value representing the point at which the distribution of activity density within the lung falls by half was calculated from 0.693/slope. This value was called the intensity half-distance.

Finally, the line from the hilum to the lung edge was divided into ten equidistant sections. Effectively, this has the effect of dividing the lung into 'shells', shell 1 being the inner shell, and shell 10 the outer shell (fig 6.1). Within each shell, it was possible to determine the total deposited activity from the product of the number of voxels in that shell and the mean voxel activity corrected for blood background. The cumulative total voxel intensity within each shell was plotted against the shell number. By taking the mid-point of the height of the resulting curve, a figure was derived which represented the shell position above and below which 50% of the total activity was distributed; this was termed the median dose position. A further analysis was performed by comparing the percentage of the total activity in the right lung within each shell between the two aerosols.

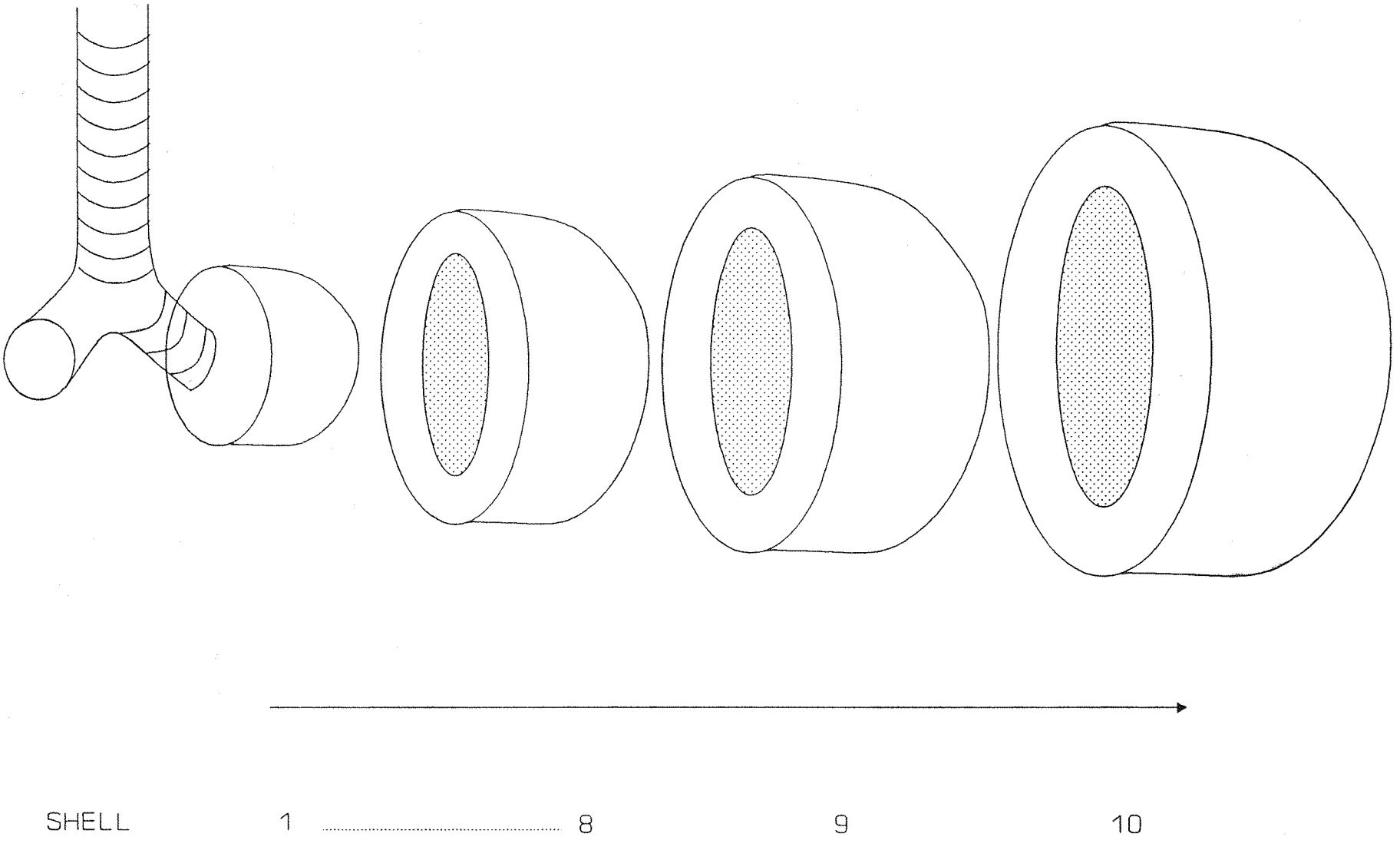

Fig 6.1 Diagrammatic representation of the effect of dividing the hilum to lung line into 'shells'.

6.3.5 Drug and Tc^{99m} pharmacokinetics.

The time course of plasma concentrations of nedocromil sodium after inhalation was analysed as described in chapter 2.5.3. For Tc^{99m} measurements, each value for plasma radioactivity was corrected to the time of inhalation. A model of first order absorption in a one compartment system was fitted to the time course of plasma activity after inhalation using a non-linear least-squares regression program (Enzfit, Elsevier-Biosoft, Amsterdam), from which the absorption rate constant and absorption half-life for Tc^{99m} were derived. The Cmax, Tmax and AUC for the two different nedocromil formulations were compared, as were the absorption rate constants and absorption half-life for Tc^{99m}.

6.4 Results.

Because of the large volume of data generated in this study to ease interpretation of the results, summary statistics only are given here. The raw and derived data are presented in appendix D.

All subjects completed the study. The radiolabelling procedure had a mean efficiency of 84.9 (0.36%) for the fine aerosol, and 85.3 (0.92%) for the coarse aerosol (NS). The coefficient of variation of the labelling procedure for the two formulations was 1.33% and 3.39% respectively (NS). The mean inspiratory parameters for the two aerosols did not differ significantly (table 6.1), confirming that inhalation of the two aerosols did not differ.

The mean radioactivity contained in two actuations of the fine aerosol was 337 (25.78) MBq, and was not significantly different from the activity delivered by the coarse aerosol, 371.2 (15.24) MBq. These figures were not significantly different to the activity delivered by the test shots, 311 (21) MBq (fine) against 351 (19.52) MBq (coarse). However, when these figures were compared to the delivered dose as assessed by the γ-camera, significant differences were found. The γ-camera assessment of delivered activity by the fine aerosol was 252.25 (12.8) MBq ($p = 0.001$ for test shots; $p = 0.004$ for dose assessed by calibrator), and 284.21 (19.34) MBq ($p = 0.001$ for both) from the coarse aerosol.

There were no differences detected in the percentage of the aerosols found in the chest, expiratory filters, MDI adaptors and gastrointestinal tract (table 6.2). When the results are pooled for all twenty studies, a mean of 7.6% (0.78%) of the delivered

dose was found in the chest, 77.0% (1.89%) was impacted, 13.3% (1.33%) remained on the adaptor and 1.8% (0.57%) was exhaled.

Analyses of the planar images showed that the two aerosols did not differ in the amount of drug delivered to the lungs. Thus, the amount of nedocromil sodium deposited in the whole chest was 0.311 (0.048) mg from the fine aerosol, and 0.286 (0.041) mg from the coarse aerosol (NS). When the right lung was analysed, the fine aerosol delivered 0.132 (0.022), and the coarse aerosol 0.109 (0.015) mg of drug (NS). However, when estimated from the SPECT images, the fine and coarse aerosols delivered 0.05 (0.005) and 0.045 (0.006) mg respectively to the right lung, which was significantly less than that calculated from the planar images ($p < 0.0001$).

Figures 6.2-6.6 show examples of the different lung images. The SPECT images were remarkably similar between subjects. When comparing penetration indices obtained from the planar and SPECT images for the two aerosol formulations, no differences were found (table 6.3). However, for all indices there was a trend for the coarse aerosol to have a higher PI, reflecting a more central deposition than the fine aerosol, but this failed to reach statistical significance. On comparing the PI derived from the planar images before and after SPECT, the latter was significantly less for both the fine (1.45 vs 1.94; $p = 0.0069$) and coarse (1.42 vs 2.09; $p = 0.0051$) formulations. The penetration indices corrected for blood background activity were not significantly different from those in which the correction was not made, but both the coronal and transverse corrected PI showed a trend towards higher values than the non-corrected data. In addition, the differences between the fine and coarse aerosol were greater for the SPECT data than for the planar data.

For the group as a whole, no significant differences were observed in the standard deviation, kurtosis or skew of the aerosols' distribution within the right lung, the median intensity half-distance or the shell median dose position (table 6.4). Figure 6.7 illustrates the relationship between voxel activity and the position of aerosol deposition for both aerosols in one subject. The highest activity intensity is found near the hilum, where the spread of activity intensity is also greatest, and both the spread and amount of activity intensity decrease toward the lung periphery.

When the deposition data were analysed in terms of the volume activity in serial shells (fig 6.8), for both aerosols the activity increased progressively from the central to the

peripheral lung shell in all subjects except one (no 10). This subject had a higher planar C/P ratio than all the other subjects (5.03 for the fine and 5.68 for the coarse aerosol, the range of planar PI in the other subjects being 1.28-3.02 and 1.31-2.5 respectively), and his predominantly central deposition is mirrored by the peak shell activity occurring toward the lung centre. The activity deposited in each shell expressed as a percentage of the total activity in the right lung was found to increase linearly from the hilum to the periphery, but no difference was found between the two aerosols (fig 6.9). For both aerosols, it can be seen that 50% of the dose in the right lung was deposited in the outer three shells.

Three subjects were excluded from the analysis of plasma nedocromil sodium pharmacokinetics. Two of these (nos 1 and 10) had unexpectedly high plasma levels at some of the time points, levels which were more than 2 standard deviations outside the mean value for that time point, and the other subject (no 9) had levels that generally did not reach the limit of detection in the majority of plasma samples on both study days.The pharmacokinetic profile of both nedocromil sodium and pertechnetate did not differ between the aerosols (table 6.5). Figure 6.12 shows the mean plasma concentration-time curves for the different aerosols for the drug and radioisotope. With both aerosols, plasma Tc^{99m} rose to a peak at betweeen 30 and 60 minutes after inhalation (fig 6.12), and then declined slowly. Plasma nedocromil sodium concentrations increased rapidly during the first 10 min post-dosing in all subjects with both formulations (fig 6.12), and in many cases the concentrations in the first sample (2.5 min) approached that of the subsequent observed maximum concentrations. The fine formulation had a higher Cmax and AUC for nedocromil sodium and a faster absorption half-life for Tc^{99m} than the coarse aerosol, but these differences did not reach statistical significance.

Figure 6.2 (overleaf). In these and the subsequent figures, the most intense areas of γ-emitting activity are shown in red, and the least intense as dark blue. Panels a & c show an anteroposterior geometric mean planar image of the thorax taken immediately after inhalation of radioactive nedocromil sodium, and before the SPECT study. This is contrasted with a similar image acquired immediately following the completion of the SPECT study (panel b), and with a coronal reconstruction taken from the SPECT study in the same subject (panel d). The pre-SPECT planar image (a&c) clearly shows that the most intense areas of activity are found in the oropharynx and stomach, with lesser degrees of activity in the lungs. The more intense activity in the left lung (yellow area) compared with that in the right lung is considered to be due to the scatter of radioactivity from the stomach. The post-SPECT planar image (b) shows a reduction of activity in the stomach, oropharynx and lung fields when compared to (a), and there are more extensive areas of low activity outside the lung fields, considered to be due to the build-up and recirculation of blood-borne activity in extrathoracic structures. The coronal SPECT image (d) shows the degree of detail that can be achieved, and the enhanced information that this imaging technique provides. Stomach activity remains high when compared to (a), but it can also be seen that there is an area of intense activity in the mediastinum , which is thought to be the main carina; activity can be seen extending from that point downward toward the stomach, presumably within the oesophagus. It is not possible to separate activity within the trachea and oesophagus. In addition, both major bronchi are outlined.

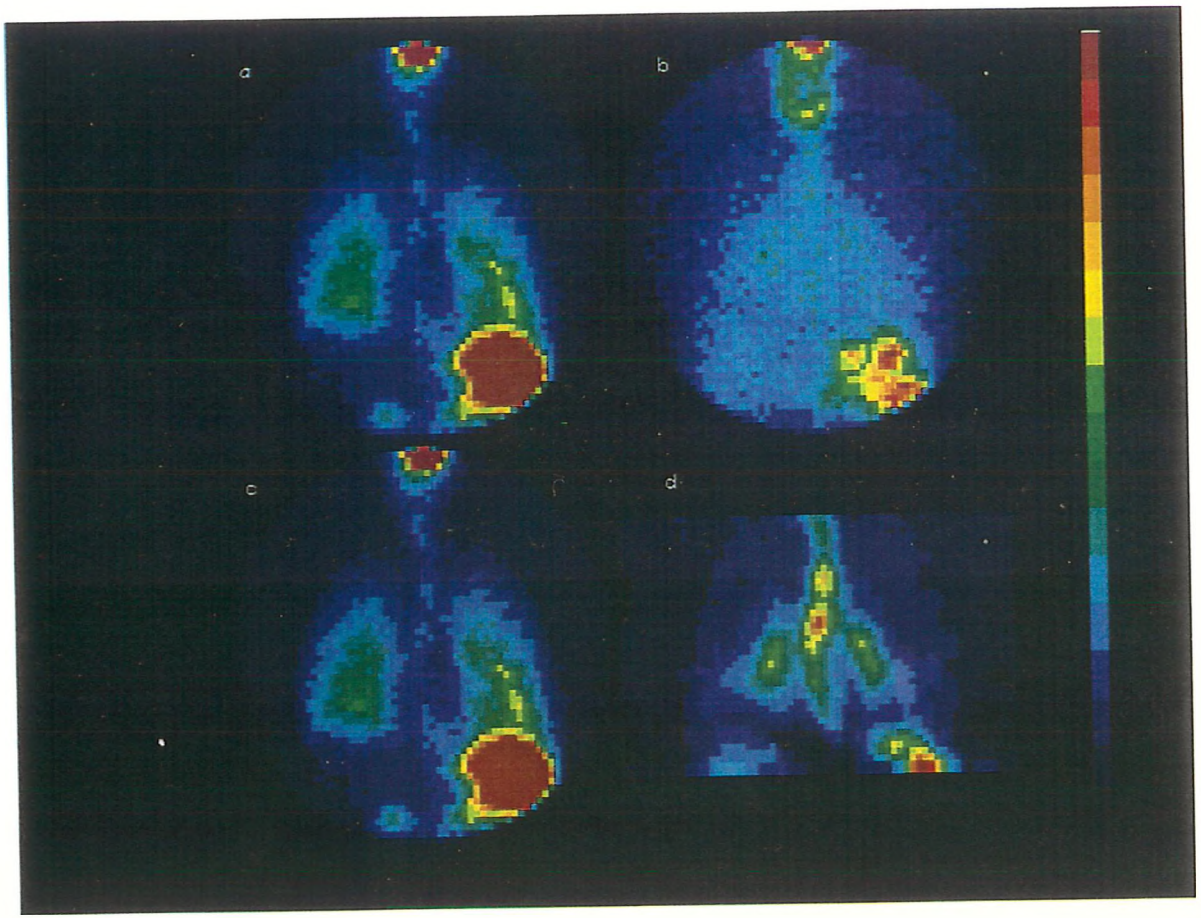
a
b
c
d

Figure 6.3 (overleaf). This illustrates the various stages in converting a CT image of a subject's thorax to an attenuation coefficient map for use in attenuation correction in SPECT. Panel (a) shows the original CT image of the thorax, which has been minified to SPECT imaging size. Note that the CT bed is visible, as are the prongs of both metallic markers placed on the chest wall for image alignment. Panel (b) shows conversion to a 64 x 64 matrix, and removal of the CT bed. Panel (c) shows the CT aligned with the SPECT image, and (d) shows the completed image with CT numbers converted to represent linear attenuation coefficients of Tc^{99m}, and the addition of the SPECT bed. Note that the most dense tissues are represented in red, and the least dense tissues in blue. These images (and all subsequent transverse images) are viewed as if the observer is at the feet of the subject; therefore the right side of the image represents the left side of the subject.

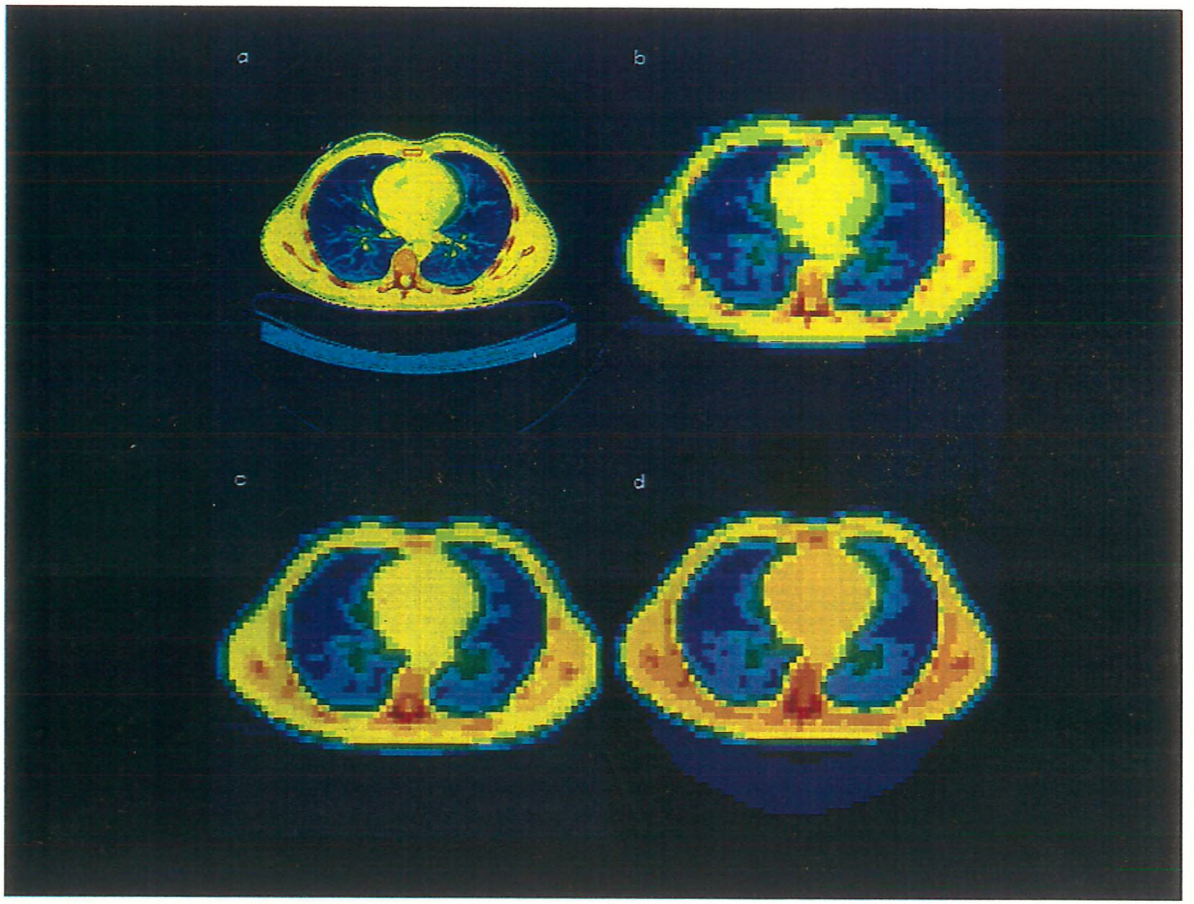
a
b
c
d

Figure 6.4 (overleaf). Panels (a) and (b) represent coronal reconstructions of CT (a) and the equivalent SPECT (b) images posterior to the heart. The coronal image is the same as that represented in figure 6.2 (d). Panels (c) and (d) represent CT and SPECT transverse reconstructions through the level of the distal trachea. The most intense activity is seen centrally, and when the images are overlayed, this is seen to correspond to the position of the trachea and oesophagus. Because of the close proximity of these organs, it is not possible to separately resolve the structures. Lesser degrees of activity are seen in the lung fields, and careful perusal of the SPECT image (d) illustrates the characteristic pattern of scatter of radiation when imaged by this technique.

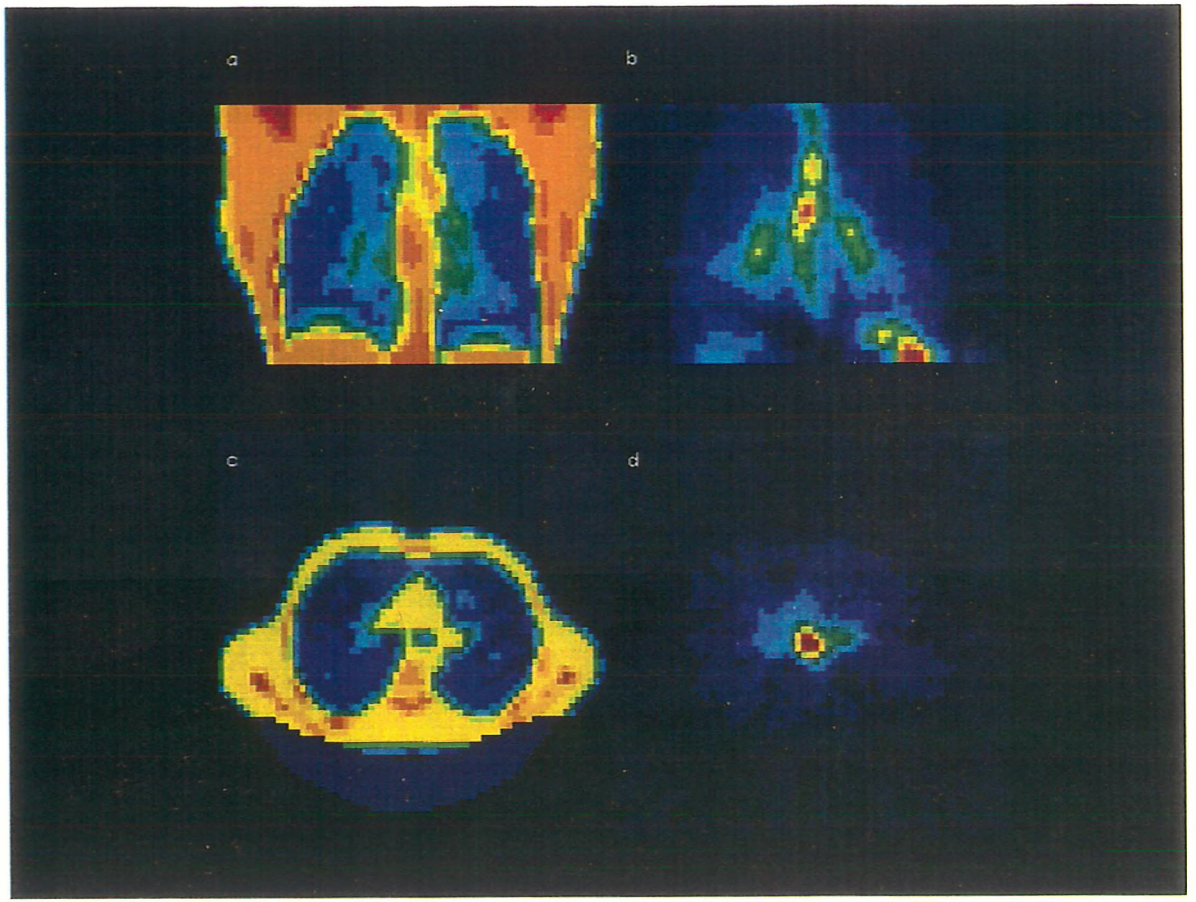
a
b
c
d

Figure 6.5 (overleaf). The four panels shown here are exactly the same as the previous figure (6.4), but the central and peripheral regions of interest are illustrated. The regions are first outlined on the CT images (a & c). The central region is defined as a box drawn along the medial edge of the right lung, centred on a point mid-way along the medial edge, and having the dimensions of half the lung height and half the lung width and the peripheral region defined by a line starting from a point mid-way on the medial border of the right lung, and describing a strip equal to one-third of the lung height inside the outer lung boundary. These regions can then be transferred directly to the correctly aligned SPECT images (b & d), and the activity contained within them measured.

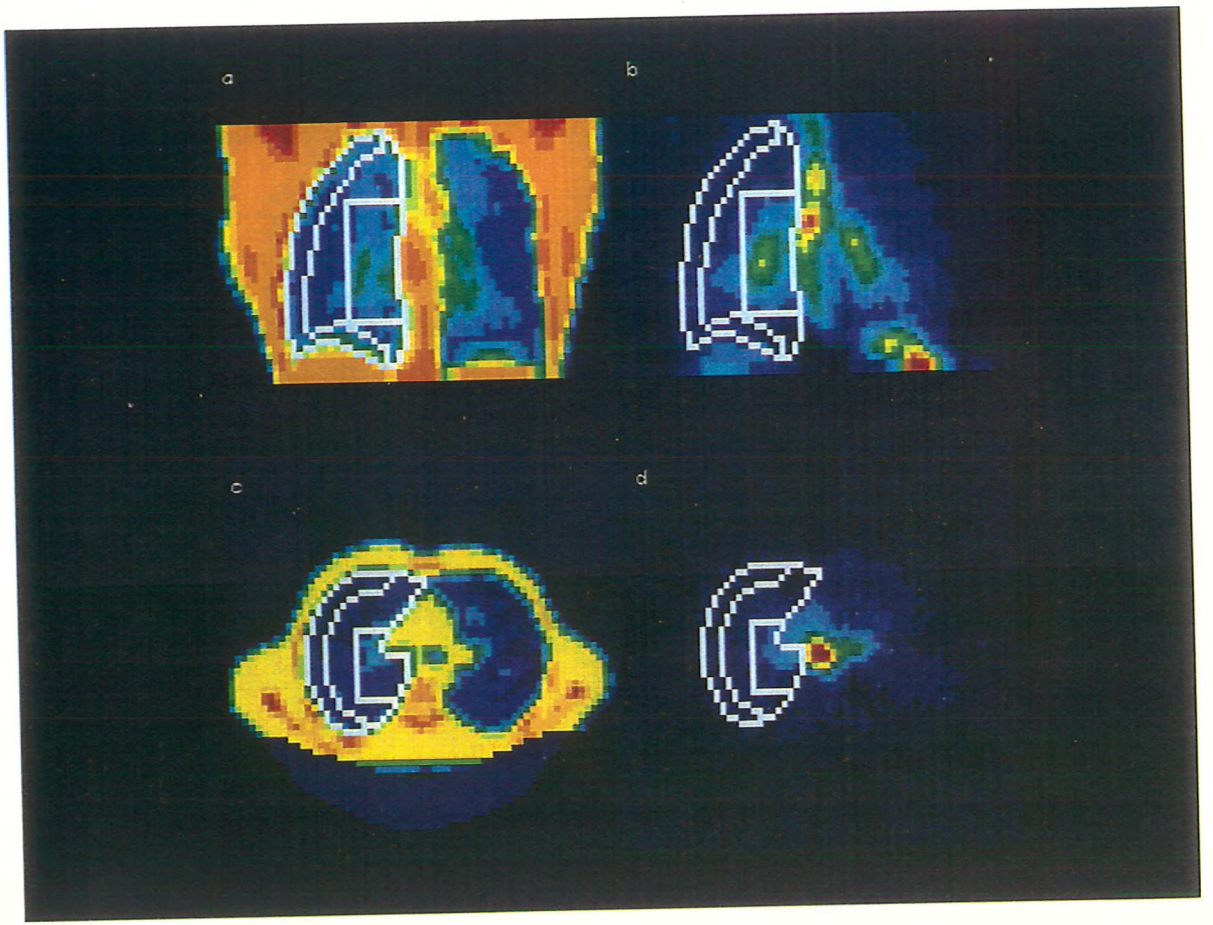
a
b
c
d

Figure 6.6 (overleaf). This illustrates a series of transverse SPECT images at the level of the proximal trachea (a), at just beyond the tracheal bifurcation (b), at the level of the heart (c), and at the level of the upper pole of the stomach (d). Activity intensity is highest within the trachea and oesophagus (a), and in panel (b), the most intense activity is seen centrally, with less intense activity on either side of this. Since this slice is beyond the tracheal bifurcation, the central activity must be located within the oesophagus, the 2 other areas of high activity being in the major bronchi. Panel (c) illustrates the problem of blood-borne activity. Once again, the most intense activity is seen within the oesophagus centrally, with activity also well seen in the lower lobe bronchi. Just anterior to the oesophageal activity, it can be seen that there are 2 well-defined areas of activity which represent blood in both sides of the heart. The final image (d) once again shows high activity within the oesophagus and stomach. In all four images, the lung fields contain only low activity intensity.

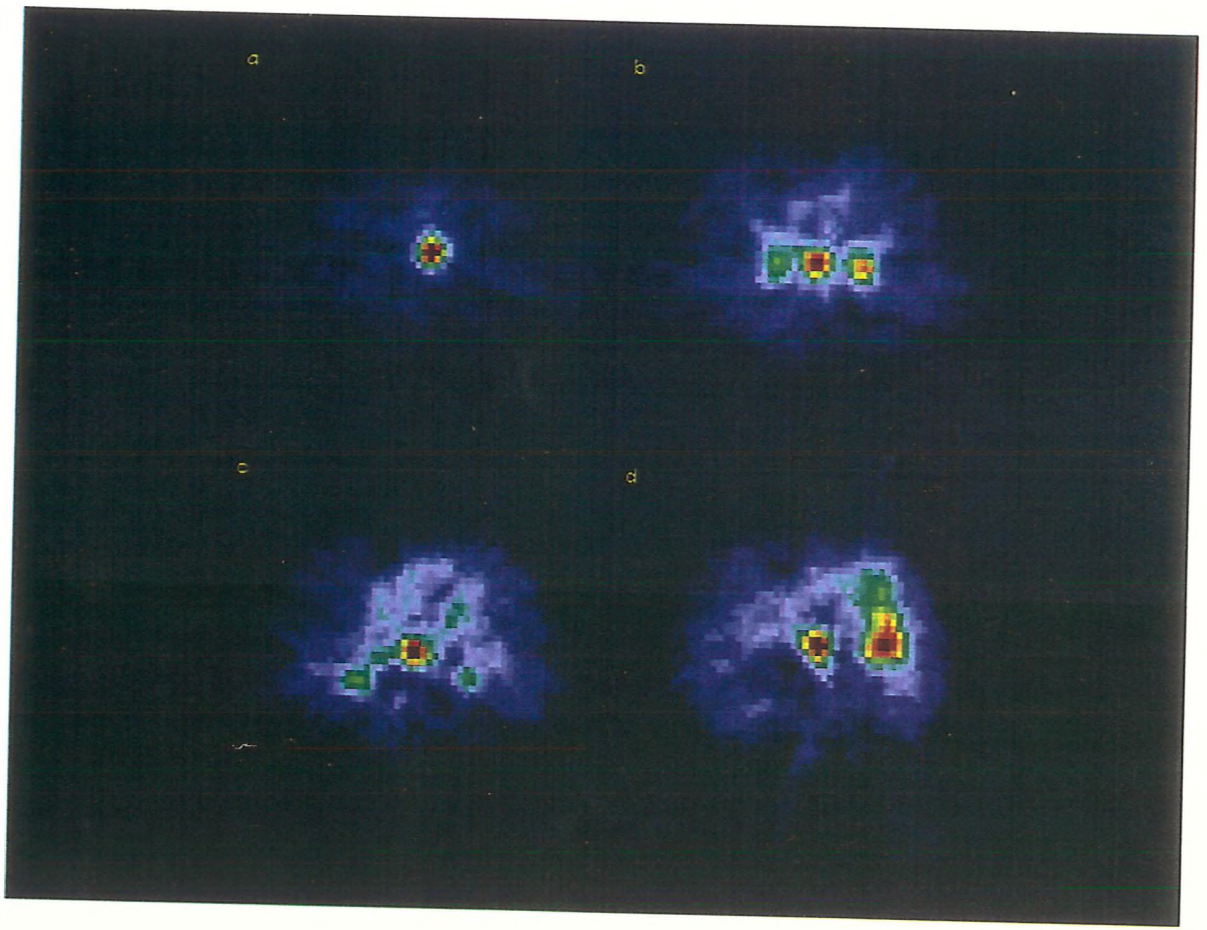
a
b
c
d

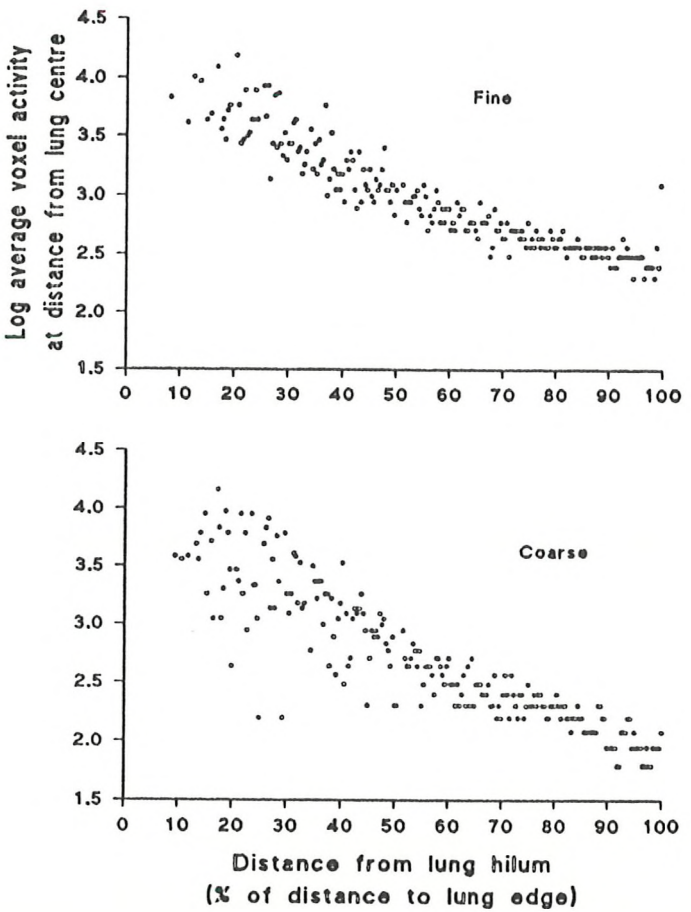

Fig 6.7 Relationship between voxel activity and deposition position in one subject after inhaling 2 radiolabelled aerosols of nedocromil sodium.

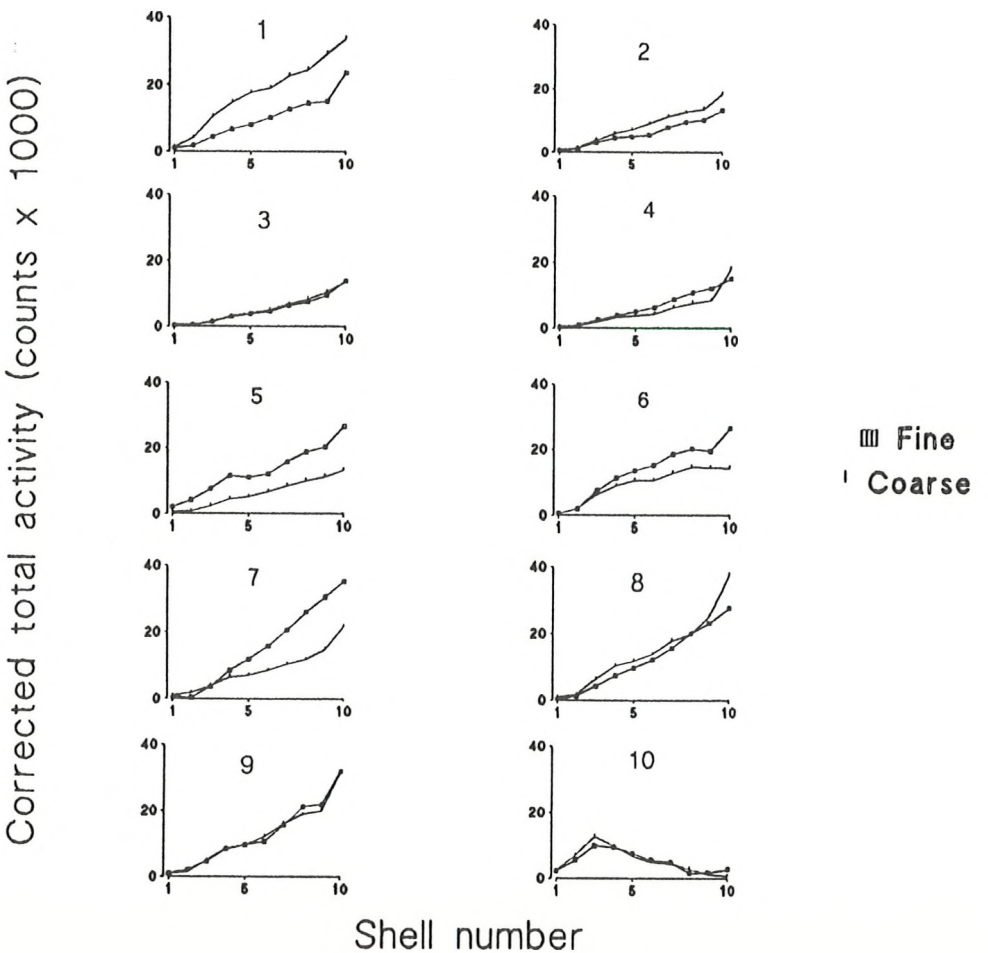

Fig 6.8 Activity in each shell (1 = hilum, 10 = periphery) of the right lung after inhaling 2 aerosols of radiolabelled nedocromil sodium in 10 subjects.

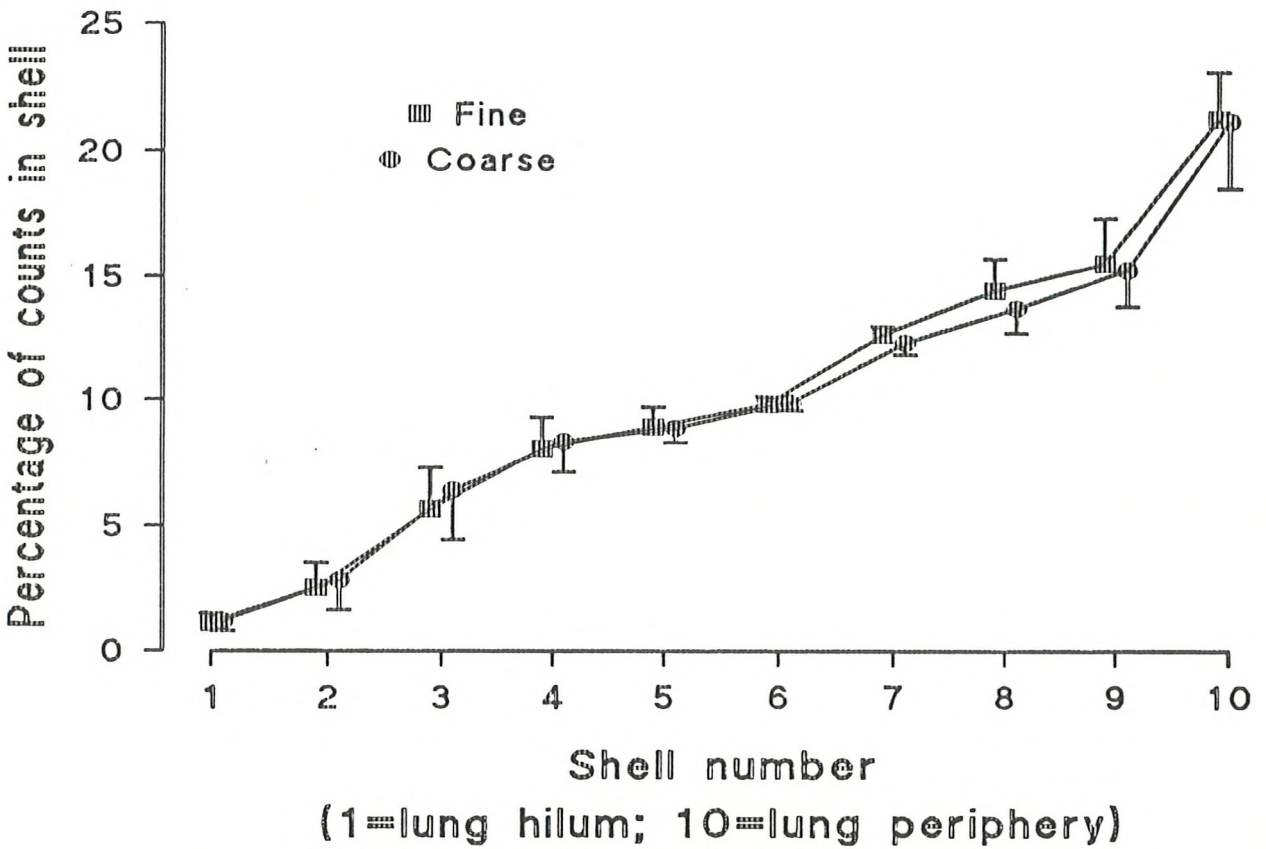

Fig 6.9 Percentage (mean ± SEM) of total activity in the right lung within each shell after inhaling 2 radioaerosols of nedocromil sodium.

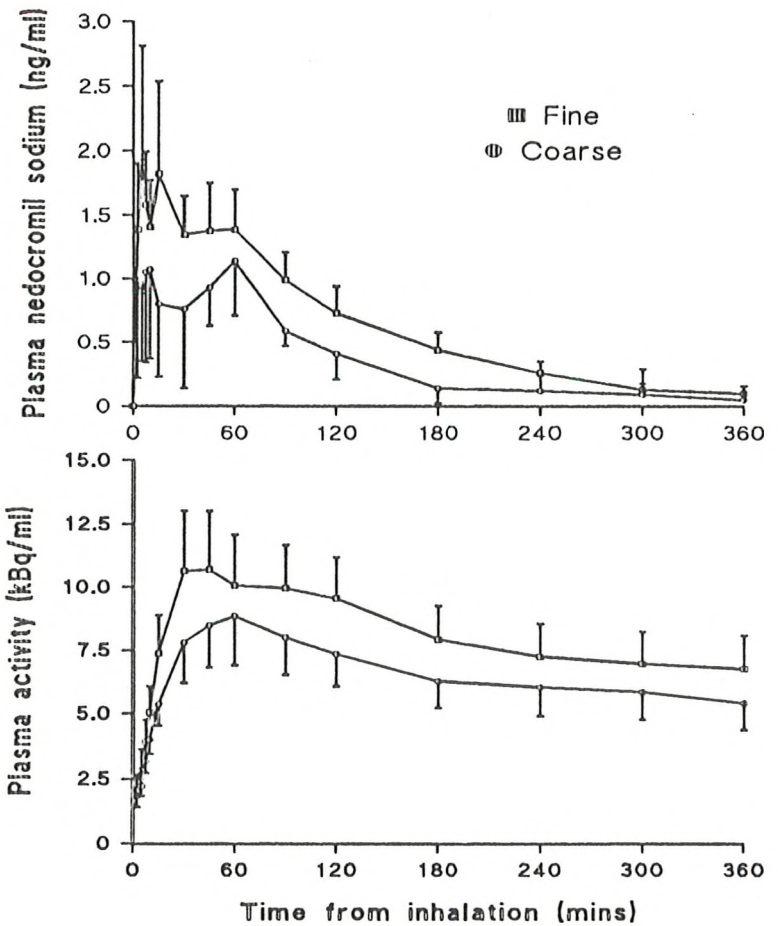

Fig 6.12 Mean (SEM) time course of plasma nedocromil (7 subjects) and Tc^{99m} (10 subjects) after inhalation of 2 aerosols of the drug.

6.5 Discussion.

In obtaining a 3 dimensional or volume-related description of intrapulmonary aerosol deposition, and by its subsequent conversion to a near hemispherical shape, this study has allowed the estimation of the total dose delivered to definable sites within the lung as well as the definition of the intrapulmonary distribution of aerosol. Thus, for the whole group of subjects, a mean 50% of the dose in the right lung was found to deposit in the outer 3½ shells, suggesting that the predominant mechanism of aerosol deposition was gravitational sedimentation. By contrast, the power of this technique is highlighted by the one subject who had a predominantly central deposition pattern (subject 10, fig 8) as assessed by the C/P ratio, in whom the distribution of activity within successive shells was seen to differ markedly from the other subjects, in that the peak activity was found at shell 3, whereas in all other cases the peak activity was located in the outer shell. The predominant mechanism of aerosol deposition in this subject was likely to be inertial impaction, a finding that would be expected in patients with airways disease or as a result of inhaling an aerosol with a large MMAD, but was unexpected in a normal subject. SPECT holds great promise in the investigation of the response to therapeutic aerosols, because it is now possible to measure accurately the site and extent of deposition, and to correlate this with response. The accuracy of such measurements could be enhanced by using a radioisotope that is not absorbed as quickly as pertechnetate, thereby obviating the problems associated with the build-up of blood background activity, and by using aerosol delivery systems (such as nebulisation) that avoid the problems associated with the high degree of extrapulmonary deposition seen here.

The two new indices used to describe the sites of aerosol deposition do not represent the same phenomenon. The intensity half-distance represents the distribution of activity density at each point in the lung, and is the 3D counterpart of the penetration index derived from planar images. It can be seen (fig 6.7) that the amount and spread of voxel intensity is greatest near the lung hilum, considered to be due largely to anatomical factors. That is, in the shells nearest the hilum, there will be both large conducting airways and alveoli, and because the area available for particle deposition in the airways is very small compared to that in the small airways and alveoli, the density of particle deposition is greater at these sites. By manipulating these data, it was possible to derive an index, the median dose position, which takes into account lung volume and describes the distribution of total activity within the lung. Each successive shell from the hilum has a larger volume than the preceeding shell and, as

demonstrated here in subjects with a predominantly peripheral aerosol deposition, is likely to contain a higher total activity. Thus, this analysis is able to highlight the difference between predominantly central and peripheral deposition of the delivered dose. As seen in this study, a polydisperse aerosol such as nedocromil sodium delivered by a MDI has a low activity density distribution but a high total activity within the peripheral lung, and conversely, closer to the hilum the aerosol has a high activity density and a low total activity. This indicates that although a small amount of the drug is deposited near the lung hilum, there is more drug per unit lung area than in the periphery. It is not known if the response to a drug depends upon the total dose delivered or to the density of occupation of receptor sites. However, SPECT can now be used to examine this as well as the proposition that therapeutic aerosols need to penetrate deeply for maximum effect.

It was expected that the bulk of these aerosols would deposit more centrally because of their particle size characteristics. Thus, the finding that the amount of drug within each shell tends to increase linearly with distance from the hilum is surprising, and may be of fundamental importance. The finding that the median dose position for these aerosols was located toward the lung periphery was also unexpected. Why the dose of an aerosol within the lung should vary in direct proportion to distance from the hilum is unclear but the size distribution of particles reaching the lung, inhalation technique and the spherical geometry of the model may all be implicated. Further work is needed to clarify whether this phenomenon is restricted to polydisperse aerosols. Current theory would suggest that a monodisperse aerosol would not behave in this manner, and it may be expected that the less the size spread of particles within an aerosol the greater the correspondence between regional activity density and regional total activity. Because of their propensity to increase turbulent airflow at sites of bronchoconstriction, it is also possible that asthmatic airways may increase deposition at those sites, effectively converting an aerosol with a wide spread of particle size to one behaving as a less dispersed aerosol. However, caution should be exercised when extrapolating from studies in normal subjects to asthmatics.

This study has attempted to determine whether the site of intrapulmonary deposition of nedocromil sodium can affect its subsequent pharmacokinetic profile, when the drug is inhaled in a standardised manner. This is the first study to utilise SPECT to document the pulmonary deposition characteristics of an aerosol delivered by MDI, and few previous workers have attempted to correlate deposition and pharmacokinetics. Before

further discussion of the results, it is necessary to consider the methodology used.

Attenuation correction applied to the SPECT images was used in this study to obtain quantitative information. The use of CT images for attenuation correction meant that our volunteers were exposed to a further radiation dose. The effective whole body dose from a standard diagnostic CT examination of the thorax using a similar scanner was found to be 6.45 milliSieverts (mSv) by Nishizawa et al (1991). The scanning technique utilised in this thesis is estimated to deliver half that figure (3.2 mSv) because the acquisition of fine detail is not necessary as it is in diagnostic examinations and therefore smaller slice widths, a faster scanning time and a lower beam energy could be used. The alternative method of attenuation correction, the transmission scan, which also involves exposing the subject to an external source of radiation, does not yield as much anatomical information although the radiation dose is lower.

The use of SPECT also required the delivery of higher levels of activity to the subjects than would be the case if only planar images had been acquired since a greater number of counts is required for statistically valid images. Estimates derived from the ICRP (1987) suggest a total radiation dose to each subject of $\approx$ 9 mSv (appendix D, p 226). Although SPECT images give superior spatial information, image noise in areas of low activity such as the lung periphery may be high. A further disadvantage of SPECT is the requirement for subjects to adopt the supine posture with their arms held above their heads. This is an uncomfortable position to hold, and even though the subjects used in this study were young and fit, many complained of discomfort. This may be alleviated by shortening the acquisition time for each image, but this would lead to a loss of image quality. In turn, it could be overcome by delivering a higher dose of activity, but at the expense of safety. A further method of improving the resolution of the images would be by use of more advanced SPECT systems. The system used in this work employed a γ-camera with only a circular rotation, and in order to rotate around the subjects' shoulders, the camera was often further away from the chest wall than would otherwise be the case. Newer systems now incorporate cameras that can vary their distance from the subject, or alternatively the SPECT bed can be made to move closer to the camera when possible, so obtaining images with the maximum possible resolution. Another problem with γ-cameras is the inability to resolve accurately structures less than 10 mm in diameter - for example, it is not possible to separate activity deposited in the trachea and oesophagus, nor is it possible to follow airways toward the lung periphery as they decrease in size. Nevertheless, the ability

of SPECT to separate peripheral from central regions of interest correctly magnifies the differences in central/peripheral ratios compared to planar imaging, and confirms the main findings of Phipps et al[6].

A further problem with SPECT is that the final image is an averaged, static view of a dynamic process. That there was some alteration in the distribution of lung activity during the course of the SPECT study is attested to by the differences between the PI from the planar images before and after SPECT, indicating that there was a reduction in central activity during the study period as a result of mucociliary clearance, and/or the activity in the peripheral region of interest may have increased during the study as a result of the build-up of blood background activity. This differential clearance of activity from the lungs was thought not to influence the final images as the back-projection process reconstructs each image slice voxel by voxel, thereby minimising the effects of activity changes in one voxel on adjacent voxels. A correction to account for the loss of activity from the lungs during the scanning period could have been derived from further, separate studies in the subjects by measuring clearance, although this would have exposed subjects to further radiation and was felt to be unsafe. Once again, this problem may be alleviated by more rapid image acquisition and by use of a label that has a longer residence time in the lung.

It is important to note that the pertechnetate and drug were not directly bound, but were present in the aerosol in the same proportions, making it reasonable to assume that the image of deposited radioactivity was equivalent to drug deposition. Once the two substances deposit in the lung, their subsequent behaviours probably differ, which is supported by their different kinetic profiles (figs 6.12 & 6.13). In addition, because the thyroid gland was visible at the end of the scanning period, this indicated that the gland had trapped free pertechnetate. Moreover, one subject had very low concentrations of plasma nedocromil sodium, despite having appreciable amounts of Tc^{99m} present. It is thus apparent that the label and drug behaved differently. The peak activity of Tc^{99m} in the peripheral blood occurred at a time point roughly half way through the SPECT study, and it was therefore necessary to attempt to correct for this blood-borne activity. Two subjects who were undergoing investigation of their cardiac function were studied, and the estimate obtained from them was used. These subjects had a prior history of ischaemic cardiac disease, and indeed, both had a reduced cardiac ejection fraction, being 0.16 and 0.27 respectively (normal > 0.5). Ideally, it would have been preferable to use the subjects who actually inhaled the radioaerosols,

but it was felt unethical to subject them to further radiation. The estimates obtained may have been inaccurate in that both subjects had depressed cardiac function and it is possible that their lungs may have contained more blood than in a healthy volunteer, giving rise to an overestimate of blood volume in the peripheral lung. However, despite the reduced ejection fraction, neither subject was symptomatic and both were on appropriate therapy. A further problem with the blood background correction is the application of a single correction factor to the whole lung. It is likely that the volume of blood in the central lung is greater than that in the periphery (per voxel), and therefore the correction employed here may underestimate the contribution of blood background activity in the central lung. However, although this correction had the effect of reducing peripheral counts and therefore increasing the resultant PI, there was no statistical difference between the corrected and uncorrected PI.

The assessments of delivered radioactivity made from the γ-camera and radioisotope calibrator measurements differed in that the γ-camera derived values were significantly lower than those from the calibrator. This suggests that not all the delivered activity may have been measured, possibly because of loss of activity into the atmosphere, or more likely because of the many approximations made to derive activity from γ-camera count rates in combination with the effect of time delays between aerosol inhalation and γ-camera imaging.

The observed deposition of the aerosols in the chest amounting to 7.6% of the total ejected by the MDI was within the range of results reported for other metered-dose generated aerosols described in the literature. Thus, Newman et al (1989) reported that 10.5% of radiolabelled sodium cromoglycate, an aerosol with similar size characteristics to those used in this study, and inhaled in the same manner, deposited in the chest, while Spiro et al (1984) reported a lung deposition of 16% of inhaled ipratropium bromide. In another study (Newman et al, 1982), 14% of a pressurised aerosol of Teflon particles having a MMAD of 3.2 μm was deposited in the lung when inhaled with a technique identical to that used here.

Despite the large differences that exist between the aerosols used in this study, no clear differences were found between the intrapulmonary distribution of the two formulations. The aerosols were designed in order to maximise any differences in lung penetration; thus, the fine aerosol contained twice the mass of particles < 10 μm in diameter than the coarse aerosol, and it was expected that more of the fine aerosol

would enter the lungs to be deposited in the large airways. Moreover, the difference between the two formulations for particles < 4 μm in diameter was of the same magnitude, and a similar variation in peripheral deposition was expected. The failure to detect a difference between the lung deposition of the aerosols may be because no in vivo aerodynamic difference exists between them, although this is not consistent with current aerosol theory. A further possibility is that the imaging system is not able to detect very small differences, although it was considered that the anticipated large differences would have been detectable.

A consistent trend was seen toward the fine aerosol having a greater pulmonary deposition and a higher peripheral and/or a lower central deposition than the coarse aerosol. Thus, after inhalation, the fine aerosol had a higher maximal plasma concentration and area under the plasma concentration-time curve than the coarse aerosol, and the penetration index, no matter which image it was derived from, was always lower for the fine aerosol. Furthermore, the trend toward greater peripheral deposition of the fine aerosol was also reflected by the faster absorption half-life of Tc^{99m} after the fine aerosol since it has been demonstrated that the clearance of technetium from the lung is faster from the periphery than from the large conducting airways (Bennett & Ilowhite, 1989).

It is felt that the major reason for the failure to detect a difference between the aerosols is the inspiratory procedure used. A slow inhalation has been suggested as the optimal way to inhale an aerosol, and this technique was employed in this study. In order to entrain an aerosol in an airstream, it is necessary to overcome the inertia of that aerosol. Aerosols generated by pressurised canisters have a very high iunitial forward velocity (Rance, 1974) and therefore high inertia, and it may be that a slow inspiratory flow rate may not be enough to overcome the force tending to direct the aerosol in a straight line toward the oropharynx. Conversely, a rapid inspiration has the effect of increasing turbulence within the aerosol and increasing impaction in the oropharynx. It is proposed that there is an optimal range of inspiratory flow rates, above and below which such fast moving and large aerosols will impact before penetrating the lung. This mechanism would explain the similar deposition profiles of the two aerosols, since the low inspiratory flow rate could only entrain those particles of low mass or velocity. However, this does not fully explain the findings, as the fine aerosol had twice the mass of small particles contained in the coarse aerosol.

The absence of a difference between the amount of drug found in the lungs, and between the pharmacokinetic profiles of both drug and radioisotope is not surprising given the similar deposition of the two aerosols. The two-fold difference between the SPECT and planar assessments of the amount of drug in the right lung is considered to due to the time difference between the scans.

Three subjects were excluded from the analysis of plasma nedocromil sodium pharmacokinetics, two because of massive and unexpected increases in plasma drug concentration at individual time points, which had returned to their expected levels by the next measurement. These large increases are unexplained. It is most likely that the relevant specimens had become contaminated even though precautions against contamination were extensive. It is also possible that the subjects may have performed some activity known to cause sudden rises in plasma nedocromil sodium concentration (Ghosh et al, 1988; chapter 4), or some substance may have been present in the subjects' plasma to cause a cross-reaction. However, the subjects rested throughout the study period and any substance in the plasma causing a cross-reaction would be unlikely to appear transiently.

The derived pharmacokinetic parameters for nedocromil sodium are similar to those reported in chapter 3 and elsewhere (Neale et al, 1987), except for the time taken to achieve maximal plasma concentration. Neale reported a time of 20 (6) min in normal subjects, and in the group of asthmatics used in chapter 3, 19 (5) min, whereas in this study the fine aerosol had a Tmax of 31.71 (8.98) min and the coarse aerosol a Tmax of 38.57 (15.70) min. Whether this difference is significant is unclear, and there is no obvious reason for a slower absorption of nedocromil sodium in this study. It may be that the co-deposition of Tc^{99m} may be responsible for this finding, perhaps by interfering with the process of drug absorption. The corollary cannot be examined as there is no other study in which the plasma pharmacokinetics of Tc^{99m} as pertechnetate have been studied.

In conclusion, this study has shown that SPECT is a valuable tool for showing the volume distribution of an inhaled drug and provides a unique opportunity for relating this to pharmacodynamic and pharmacokinetic indices. SPECT was not able to demonstrate a clear difference in the deposition of two polydisperse aerosols of nedocromil sodium, although there was a tendency for more of the fine formulation to deposit in the lung and reach the periphery.

Table 6.1. Inspiratory parameters for the formulations of nedocromil sodium.

	Fine aerosol	Coarse aerosol
Breath holding time (sec)	10.35 (0.36)*	10.47 (0.33)
Peak inspiratory flow rate (l/min)	45.7 (2.15)	47.53 (2.18)
Inspiratory flow rate at actuation (l/min)	37.25 (1.94)	40.26 (2.11)
Time of aerosol actuation (sec)	1.7 (0.05)	1.65 (0.06)
Inspiratory volume at actuation (l)	0.99 (0.04)	0.99 (0.05)
Percentage of inspired volume at actuation	22.05 (0.86)	20.79 (0.87)

* - mean (SEM) for 10 subjects.

Table 6.2. Proportion of two formulations of radiolabelled nedocromil sodium deposited at different locations.

	Fine aerosol	Coarse aerosol
Chest	7.91 (1.21)*	7.26 (1.04)
Gastrointestinal tract	78.56 (1.71)	75.49 (3.41)
MDI adaptor	12.76 (1.01)	13.92 (2.52)
Exhaled	0.77 (0.23.)	2.87 (1.04)

* - proportion expressed as a percentage of the total. Mean (SEM) for 10 subjects.

Table 6.3. Penetration indices derived from planar and SPECT gamma camera images after inhalation of two formulations of nedocromil sodium.

	Fine aerosol	Coarse aerosol
Planar image before SPECT	1.94 (1.28-5.03)*	2.09 (1.31-5.68)
Planar image after SPECT	1.45 (1.34-1.84)	1.42 (1.23-2.61)
Coronal SPECT (not corrected)	2.08 (1.45-4.42)	2.46 (1.58-6.84)
Coronal SPECT (corrected)	2.75 (1.72-9.80)	3.22 (1.86-14.05)
Transverse SPECT (not corrected)	2.14 (1.63-5.09)	2.51 (1.67-7.75)
Transverse SPECT (corrected)	2.98 (1.93-14.07)	3.49 (2.07-17.63)

* - median and range of values for 10 subjects.

Table 6.4. Three dimensional analyses of SPECT data after inhalation of 2 formulations of radiolabelled nedocromil sodium.

	Fine aerosol	Coarse aerosol
Distribution of aerosol*:		
Standard deviation	0.511 (0.025)	0.569 (0.025)
Skew	-0.165 (0.107)	-0.164 (0.174)
Kurtosis	1.636 (0.142)	1.976 (0.23)
Intensity half-distance+	43.3 (9.9-69.3)	42.1 (9.1-69.3)
Median dose position (shell no)+	6.84 (3.2-7.21)	6.76 (2.93-7.28)

* - mean (SEM) for 10 subjects; + - median (range) for 10 subjects.

Table 6.5. Pharmacokinetic parameters of drug and Tc^{99m} following inhalation of 2 formulations of radio-labelled nedocromil sodium.

	Fine aerosol	Coarse aerosol
Nedocromil sodium:		
C max (ng/ml)	2.33 (0.67)*	1.43 (0.27)
T max (min after inhalation)	31.71 (8.98)	38.57 (8.43)
$AUC_{0\text{-}360}$ (ng.min/ml)	215.76 (44.18)	123.48 (15.70)
Tc^{99m} absorption half-life (min)	11.84 (1.10)+	21.37 (4.51)
Tc^{99m} absorption rate constant	0.0646 (0.0078)	0.0455 (0.0086)

* - mean (SEM) for 7 subjects; + - mean (SEM) for 10 subjects.

Chapter 7. Discussion.

The anti-asthmatic properties of nedocromil sodium are well documented, and are due to a combination of effects on the cells, inflammatory mediators, vessels and nerves that participate in the inflammatory response that underlies asthma. The drug is taken by the inhaled route, and the therapeutic aerosol is most often generated by MDI, as are most therapeutic aerosols. Therefore, a method was developed for the easy addition of technetium-99m (Tc^{99m}) as pertechnetate to nedocromil sodium for delivery by MDI (chapter 5). The labelling method preserves the particle size characteristics of the aerosol, and because drug and label are distributed together, the assumption that a γ-camera image of the intrapulmonary distribution of the radiolabel is equivalent to that of the drug is reasonable. The labelling procedure is easy and straightforward, and can be done safely providing stringent precautions are taken against exposure to radiation. The procedure does not involve the addition of substances such as particulates or propellants to the aerosol, and as such it should be applicable to every agent delivered in this manner.

The fine nedocromil sodium aerosol was composed mainly of droplets that would be unable to enter the airways, with 50% being > 16.5 μm, and only 44% of droplets < 10 μm in diameter. That fraction of an aerosol considered likely to penetrate the respiratory tract has been named the 'respirable fraction', and conventionally is considered to be composed of particles < 5-6 μm in diameter. However, because it is not known where in the respiratory tract an aerosol should be deposited for maximum effect, and because 10 μm particles can deposit in the proximal respiratory tract to a greater extent than particles of most other sizes (Task Group on Lung Dynamics, 1966; Stahlhofen et al, 1980; Heyder et al, 1982), the term 'respirable fraction' should either be abandoned or redefined.

There have been few reports of radiolabelling techniques for aerosols, and the work described here emphasises the need to measure the particle size of an aerosol before and after any manipulation, and also emphasises the necessity of sizing aerosols under conditions as near as possible to the those in which they are inhaled, and not, as many authors have done, after the aerosol has been allowed to collect in a chamber before measurement. Thus, while authors such as Kim et al (1985) and Bouchikhi et al (1988) report that the MMAD of salbutamol delivered by MDI is about 2.5μm, Zainudin and co-workers (1990) found that salbutamol delivered by MDI had an MMAD of greater

than 6.5 μm. The difference is due to the fact that Zainudin measured the aerosol as it is inhaled, and not after evaporation of propellant. A similar phenomenon is described here, as the dry powder from which the nedocromil sodium MDI was constituted had an MMAD of 2 μm, while the generated aerosol is much bigger. While sizing aerosols in this way gives a much better estimate of the amount entering the lungs, it is still inaccurate, in that actual deposition is less than the predicted figure. For instance, the pressurised salbutamol aerosol described by Zainudin et al (1990) should have deposited in the lungs in much greater amounts than described (11% of the delivered dose), and similarly the fine nedocromil sodium aerosol used here would also be expected to have a higher intra-pulmonary deposition than was observed. The difference is almost certainly due the velocity at which these aerosols are ejected (Rance, 1974).

The failure to demonstrate a significant difference in the intra-pulmonary deposition between the 2 aerosols was disappointing, although a consistent trend was seen that suggested the fine aerosol may have had a greater peripheral deposition (Chapter 6). Nevertheless, the ability of SPECT to separate peripheral from central regions of interest correctly magnifies the differences in central/peripheral ratios compared to planar imaging, and confirms the main findings of Phipps et al (1989). The pulmonary deposition characteristics of inhaled nedocromil sodium described by the 3-dimensional imaging techniques employed in this thesis were surprising, and somewhat at odds with the analysis of the planar images, which in all cases suggested that the bulk of the inhaled drug was in the central region of interest. That 50% of the dose was found in the peripheral lung highlights the difference in the information provided by SPECT when compared with planar scintigraphy. No other study has described aerosol deposition in this manner, and although Phipps et al (1989) demonstrated the power of SPECT, they failed to make use of all the data at their disposal by describing aerosol deposition only in terms of central and peripheral volumes of interest. It should now be possible to take this technique further, by attempting to define the anatomical structures contained within each shell in order to better study inhaled drug kinetics and dynamics. By taking care to deliver matching doses of different particle size aerosols of the same drug, it should be possible to describe with precision the site of action of a therapeutic aerosol, and to study the relationship between deposition site, drug pharmacokinetics and pharmacodynamics. The uses of SPECT could also extend to the study of ventilation in both normal and abnormal lungs, for example by SPECT imaging of ^{81}Kr inhalation, and comparison with the deposition and efficacy of inhaled

therapeutic agents. The problem of the rapid absorption of the radioisotope into the blood stream and its subsequent recirculation may be overcome by using nebulised radiolabelled aerosols in which the label can be attached to a non-absorbable substance, such as stannous phytate, without disturbing the particle size characteristics of the delivered aerosol. The use of nebulised aerosols has a further advantage over the MDI in that it is easier to produce aerosols of widely differing sizes. Clearly, though, further work needs to be done to attempt to identify a labelling technique for drugs contained within MDIs that will allow the delivery of an isotope that is not rapidly absorbed.

Any comparison of radiolabelled drug deposition and kinetics must take into account the possibility that the absorption of one compound may be influenced by the presence of the other. Thus, it seems as if the Tc^{99m} may have slowed at least the initial absorption phase of nedocromil sodium since in the SPECT study Tmax was longer than in the other 2 studies in this thesis in which nedocromil sodium Tmax was measured (chapters 3 & 4). Because there is no similar information available from other studies it was not possible to establish if the absorption of Tc^{99m} may have been similarly affected by the presence of nedocromil sodium. Why the absorption of nedocromil sodium should be affected by the presence of the radioisotope is not clear. It seems unlikely that the two molecules share the same pathway for absorption as nedocromil sodium is poorly absorbed from the gastro-intestinal tract, whereas close to 100% of an oral dose of technetium will be absorbed (Beasley et al, 1966).

Once inhaled, how is nedocromil sodium absorbed, and where is its site of action? The work presented in this thesis confirms that both in normal subjects and asthmatic volunteers, the drug displays absorption-limited pharmacokinetics. That is, the rate of appearance of the drug in the peripheral blood is dependant upon its concentration in the airways, and as shown here, absorption of the drug can be influenced both by multiple FEV_1 manoeuvres and deep inspiration with prolonged breath-holding, and also by premedication with probenecid. It is not known where in the lung the increased absorption occurs, although the finding that 50% of the drug reaching the lungs is in the outer 3 shells (chapter 6) suggests that any rapid changes in absorption as a consequence of respiratory manoeuvres is most likely to involve the lung periphery. It may be possible to investigate this by delivering matching doses of nedocromil sodium delivered as aerosols of very different sizes in order to achieve predominantly central or peripheral deposition, and then to repeat the respiratory manoeuvres and compare

the subsequent rises in plasma nedocromil sodium. It is also important to determine if the increases in nedocromil sodium absorption can influence its pharmacodynamics; if, as seems likely, it is most effective at the airway surface, then more rapid absorption from the airways may reduce either the degree or duration of efficacy. This could be investigated by firstly determining its duration of action by repeated AMP inhalation challenges over an 8 hour period in asthmatic subjects after the inhalation of nedocromil sodium, and then repeating the study during which subjects would perform repeated manoeuvres to increase drug absorption from the airways. The knowledge that probenecid premedication appears to hold up some fraction of the drug at the airway surface can also be used to compare the extent and duration of protection against inhaled AMP challenge in asthmatic subjects premedicated with a placebo substance or probenecid. The role of circulatory changes in the rapid increases induced by respiratory manoeuvres remains unclear. The work described here with inhaled methoxamine suggests that a reduction in mucosal blood flow does not influence the increases, but as discussed in chapter 4, it is possible that the manoeuvres influence intrathoracic blood flow at sites other than the mucosa. Another way to examine this would be to increase blood flow through the lung in resting subjects by, for example, the intravenous infusion of drugs that raise cardiac rate and output, and comparing the drug kinetics in 'stimulated' and 'unstimulated' subjects. Finally, this work begs the question whether the pharmacokinetics of other inhaled drugs can also be altered in the same manner by respiratory manoeuvres, and clearly this should be investigated.

The site of action of nedocromil sodium in protecting against AMP-induced bronchoconstriction appears to be at the airway surface, as the work in chapter 3 showed that the drug was much more effective when delivered by inhalation compared to either the oral or intravenous route in the group of asthmatics studied. However, the demonstration that equivalent protection was conferred by all 3 routes of administration in 2 subjects suggests that either it may have some action at sites deep to the airway lumen, or more likely that the drug was able to reach the airway surface through passage out of the blood vessels into the lumen. It is known that plasma can move from vessels into the lumen in response to inflammatory provocations at the mucosal surface (Persson et al, 1991). Subjects with high degrees of atopy and baseline airway hyperresponsiveness may have prominent inflammatory changes, and it is therefore possible that the drug is more easily able to leak out of mucosal blood vessels and into the airway tissues when compared to subjects with lesser degrees of inflammation.

The study in chapter 3 was done in order to assess the importance of drug delivery to the airways by the bronchial circulation. The ability of the bronchial circulation to deliver drugs to the lung is unquestioned, as evidenced by the therapeutic efficacy of such orally administered agents as corticosteroids and theophylline. However, the possibility that this circulation can redistribute drug from its site of deposition in proximal airways to sites of action downstream is intriguing. The fact that asthmatics with acute severe bronchoconstriction respond to inhaled drugs which would not be expected to penetrate the lung to any great extent lends support to this concept, and the anatomy of the bronchial circulation would lend itself to this function. This could be examined by using inspiratory manoeuvres to deliver a therapeutic aerosol to the proximal (preferably extrapulmonary) airways, and comparing the subsequent efficacy and pharmacokinetics to that of a similar dose delivered in such a way as to deposit in the periphery. A more invasive way to undertake this work would be instill the drug directly at discrete locations within the airways or lungs by use of a bronchoscope, and to compare the pharmacokinetics and efficacy with that of a matching inhaled dose.

The work described in chapter 3 may be interpreted in another way. The place of nedocromil sodium in the treatment of asthma is not yet clear (Geddes et al, 1989), and while the drug is undoubtedly effective in the treatment of asthma, it is unlikely to replace corticosteroids, but may be used in poorly-controlled asthmatics already taking corticosteroids, or in those poorly tolerant of inhaled corticosteroids. However, the bitter taste of the inhaled drug may prevent a significant number of patients from its prolonged use (Thomson, 1989). The observation that the drug was effective by the systemic route in highly atopic and hyperreactive asthmatics suggests that an oral preparation of nedocromil sodium may have some activity. It is those asthmatics who are poorly controlled on maximal therapy with inhaled or oral corticosteroids who may benefit, especially if the drug can be delivered in high enough doses without deleterious side-effects. This group of subjects are likely to be taking many doses of inhaled drug each day, and may appreciate the possibility of taking an active, safe and side-effect free oral preparation.

In conclusion, the work in this thesis has shown that when inhaled from a metered-dose inhaler, little nedocromil sodium deposits in the lungs, with approximately 8% of the inhaled dose found in the chest, of which approximately 50% is found in the lung periphery, as demonstrated by the new analytic techniques applied to 3-dimensional images of aerosol deposition. The drug exhibits absorption rate-limited

pharmacokinetics, and a proportion of its absorption is by a probenecid-sensitive facilitated transport mechanism. Its absorption from the lungs can be increased by manoeuvres that induce disruption of epithelial tight junctions. The drug is most effective when taken by inhalation, and may display activity in some asthmatics when delivered to the lungs by the systemic route. Although there is no correlation between plasma blood levels and the efficacy of the drug, there is a correlation between baseline airways responsiveness to inhaled AMP and the therapeutic efficacy of nedocromil sodium, suggesting that it may be of most benefit in asthmatics with high degrees of airways hyperreactivity.

References

Abraham WM, Stevenson JS, Eldridge M, Garrido R, Nieves L. 1988. Effect of nedocromil sodium in allergen-induced early and late bronchial responses and allergen-induced airway hyperresponsiveness in allergic sheep. J Appl Physiol 65; 1062-1068.

Allen J, Husar RB, Macias ES. 1979. Aerosol size and shape determination using a laser light scattering spectrometer. In: Lundgren et al, eds. Aerosol Measurement, University Presses of Florida, Gainesville, pp 313-320.

Altounyan REC, Cole M, Lee TB. 1986. Inhibition of sulphur dioxide-induced bronchoconstriction by nedocromil sodium and sodium cromoglycate in non-asthmatic atopic subjects. Eur J Respir Dis 69 (suppl 147); 274-276.

Anthracite RF, Vachon L, Knapp PH. 1971. Alpha-adrenergic receptors in the human lung. Psychosomatic Med 33; 481-489.

Axelsson B, Msaki P, Israelsson A. 1984. Subtraction of compton-scattered photons in single photon emission computed tomography. J Nucl Med 25; 490-494.

Baier H, Long WM, Wanner A. 1985. Bronchial circulation in asthma. Respiration 48; 199-205.

Baile EM, Albert RA, Kirk W, Lakshminarayan S, Wiggs BJR, Paré PD. 1984. Positive end-expiratory pressure decreases bronchial blood flow in the dog. J Appl Physiol 56; 1289-1293.

Barnes PJ, Basbaum CB, Nadel JA, Robert JM. 1982. Localisation of beta-adrenoceptors in the mammalian lung by light microscopic autoradiography. Nature 229; 444-447.

Barnes PJ & Pride NB. 1983. Dose-response curves to inhaled β-adrenoceptor agonists in normal and asthmatic subjects. Br J Clin Pharmac 15; 677-682.

Barnes PJ. 1986. Asthma as an axon reflex. Lancet 1; 242-245.

Bartosch R, Feldberg W, Nagel E. 1932. Das freinwerden eines histaminahulichen stoffes bei der anaphylaxie des merschweinchens. Pflugers Arch 230; 129.

Beasley R, Roche WR, Roberts JA, Holgate ST. 1989. Cellular events in the bronchi in mild asthma and after bronchial provocation. Am Rev Respir Dis 137; 806-817.

Beasley TM, Palmer HE, Nelp WB. 1966. Distribution and excretion of technetium in humans. Health Phys 12; 1425-1435.

Bel EH, Timmers MC, Hermans J, Dijkman JH, Sterk PJ. 1990. The long term effects of nedocromil sodium and beclomethasone dipropionate on bronchial responsiveness to methacholine in nonatopic asthmatic subjects. Am Rev Respir Dis 141; 21-28.

Bennett WD & Ilowite JS. 1989. Dual pathway clearance of ^{99m}Tc-DTPA from the bronchial mucosa. Am Rev Respir Dis 139; 1132-1138.

Bergmann KC, Bauer CP, Overlack A. 1990. A placebo-controlled blinded comparison of nedocromil sodium and beclomethasone dipropionate in bronchial asthma. Lung (suppl 1); 230-239.

Best CH. 1927. The nature of the vasodilator constituents of certain tissue extracts. J Physiol 62; 397.

Bick RL & Ross ES. 1985. Clinical use of intrapulmonary heparin. Semin Thromb Haemost 11; 213-217.

Black JL, Salome CM, Yan K, Shaw J. 1982. Comparison between airways response to an α-adrenoceptor agonist and histamine in asthmatic and non-asthmatic subjects. Clin Pharmac 14; 464-466.

Bone MF, Kubik MM, Keaney NP, Summers GD, Connolly CK, Sherwood Burge P, Dent RG, Allan GW. 1989. Nedocromil sodium in adults with asthma dependant on inhaled corticosteroids: a double blind, placebo controlled study. Thorax 44; 654-659.

Boschetto P, Roberts NM, Rodgers DF, Barnes PJ. 1989. Effects of anti-asthma drugs on microvascular leakage in guinea-pig airways. Am Rev Respir Dis 139; 416-421.

Boucher RC, Ranga V, Paré PD, Inoue S, Moroz LA, Hogg JC. 1978. Effect of histamine and methacholine on guinea pig tracheal permeability to HRP. J Appl Physiol 45; 939-948.

Bouchikhi A, Becquemin MH, Bignon J, Roy M, Teillac A. 1988. Particle size study of nine metered dose inhalers, and their deposition probabilities in the airways. Eur Respir J 1; 547-552.

Boulet LP, Cartier A, Cockcroft DW, Gruber JM, Laberge F, MacDonald GF, Malo JL, Mazza JA, Moote WD, Sandham JD, Thomas P. 1990. Tolerance to reduction of oral steroid dosage in severely asthmatic patients receiving nedocromil sodium. Respir Med 84; 317-323.

Boushey HA, Holtzmann MJ, Sheller JR, Nadel JA. 1980. Bronchial hyperreactivity. Am Rev Respir Dis 121; 389-413.

Brain JD, Knudson DE, Sorokin SP, Davis MA. 1976. Pulmonary distribution of particles given by intratracheal instillation or by aerosol inhalation. Env Res 11; 13-33.

Briscoe WA & DuBois AB. 1958. The relationship between airway resistance, airway conductance and lung volume in subjects of different age and body size. J Clin Invest 37; 1279-1285.

Bruijnzeel PLB, Warringa RAJ, Kok PTM. 1989. Inhibition of platelet-activating factor- and zymosan-activated serum-induced chemotaxis of human neutrophils by nedocromil sodium, BN 52021 and sodium cromoglycate. Br J Pharmac 97; 1251-1257.

Burch SG, Erbland ML, Gann LP, Hiller FC. 1988. Plasma nicotine levels after inhalation of aerosolised nicotine. Am Rev Respir Dis 137; A159.

Butler J, Caro C, Alkaler R, DuBois B. 1960. Physiological factors affecting airway resistance in normal subjects and in patients with obstructive airways disease. J Clin Invest 39; 584-591.

Carrasco E & Sepulveda R. 1986. The acceptability, tolerability and safety of nedocromil sodium in long term clinical use. Eur J Respir Dis 69; 327-329.

Chai H, Farr RS, Froelich LA, Mathison DA, McLean JA, Rosenthal RR, Sheffer AL, Spector SL, Townley RG. 1975. Standardization of bronchial inhalation challenge procedures. J Allergy Clin Immunol 56; 323-327.

Chan TL & Yu CP. 1982. Charge effects on particle deposition in the human tracheobronchial tree. In Walton WH, ed. Inhaled particles V. Oxford: Pergamon Press, 65-75.

Cheema MS, Groth S, Marriott C. 1988. Binding and diffusion characteristics of ^{14}C EDTA and ^{99m}Tc DTPA in respiratory tract mucus glycoprotein from patients with chronic bronchitis. Thorax 43; 669-673.

Chen KK & Schmidt CF. 1926. The action and use of ephedrine. JAMA 87; 836-841.

Chung KF, Jeyasingh K, Snashall PD. 1988. Influence of airway calibre on the intrapulmonary dose and distribution of inhaled aerosol in normal and asthmatic subjects. Eur Respir J 1; 890-895.

Church MK. 1978. Cromoglycate-like anti-allergic drugs, a review. Drugs Today 14; 281-341.

Clarke SW. 1984. Anatomy and physiology of the human lung: aspects relevant to aerosols. In: Clarke SW, Pavia D, eds. Aerosols and the lung. Butterworths, London, pp 9-18.

Clay MM, Pavia D, Clarke SW. 1986. Effect of aerosol particle size on bronchodilatation with nebulised terbutaline sulphate in asthmatic subjects. Thorax 41; 364-368.

Cotes JE. 1979. Lung function: Assessment and Applications in Medicine. 4th ed. Blackwell Scientific, Oxford.

Crimi E, Brusasco V, Brancatisano M, Losurdo E, Crimi P. 1987. Effect of nedocromil sodium on adenosine- and methacholine-induced bronchospasm in asthma. Clin Allergy 17; 135-141.

Crimi N, Palermo F, Oliveri R, Palermo B, Vancheri C, Polosa R, Mistretta A. 1988. Effect of nedocromil on bronchospasm induced by inhalation of substance P. Clin Allergy 18; 375-382.

Cushley MJ, Tattersfield AE, Holgate ST. 1984. Adenosine induced bronchoconstriction in asthma: antagonism by inhaled theophylline. Am Rev Respir Dis 129; 380-384.

Dahlén S-E, Bjork T, Kumlin M, Sydbom A, Raud J, Palmertz U, Franzen L, Gronneberg R, Hedqvist P. 1989. Dual inhibitory action of nedocromil sodium on antigen-induced inflammation. Drugs 37 (suppl 1); 63-68.

Damon M, Chavis C, Daures JP, Crastes de Paulet A, Michel FB, Godard PH. 1989. Increased generation of the arachidonic metabolites LTB4 and 5-HETE by human alveolar macrophages in patients with asthma: effect in vitro of nedocromil sodium. Eur Respir J 2; 202-209.

Deffebach ME, Charan NB, Lakshminarayan S, Butler J. 1987. The bronchial circulation. Am Rev Respir Dis 135; 463-481.

Dinh Xuan AT, Chaussain M, Regnard J, Lockart A. 1989. Pretreatment with an inhaled α-adrenergic agonist, methoxamine, reduces exercise-induced asthma. Eur Respir J 2; 409-414.

Dixon CMS & Barnes PJ. 1989. Bradykinin-induced bronchoconstriction: inhibition by nedocromil sodium and sodium cromoglycate. Br J Clin Pharmac 27; 831-836.

Djukanović R, Roche WR, Wilson JW, Beasley CRW, Twentyman OP, Howarth PH, Holgate ST. 1990. Mucosal inflammation in asthma. Am Rev Respir Dis 142; 434-457.

Dolovich M, Ryan G, Newhouse MT. 1981a. Aerosol penetration into the lung; influence on airway responses. Chest 80 (suppl); 834-836.

Dolovich M, Ruffin RE, Roberts R, Newhouse MT. 1981b. Optimal delivery of aerosols from metered dose inhalers. Chest 80 (suppl); 911-915.

Dolovich M. 1989. Physical principles underlying aerosol therapy. J Aerosol Med 2; 171-186.

Donna E, Danta I, Kim CS, Wanner A. 1989. Relationship between deposition of and responsiveness to inhaled methacholine in normal and asthmatic subjects. J Allergy Clin Immunol 83; 456-461.

Dorow P. 1986. A double-blind group comparative trial of nedocromil sodium and placebo in the management of bronchial asthma in steroid-dependant patients. Eur J Respir Dis 69 (suppl. 147); 317-319.

Douglas JG, Leslie JK, Crompton GK, Grant IWB. 1985. Is the flow rate used to drive a jet nebuliser clinically important? Br J Dis Chest 290; 29.

Drazen JM, Hirschman C, Macklem PT, Pauwels R, Permutt S, Persson C. 1989. Physiology. In: Holgate ST ed. The Role of Inflammatory Processes in Airway Hyperresponsiveness. Blackwell Scientific, Oxford, U.K., pp 108-150.

DuBois AB, Botelho SY, Comroe JH Jr. 1956. A new method for measuring airway resistance in man using a body plethsmograph: values in normal subjects and in patients with respiratory disease. J Clin Invest 35; 327-335.

Dusser DJ, Minty BD, Collignon M-AG, Hinge D, Barritault G, Huchon GJ. 1986. Regional respiratory clearance of aerosolised ^{99m}Tc-DTPA: posture and smoking effects. J Appl Physiol 60; 2000-2006.

Eady RP. 1986. The pharmacology of nedocromil sodium. Eur J Respir Dis 69 (Suppl 147); 112-119.

Egan AE. 1980. Response of alveolar epithelial solute permeability to changes in lung inflation. J Appl Physiol 49; 1032-1036.

Elwood RK, Kennedy S, Belzberg A, Hogg JC, Pare PD. 1983. Respiratory mucosal permeability in asthma. Am Rev Respir Dis 128; 523-527.

Erjefalt I & Persson CGA. 1986. Anti-asthma drugs attenuate inflammatory leakage into airway lumen. Acta Physiol Scand 128; 653-655.

Erjefalt I & Persson CGA. 1989. Inflammatory passage of plasma macromolecules into airway wall and lumen. Pulm Pharmacol 2; 93-102.

Evander E, Wollmer P, Jonson B, Lachmann B. 1987. Pulmonary clearance of inhaled ^{99m}Tc-DTPA: effects of surfactant depletion by lung lavage. J Appl Physiol 62; 1611-1614.

Evans TW, Rogers DF, Aursudkij B, Chung KF, Barnes PJ. 1987. Role of mediators in airway vascular permeability induced by antigen. Am Rev Respir Dis 135; 315 (Abstract).

Fairshter RD & Wilson AF. 1980. Relationship between the site of airflow limitation and the bronchodilator response in asthma. Am Rev Respir Dis 122; 27-32.

Fleming J. 1979a. Technique for contralateral subtraction in lateral lung radionuclide imaging. Med Biol Eng & Comput 17; 751-756.

Fleming J. 1979b. A technique for the absolute measurement of activity using a gamma camera and computer. Phys Med Biol 24; 176-180.

Fleming J, Britten AJ, Blake GM, Gray J, Howlett PJ. 1987. A general software system for the handling of medical images. Nuc Med Comm 8; 270.

Fleming J. 1989. A technique for using CT images in attenuation correction and quantification in SPECT. Nuc Med Comm 10; 83-97.

Fuller RW & Collier JG. 1983. The pharmacokinetic assessment of sodium cromoglycate. J Pharm Pharmacol 35; 289-292.

Fyans PG, Chatterjee PC, Chatterjee SS. 1986. A trial comparing nedocromil sodium (Tilade) and placebo in the management of bronchial asthma. Clin Allergy 16; 505-511.

Fyans PG, Chatterjee PC, Chatterjee SS. 1989. Effects of adding nedocromil sodium (Tilade) to the routine therapy of patients with bronchial asthma. Clin Exp Allergy 19; 521-528.

Gale AE. 1985. Drug degeneration during ultrasonic nebulisation. J Aerosol Sci 16; 265-7.

Gardiner TH & Schanker LS. 1974. Absorption of disodium cromoglycate from the rat lung: evidence of carrier transport. Xenobiotica 12; 725-731.

Gardner JJ, Preston JR, Gilbert CM, Wilkinson DJ, Lockley WJS, Brown K. 1988. A radioimmunoassay method for the determination of nedocromil sodium in plasma and urine. J Pharm Biomed Anal 6; 285-297.

Geddes DM, Turner-Warwick M, Brewis RAL, Davies RJ. 1989. Nedocromil sodium workshop. Respir Med 83; 265-267.

Gemmell HG. 1989. Single photon emission computed tomography. In: Sharp PF, Gemmell HG, Smith FW, eds. Practical nuclear medicine. IRL Press, Oxford. pp 39-51.

Ghosh S, Neale MG, McIlroy I, Patel KR. 1989. Effect of physiological manoeuvres on the absorption of inhaled nedocromil sodium. Thorax 44; 888P.

Gibaldi M & Perrier D. 1982. Pharmacokinetics, 2nd ed. Marcel Dekker, Madison Ave, New York.

Gibaldi M. 1984. Noncompartmental pharmacokinetics. In: Gibaldi M, ed. Biopharmaceutics and Clinical Pharmacokinetics. Lea and Febiger, Philadelphia, pp 17-28.

Gillett MK, Briggs BA, Snashall PD. 1989. The influence of aerosol retention and pattern of deposition on bronchial responsiveness to atropine and methacholine in humans. Am Rev Respir Dis 140; 1727-1733.

Godfrey S, Zeidifard E, Brown K, Bell JH. 1974. The possible site of action of sodium cromoglycate assessed by aerosol challenge. Clin Sci Mol Med 46; 265-272.

Goldin JG & Bateman ED. 1988. Does nedocromil sodium have a steroid sparing effect in adult asthmatic patients requiring maintenance oral corticosteroids? Thorax 43; 982-986.

Gonzalez JP & Brogden RN. 1987. Nedocromil sodium: a preliminary review. Drugs 34; 560-577.

Goodwin PN & Rao DV. 1977. The structure of matter. In: The physics of nuclear medicine. Charles C Thomas, Springfield, Illinois, USA. pp 2-24.

Graeser JB & Rowe AH. 1935. Inhalation of epinephrine for the relief of asthmatic symptoms. J Allergy 6; 415-420.

Graham JR, Malvea BP, Gramm HF. 1960. Aerosol ergotamine tartrate for migraine and Horton's syndrome. N Eng J Med 263; 802-804.

Grega GJ, Svensjo E, Haddy FJ. 1982. Macromolecular permeability of the microvascular membrane: physiological and pharmacological regulation. Microcirculation 1; 325-341.

Griffiths WD, Iles PJ, Vaughan NP. 1986. The behaviour of liquid droplet aerosols in an APS 3300. J Aerosol Sci 17; 921-930.

Gumbiner B. 1987. Structure, biochemistry, and assembly of epitheliial tight junctions. Am J Physiol 253; C749-C758.

Hadfield JW, Windebank WJ, Bateman JRM. 1986. Is driving gas flow rate clinically important for nebuliser therapy? Br J Dis Chest 80; 50-54.

Hallworth GW & Andrews UG. 1976. Size analysis of suspension inhalation aerosols by inertial separation methods. J Pharm Pharmacol 28; 898-907.

Hallworth GW & Hamilton RR. 1976. Size analysis of metered suspension pressurized aerosols with the Quantimet 720. J Pharm Pharmacol 28; 890-897.

Hallworth GW & Westmoreland DG. 1987. The twin impinger: a simple device for assessing the delivery of drugs from metered dose pressurised aerosol inhalers. J Pharm Pharmacol 39; 966-972.

Heyder J. 1982. Particle transport onto human airway surfaces. Eur J Respir Med 63 (suppl 119); 29-50.

Heyder J, Gebhart J, Rudolf G, Schiller CF, Stahlhofen W. 1986. Deposition of particles in the human respiratory tract in the size range 0.005-15 μm. J Aerosol Sci 17; 811-825.

Hiller FC, Mazumder M, Wilson D, Bone R. 1978. Aerodynamic size distribution of metered-dose bronchodilator aerosols. Am Rev Respir Dis 118; 311-317.

Hiller FC, Mazumder MK, Wilson JD, Bone RC. 1980a. Effect of low and high relative humidity on metered-dose bronchodilator solution and powder aerosols. J Pharm Sci 69; 334-337.

Hiller FC, Mazumder MK, Wilson JD, Bone RC. 1980b. Aerodynamic size distribution, hygroscopicity and deposition estimation of beclomethasone dipropionate aerosol. J Pharm Pharmacol 32; 605-609.

Hiller FC, Mazumder MK, Wilson JD, Wison FJ, Bone RC. 1983. Aerodynamic size distribution of therapeutic aerosols: a review of studies of several devices using the single particle aerodynamic relaxation time analyser. Aerosol Science Technology 2; 298.

Hiscock NRJ. 1980. Plethysmographic instrumentation. M Sc Dissertation. University of Southampton.

Holtzman MJ, Sheller JR, Dimeo M, Nadel JA, Boushet HA. 1980. Effect of ganglionic blockade on bronchial reactivity in asthmatic subjects. Am Rev Respir Dis 122; 17-25.

Honda I, Shimura S, Sasaki T, Sasaki H, Takishima T, Nakamura M. 1988. Airway mucosal permeability in chronic bronchitics and bronchial asthmatics with hypersecretion. Am Rev Respir Dis 137; 866-871.

Hutson PA, Holgate ST, Church MK. 1988. Inhibition of nedocromil sodium of early and late phase bronchoconstriction and airway cellular infiltration provoked by ovalbumin inhalation in conscious sensitised guinea pigs. Br J Pharmacol 94; 6-8.

ICRP, 1987. Annals of the International Commission on Radiation Protection, publication 53. Pergamon Press, Oxford, UK, vol 18, nos 1-4.

Ilowhite JS, Bennett WD, Sheetz MS, Groth ML, Nierman DM. 1989. Permeability of the bronchial mucosa to ^{99m}Tc-DTPA in asthma. Am Rev Respir Dis 139; 1139-1143.

Jackson DM & Eady RP. 1988. Acute transient SO2-induced airway hyperreactivity: effects of nedocromil sodium. J Appl Physiol 65; 1119-1124.

Jackson DM, Norris AA, Eady RP. 1989. Nedocromil sodium and sensory nerves in the dog lung. Pulmonary Pharmacology 2; 179-184.

Jay SJ. 1979. Pulmonary alveolar proteinosis: successful treatment with aerosolised trypsin. Am J Med 66; 348-354.

Johnson MA, Newman SP, Bloom R, Talaee N, Clarke SW. 1989. Delivery of albuterol and ipratropium bromide from two nebuliser systems in chronic stable asthma. Chest 96; 1-10.

Jones JG, Minty BD, Royston D. 1982. The physiology of leaky lungs. Br J Anaesth 54; 705-721.

Joos GS, Pauwels RA, Van Der Straeten ME. 1988. The effect of nedocromil sodium on the bronchoconstrictor effect of neurokinin A in asthmatics. J. Allergy Clin Immunol 81; 276.

Juniper EF, Kline PA, Morris MM, Hargreave FE. 1987. Airway constriction by isocapnic hyperventilation of cold, dry air: comparison of magnitude and duration of

protection by nedocromil sodium and sodium cromoglycate. Clin Allergy 174; 523-528.

Kim CS, Trujillo D, Sackner MA. 1985. Size aspects of metered-dose inhaler aerosols. Am Rev Respir Dis 132; 137-142.

Kirk WF. 1972. In vitro method of comparing clouds produced from inhalation aerosols for efficiency in penetration of airways. J Pharm Sci 61; 262-265.

Köhler D, Fleischer W, Matthys H. 1988. New method for easy labelling of beta-2-agonists in the metered dose inhaler with technetium-99m. Respiration 53; 65-73.

Konzett H. 1940. News zur asthma therapie. Klin Wochenschr 19; 1305-1306.

Laitinen LA, Heino M, Laitinen A, Kava T, Haahtela T. 1985. Damage to the airway epithelium and bronchial reactivity in patients with asthma. Am Rev Respir Dis 131; 599-606.

Laitinen LA, Laitinen A, Widdicombe J. 1987. Effects of inflammatory and other mediators on airway vascular beds. Am Rev Respir Dis 135; S67-S70.

Lal S, Malhotra S, Gribben D, Hodder D. 1986. An open assessment study of the acceptability, tolerability and safety of nedocromil sodium in long term clinical use in patients with perennial asthma. Eur J Respir Dis 69; 136-142.

Laube BL, Swift DL, Wagner HN, Norman PS, Adams GK. 1986. The effect of bronchial obstruction on central airway deposition of a saline aerosol in patients with asthma. Am Rev Respir Dis 133; 740-743.

Legros F, Akodad EM, De Mayer P, Yernault JC, Van Vooren JP. 1990. Liposomal encapsulation of gentamicin decreases blood levels after intratracheal administration. Eur Respir J 3 (suppl 10); 281s.

Leung KBP, Flint KC, Brostoff J, Hudspith BN, Johnson N McI, Lau HYA, Liu WL, Pearce FL. 1988. Effects of sodium cromoglycate and nedocromil sodium on histamine secretion from human lung mast cells. Thorax 43; 756-761.

Lewis RA. 1984. Inhalation drugs in asthma management: state of the art, factors affecting delivery, and clinical response to inhaled drugs. NER Allergy Proc 5; 23-33.

Logus JW, Trajan M, Hooper HR, Lentle BC, Man SFP. 1984. Single photon emission tomography of lungs imaged with ^{99m}Tc-labelled aerosol. J Can Assoc Radiol 35; 133-138

Lorino AM, Meignan M, Bouissou P, Atlan G. 1989. Effects of sustained exercise on pulmonary clearance of aerosolised ^{99m}Tc-DTPA. J Appl Physiol 67; 2055-2059.

Machin D & Cambell MJ. 1987. Statistical tables for the design of clinical trials. Blackwell Scientific, Oxford, UK.

Mann JS, Holgate ST, Renwick AG, Cushley MJ. 1986. Airway effects of purine nucleosides and nucleotides and release with bronchial provocation in asthma. J Appl Physiol 61; 1667-1676.

Marks JD, Luce JM, Lazar NM, Ngao-sun Wu J, Lipavsky AJA, Murray JF. 1985. Effect of increases in lung volume on clearance of aerosolised solute from human lungs. J Appl Physiol 59; 1242-1248.

Marple VA & Willeke K. 1979. Inertial impactors. In: Lundgren et al, eds. Aerosol Measurement. University Presses of Florida, Gainesville, pp 91-107.

Marple VA & Rubow KL. 1980. Aerosol generation: concept and parameters. In: Willeke K, ed. Generation of aerosols and facilities for exposure experiments. Ann Arbor Science Publishers, pp 3-29.

May KR. 1966. Multistage liquid impinger. Bacteriological Reviews 30; 559-570.

McDonald DM. 1987. Neurogenic inflammation in the respiratory tract: actions of sensory nerve mediators on blood vessels and epithelium of the mucosa. Am Rev Respir Dis 136; S65-S72.

Mead J, Turner JM, Macklem PT. 1967. Significance of the relationship between lung recoil and maximal expiratory flow. J Appl Physiol 22; 95-108.

Meakin BJ & Stroud N. 1983. An evaluation of some metered dose aerosols using a twin stage impinger sampling device. J Pharm Pharmacol 35 (suppl); 7P.

Meignan M, Rosso J, Leveau J, Katz A, Cinotti L, Madelaine G, Galle P. 1986. Exercise increases the lung clearance of inhaled technetium-99m DTPA. J Nucl Med 27; 274-280.

Melandri C, Prodi V, Tarroni G, Formignani M, De Zaiazomo T, Bompane GF, Maestri G. 1977. On the deposition of unipolar charged particles in the human respiratory tract. In: Walton WH, ed. Inhaled particles IV. Pergamon Press, Oxford, pp 193-200.

Miller RF, Godfrey-Faussett P, Semple SJG. 1989. Nebulised pentamidine as treatment for *Pneumocystis carinii* pneumonia in the acquired immunodeficiency syndrome. Thorax 44; 565-569.

Mitchell DM, Solomon MA, Tolfree SEJ, Short M, Spiro SG. 1987. Effect of particle size of bronchodilator aerosols on lung distribution and pulmonary function in patients with chronic asthma. Thorax 42; 457-461.

Modell HL, Beck K, Butler J. 1981. Functional aspects of canine broncho-pulmonary vacular communications. J Appl Physiol 50; 1045-1051.

Moqbel R, Cromwell O, Walsh GM, Wardlaw AJ, Kurlak L, Kay AB. 1988. The effects of nedocromil sodium (Tilade) on activation of human eosinophils, neutrophils and histamine release from mast cells. Allergy 43; 268-276.

Moqbel R, Cromwell O, Kay AB. 1989. The effect of nedocromil sodium on human eosinophil activation. Drugs 37 (suppl 1); 19-22.

Morén F. 1978. Drug deposition of pressurized inhalation aerosols. II Influence of vapour pressure and metered volume. Int J Pharm 1; 213-218.

Morén F & Andersson J. 1980. Fraction of dose exhaled after administration of pressurised inhalation aerosols. Int J Pharm 6; 295-300.

Morrow PE. 1974. Aerosol characterisation and deposition. Am Rev Respir Dis 110; 88-99.

Nair N, Hopp RJ, Townley R. 1989. Effect of nedocromil on antigen-induced bronchoconstriction in asthmatic subjects. Ann Allergy 62; 329-331.

Neale MG, Brown K, Hodder RW, Auty RM. 1986. The pharmacokinetics of sodium cromoglycate in man after intravenous and inhalation administration. Br J Clin Pharmac 22; 373-382.

Neale MG, Brown K, Foulds RA, Lal S, Morris DA, Thomas D. 1987. The pharmacokinetics of nedocromil sodium, a new drug for the treatment of reversible obstructive airways disease, in human volunteers and patients with reversible obstructive airway disease. Br J Clin Pharmac 24; 493-501.

Neale MG, Albazzaz M, Patel KR. 1988. Absorption of nedocromil sodium from the lungs: effect of exercise challenge. Thorax 43; 251P.

Newman SP, Pavia D, Clarke SW. 1980. Simple instructions for using pressurized aerosol bronchodilators. J Royal Soc Med 73; 776-779.

Newman SP, Morén F, Pavia D, Little F, Clarke SW. 1981a. Deposition of pressurised suspension aerosols inhaled through extension devices. Am Rev Respir Dis 124; 317-320.

Newman SP, Morén F, Pavia D, Sheahan NF, Clarke W. 1981b. Deposition of pressurised aerosols in the human respiratory tract. Thorax 36; 52-55.

Newman SP, Morén F, Pavia D, Corrado O, Clarke SW. 1982a. The effects of changes in metered volume and propellant vapour pressure on the deposition of pressurized aerosols. Int J Pharm 11; 337-344.

Newman SP, Pavia D, Garland N, Clarke SW. 1982b. Effects of various inhalation modes on the deposition of radioactive pressurised aerosols. Eur J Respir Dis 63 (suppl 119); 57-65.

Newman SP & Clarke SW. 1983. Therapeutic aerosols I - Physical and practical considerations. Thorax 38; 881-886.

Newman SP, Pellow PGD, Clarke SW. 1986. Droplet size distributions of nebulised aerosols for inhalation therapy. Clin Phys Physiol Meas 7; 139-146.

Newman SP, Clark AR, Talaee N, Clarke SW. 1989a. Pressurised aerosol deposition in the human lung with and without an "open" spacer device. Thorax 44; 706-710.

Newman SP, Morén F, Trofast E, Talaee N, Clarke SW. 1989b. Deposition and clinical efficacy of terbutaline sulphate from Turbuhaler, a new multi-dose inhaler. Eur Respir J 2; 247-252.

Nishizawa K, Maruyama T, Takayama M, Okada M, Hachiya J, Furuya Y. 1991. Determinations of organ doses and effective dose equivalents from computed tomographic examination. Br J Radiol 64; 20-28.

Nogrady SG & Beven C. 1981. H_2-receptor blockade and bronchial hyperreactivity to histamine in asthma. Thorax 36; 268-271.

Nolop KB, Maxwell DL, Royston D, Hughes JMB. 1986. Effect of raised thoracic pressure and volume on ^{99m}Tc-DTPA clearance in humans. J Appl Physiol 60; 1493-1497.

Norušis MJ. 1988. Statistical program for the social sciences. SPSS Inc, Chicago, USA.

O'Brodovich H & Coates G. 1987. Pulmonary clearance of ^{99m}Tc-DTPA: a noninvasive assessment of epithelial integrity. Lung 165; 1-16.

O'Byrne PM, Dolovich M, Dirks R, Roberts RS, Newhouse MT. 1984. Lung epithelial permeability: relation to nonspecific airway responsiveness. J Appl Physiol 57; 77-84.

O'Donnell S & Barnett CJK. 1987. Microvascular leakage due to platelet activating factor in guinea-pig trachea and bronchi. Eur J Pharmacol 138; 385-396.

Paananen M, Karakarop T, Kreus KE. 1986. Withdrawal of inhaled corticosteroids under cover of nedocromil sodium. Eur J Respir Dis 69; 330-335.

Padfield JM, Winterborn IK, Pover GM, Tattersfield A. 1983. Correlation between inertial impactor performance of a bronchodilator aerosol. J Pharm Pharmacol 35 (suppl); 10P.

Patel P, Mukai D, Wilson AF. 1990. Dose-response effects of two sizes of monodisperse isoproterenol in mild asthma. Am Rev Respir Dis 141; 357-360.

Paterson JW, Woolcock AL, Shenfield GM. 1979. Bronchodilator drugs. Am Rev Respir Dis 120; 1149-1188.

Pauwels R. 1986. Pharmacokinetics of inhaled drugs. In: Morén F, Newhouse MT, Dolovich MB. Aerosols in Medicine: Principles, Diagnosis and Therapy. Elsiever, Amsterdam, 219-224.

Pavia D, Thomson ML, Clarke SW, Shannon HS. 1977. Effect of lung function and mode of inhalation on penetration of aerosol into the human lung.
Thorax 32; 194-197.

Pepys J. 1975. Skin testing. Br J Hosp Med 14; 412.

Persson CGA & Svenjso E. 1983. Airway hyperreactivity and microvascular permeability to large molecules. Eur J Respir Dis 64 (suppl 131); 183-214.

Persson CGA & Erjefalt I. 1986. Inflammatory leakage of macromolecules from the vascular compartment into the tracheal lumen. Acta Physiol Scand 126; 615-616.

Persson CGA. 1986. Role of plasma exudation in asthmatic airways. Lancet ii, 1126-1129.

Persson CGA. 1987. Leakage of macromolecules from the tracheobronchial circulation. Am Rev Respir Dis 135; S571-S575.

Persson CGA, Erjefalt I, Alkner U, Baumgarten C, Greiff L, Gustafsson B, Luts A, Pipkorn U, Sundler F, Svensson C, Wollmer P. 1991. Plasma exudation as a first line respiratory defence. Clin Exp Allergy 21; 17-24.

Persson G & Wirén JE. 1989. The bronchodilator response from inhaled terbutaline is influenced by the mass of small particles: a study on a dry powder inhaler (Turbuhaler®). Eur Respir J 2; 253-256.

Phillips GD, Rafferty P, Beasley R, Holgate ST. 1987. Effect of oral terfenadine on the bronchoconstrictor response to inhaled histamine and adenosine-5'-monophosphate. Thorax 42; 939-945.

Phillips GD & Holgate ST. 1988. Absence of a late phase response or increase in histamine responsiveness after bronchial provocation with adenosine-5'-monophosphate in atopic and non-atopic asthma. Clin Sci 75; 429-436.

Phillips GD, Scott VL, Richards R, Holgate ST. 1989. Effect of nedocromil sodium and sodium cromoglycate against bronchoconstriction induced by inhaled adenosine-5'-monophosphate. Eur Respir J 2; 210-217.

Phipps PR, Gonda I, Bailey DL, Borham P, Bautovich G, Anderson SD. 1989. Comparisons of planar and tomographic gamma scintigraphy to measure the penetration index of inhaled aerosols. Am Rev Respir Dis 139; 1516-1523.

Phipps PR & Gonda I. 1990. Droplets produced by medical nebulisers. Chest 97; 1327-1332.

Polli GP, Grim WM, Bacher FA, Yunker MH. 1969. Influence of formulation on aerosol particle size. J Pharm Sci 58; 484-486.

Polosa R, Holgate ST, Church MK. 1989. Adenosine as a pro-inflammatory mediator in asthma. Pulmonary Pharmacology 2; 21-26.

Pride NB. 1971. The assessment of airflow obstruction. Role of measurements of airways resistance and tests of forced expiration. Br J Dis Chest 65; 135-169.

Rafferty P, Beasley R, Holgate ST. 1987a. The contribution of histamine to immediate bronchoconstriction provoked by inhaled allergen and adenosine-5'-monophosphate in atopic asthma. Am Rev Respir Dis 136, 369-373.

Rafferty P & Holgate ST. 1987b. Terfenadine (Seldane) is a potent and selective histamine H_1—receptor antagonist in asthmatic airways. Am Rev Respir Dis 135; 181-184.

Rance RW. 1974. Studies of the factors controlling the action of hair sprays-III: The influence of particle velocity and diameter on the capture of particles by arrays of hair fibres. J Soc Cosmet Chem 25; 545-561.

Ranga V, Powers MA, Padilla M, Strope GL, Fowler L, Kleinerman J. 1983. Effect of allergic bronchoconstriction on airways epithelial permeability to large polar solutes in the guinea pig. Am Rev Respir Dis 128; 1065-1070.

Rao AK & Whitby KT. 1978. Non-ideal collection characteristics of inertial impactors - II. Cascade impactors. J Aerosol Sci 9; 87-100.

Redding JS, Asuncion JS, Pearson JW. 1967. Effective routes of drug administration during cardiac arrest. Anaesth Analg 46; 253-258.

Rees PJ, Clark TJH, Morén F. 1982. The importance of particle size in response to inhaled bronchodilators. Eur J Respir Dis 63 (suppl 119); 73-78.

Richards IM, Eady RP, Harper ST, Jackson DM, Orr TSC, Pritchard DI, Vendy K, Wells E. 1983. *Ascaris*-induced bronchoconstriction in primates experimentally infected with *Ascaris suum* ova. Clin Exp Immunol 54; 461-468.

Richards R, Dickson CR, Renwick AG, Lewis RA, Holgate ST. 1987. Absorption and disposition kinetics of cromolyn sodium and the influence of inhalation technique. J Pharmacol Exp Therapy 27; 1028-1032.

Richards R, Fowler C, Simpson S, Renwick AG, Britten A, Holgate ST. 1988a. Inhaled histamine increases the rate of absorption of sodium cromoglycate from the lung. Br J Clin Pharmac 25; 665P.

Richards R, Haas A, Simpson S, Britten A, Renwick A, Holgate S. 1988b. Effect of methacholine-induced bronchoconstriction on the pulmonary distribution and plasma pharmacokinetics of inhaled sodium cromoglycate in subjects with normal and hyperreactive airways. Thorax 43; 611-616.

Richards R, Fowler C, Simpson SF, Renwick AG, Holgate ST. 1989a. Deep inspiration increases the absorption of inhaled sodium cromoglycate. Br J Clin Pharmac 27; 861-865.

Richards R, Phillips GD, Holgate ST. 1989b. Nedocromil sodium is more potent than sodium cromoglycate against AMP-induced bronchoconstriction in atopic asthmatic subjects. Clin Exp Allergy 19; 285-291.

Riley PA, Mather ME, Keogh RW, Eady RP. 1987. Activity of nedocromil sodium in mast cell-dependent reactions in the rat. Int Arch Allergy Appl Immunol 82; 108-110.

Rizk NW, Luce JM, Hoeffel JM, Price DC, Murray JF. 1984. Site of deposition and factors affecting clearance of aerosolised solute from dog lungs. J Appl Physiol 56; 723-729.

Ruffin RE, Kenworthy MC, Newhouse MT. 1978a. Response of asthmatics to fenoterol inhalation: a method of quantifying the airway bronchodilator dose. Clin Pharmacol Ther 23; 338-345.

Ruffin RE, Dolovich MB, Wolff RK, Newhouse MT. 1978b. The effects of preferential deposition of histamine in the human airway. Am Rev Respir Dis 117; 485-492.

Rumble RH & Roberts MS. 1985. Detection of benylpenicillin in plasma and urine by high performance liquid chromatography. J Chromatogr 342; 436-441.

Ryan G, Dolovich M, Obminski G, Cockcroft DW, Juniper E, Hargreave FE, Newhouse MT. 1981a. Standardisation of inhalation provocation tests: Influence of nebuliser output, particle size and method of inhalation. J Allergy Clin Immunol 67; 156-161.

Ryan G, Dolovich M, Roberts R, Frith PA, Juniper EF, Hargreave FE, Newhouse MT. 1981b. Standardisation of inhalation provocation tests: two techniques of aerosol generation and inhalation compared. Am Rev Respir Dis 123; 195-199.

Schanker LS. 1978. Drug absorption from the lung. Biochem Pharmacol 27; 381-385.

Schoeffel RE, Anderson SD, Seale JP. 1981. The protective effect and duration of action of metaproteronol on exercise-induced asthma. Ann Allergy 46; 273-275.

Selroos OB. 1986. The use of budesonide in the treatment of sarcoidosis. Ann NY Acad Sci 465; 713-21.

Shaw RJ & Kay AB. 1985. Nedocromil, a mucosal and connective tissue mast cell stabiliser, inhibits exercise-induced asthma. Br J Dis Chest 79; 385-389.

Sharp PF. 1989. The gamma-camera. In: Sharp PF, Gemmell HG, Smith FW, eds. Practical nuclear medicine. IRL Press, Oxford. pp 5-14.

Shaw RJ & Kay AB. 1985. Nedocromil, a mucosal and connective tissue mast cell stabiliser, inhibits exercise-induced asthma. Br J Dis Chest 79: 385-389.

Siegel S. 1956. Nonparametric statistics for the behavioural sciences. McGraw-Hill, New York.

Simani AS, Inoue S, Hogg JC. 1974. Penetration of the respiratory epithelium of guinea pigs following exposure to cigarette smoke. Lab Invest 31; 75-81.

Simonds AK, Newman SP, Talaee N, Johnson MA, Lee CA, Clarke SW. 1989. Alveolar targeting of aerosolised pentamidine. Am Rev Respir Dis 139; A249.

Smith JE & Jordan ML. 1964. Mathematical and graphical interpretation of the log-normal law for particle size distribution analysis. J Colloid Sci 19; 549-559.

Snashall PD, Boother FA, Sterling GM. 1977. The effect of α-adrenoceptor stimulation on the airways of normal and asthmatic man. Clin Sci Mol Med 54; 283-289.

Sollis-Cohen S. 1900. The use of adrenal substance in the treatment of asthma. JAMA 34; 1164-1166.

Spiro SG, Singh CA, Tolfree SEJ, Partridge MR, Short MD. 1984. Direct labelling of ipratropium bromide aerosol and its deposition pattern in normal subjects and patients with chronic bronchitis. Thorax 39; 432-435.

Stahlhofen W, Gebhart J, Heyder J. 1980. Experimental determination of the regional deposition of aerosol particles in the human respiratory tract. Am Ind Hyg Ass 41; 385-399.

Stokes TC & Morley J. 1981. Prospects for an oral Intal. Br J Dis Chest 75; 1-14.

Svendsen UG, Frøland L, Madsen F, Nielsen NH. 1989. A comparison of the effects of nedocromil sodium and beclomethasone dipropionate on pulmonary function, symptoms, and bronchial responsiveness in patients with asthma. J All Clin Immunol 84; 224-231.

Swift DL. 1980. Generation and respiratory deposition of therapeutic aerosol. Am Rev Respir Dis 127; 71-77.

Swithenbank J, Beer JM, Taylor DS, Abbot D, McCreath GC. 1977. A laser diagnostic technique for measurement of droplet and particle size distribution. Prog Astronautics Aeronautics 53; 421-437.

Takamine DJ. 1902. Adrenaline - the active principle of the adrenal gland. Scott Med Surg J 10; 131-138.

Task Group on Lung Dynamics. 1966. Deposition and retention models for internal dosimetry of the human respiratory tract. Health Phys 12; 173-208.

Tattersfield AE & Keeping IM. 1979. Assessing changes in airway calibre - measurement of airway resistance. Br J Clin Pharmac 8; 307-319.

Taylor KMG, Taylor G, Kellaway IW, Stevens J. 1989. The influence of liposomal encapsulation on sodium cromoglycate pharamacokinetics in man. Pharm Res 6; 633-636.

Thomson NC. 1989. Nedocromil sodium: an overview. Respir Med 83; 269-276.

Thorel T, Joseph M, Tsicopoulos A, Tonnel AB, Capron A. 1988. Inhibition by nedocromil sodium of IgE-mediated activation of human mononuclear phagocytes and platelets in allergy. Int Arch Allergy Appl Immunol 85; 232-237.

Trajan M, Logus JW, Enns EG, Man SFP. 1984. Relationship between regional ventilation and aerosol deposition in tidal breathing. Am Rev Respir Dis 130; 64-70.

Van A, Chick TW, Bodman SF, Storms SW, Nathan RA. 1986. A group comparative study of the safety and efficacy of nedocromil sodium in reversible airways disease: a preliminary report. Eur J Respir Dis 69; 143-148.

Van Gundy KP, Akil B, Bill R, Boylen CT. 1988. The effect of inhaled pentamidine on the prevention of pneumocystis carinii pneumonia in patients with the acquired immunodeficiency syndrome. Am Rev Respir Dis 137; A120.

Vidgren MT, Kärkkäinen A, Karjalainen P, Paronen TP. 1987. A novel labelling method for measuring the deposition of drug particles in the respiratory tract. Int J Pharm 37; 239-244.

Voorhurst R. 1980. Perfection of skin testing technique. Allergy 35; 247-261.

Wagner EM, Mitzner WA, Bleeker ER. 1987a. Effects of airway pressure on bronchial blood flow. J Appl Physiol 62; 561-566.

Wagner EM, Mitzner WA, Bleeker ER. 1987b. Mechanism of PEEP induced increase in bronchial vascular resistance. Fed Proc 46; 6310.

Wagner EM & Mitzner WA. 1990. Bronchial circulatory reversal of methacholine-induced airway constriction. J Appl Physiol 69; 1220-1224.

Wardlaw AJ, Dunnette S, Gleich GJ, Collins JV, Kay AB. 1988. Eosinophils and mast cells in bronchoalveolar lavage in mild asthma: relationship to bronchial hyperreactivity. Am Rev Respir Dis 137; 62-69.

Wells E, Jackson CG, Harper CT, Mann J, Eady RP. 1986. Characterisation of primate bronchoalveolar mast cells. II Inhibition of histamine, LTC4 and PGD2 release from primate bronchoalveolar mast cells and a comparison with rat peritoneal mast cells. J Immunol 137; 3941-3945.

West JB. 1979. Respiratory physiology - the essentials. 2nd ed. Williams and Wilkins, Baltimore. pp 105-108.

Wigley M, Londona JH, Scott HW, Shipp JC, Waldmann RH. 1971. Insulin across respiratory mucosa by aerosol delivery. Diabetes 20; 552-556.

Young IH, Daviskas E, Keena VA. 1989. Effect of low dose nebulised morphine on exercise endurance in patients with chronic lung disease. Thorax 44; 387-390.

Yu CD, Jones RE, Henesian M. 1984. Cascade impactor method for the droplet size characterization of a metered-dose nasal spray. J Pharm Sci 73; 344-348.

Zainudin BMZ, Biddiscombe M, Tolfree SEJ, Short M, Spiro SG. 1990. Comparison of bronchodilator responses and deposition patterns of salbutamol inhaled from pressurised a metered dose inhaler, as a dry powder, and as a nebulised solution. Thorax 45; 469-473.

Appendix A. Data from chapter three: inhaled, oral and intravenous nedocromil sodium.

Table A.1: Terminal slopes of AMP dose-response curves.

Subject	Baseline	Inhaled	Oral	Intravenous
1	-65.5	-57.1	-102.4	-55.1
2	-55.0	-102.0	-68.9	-95.9
3	-31.5	-74.2	-79.2	-125.9
4	-64.0	-74.1	-71.2	-73.5
5	-75.2	-75.5	-62.2	-57.7
6	-50.5	-96.8	-116.5	-126.4
7	-70.29	-99.3	-94.4	-97.34
8	-99.9	-63.3	-75.3	-72.1
9	-93.6	-78.1	-62.9	-68.4

Table A.2: Nedocromil sodium pharmacokinetic data following inhalation.

Subject	Cmax (ng/ml)	Cchall (ng/ml)	Tmax (min)	AUC (ng.ml/min)	t½ (min)	MRT (min)	μg absorbed
1	6.37	3.39	5	1135.7	129	197	960
2	1.66	0.69	2	164.0	87	129	148
3	4.23	2.40	30	462.0	57	91	394
4	2.52	0.97	15	298.2	96	144	297
5	1.86	1.39	45	237.5	70	114	179
6	2.38	1.54	15	292.6	66	99	250
7	3.93	1.95	15	564.0	131	176	682
8	3.3	3.00	30	506.5	62	110	344
9	3.14	1.38	10	291.6	66	97	295
Mean	3.27	1.86	19	439.1	85	129	394
SD	1.45	0.91	14	292.7	28	37	263
SEM	0.48	0.30	5	97.6	9	12	88

Table A.3: Nedocromil sodium pharmacokinetic data following intravenous infusion.

Subject	Dose (μg)	Cmax (ng/ml)	Cchall (ng/ml)	Tmax (min)	AUC (ng.ml/min)	t½ (min)	MRT (min)	Cl (ml/min)	Vss (l)
1	423	10.26	1.06	20	500.6	49	38	845	31.7
2	399	7.99	0.78	15	441.4	108	80	904	72.3
3	380	8.29	0.74	20	445.2	58	50	854	42.8
4	300	7.71	0.34	25	300.9	24	20	997	20.2
5	484	11.61	2.05	20	643.0	61	59	753	44.7
6	424	10.48	0.83	20	495.3	66	44	856	37.7
7	377	8.49	0.45	25	311.8	60	35	1209	48.8
8	374	12.93	0.82	25	551.4	70	36	678	24.5
9	486	8.16	1.26	25	479.6	86	70	1013	70.7
Mean	405	9.55	0.93	22	463.2	65	48	901	43.7
SD	58	1.85	0.50	4	107.7	23	19	156	18.3
SEM	19	0.62	0.17	1	35.9	8	6	52	6.1

Table A.4: Nedocromil sodium pharmacokinetic data following oral administration.

Subject	Cmax (ng/ml)	Cchall (ng/ml)	Tmax (min)
1	2.4	1.04	45
2	1.77	1.27	240
3	4.65	4.50	150
4	3.02	1.75	240
5	3.13	2.50	60
6	2.93	1.72	120
7	1.00	0.89	180
8	0.98	0.78	150
9	5.10	2.98	45
Mean	2.78	1.94	137
SD	1.44	1.21	76
SEM	0.48	0.40	25

Table A.4: Plasma levels of nedocromil sodium (ng/ml) following inhalation.

Subject	Time from inhalation (minutes)											
	0	2	5	10	15	30	45	60	90	120	180	240
1	0.512	6.239	6.369	6.211	5.277	5.593	4.387	4.011	3.389	3.367	1.848	1.901
2	0.048	1.665	1.354	0.967	1.351	0.968	0.747	0.607	0.688	0.663	0.261	0.246
3	0.551	1.957	2.756	3.816	3.018	4.225	2.477	3.131	2.119	2.118	0.803	0.301
4	0.022	2.139	1.413	1.696	2.521	1.736	1.216	1.367	0.987	0.903	0.430	0.244
5	0.074	1.526	1.794	1.470	1.446	1.460	1.861	1.472	1.373	0.469	0.942	0.260
6	0.056	1.057	3.448	2.173	2.377	2.010	1.814	1.709	1.512	0.875	1.223	0.743
7	0.300	3.496	2.332	3.874	3.931	2.561	2.093	2.031	1.841	1.748	1.123	0.506
8	0.004	1.286	3.075	2.888	3.264	3.264	2.810	2.999	3.034	1.649	0.357	0.289
9	0	1.224	ND	3.135	2.878	2.878	2.121	1.585	1.300	0.870	ND	ND
Mean	0.174	2.288	2.818	2.914	2.896	2.744	2.170	2.101	1.805	1.407	0.873	0.561
SD	0.222	1.652	1.625	1.603	1.214	1.457	1.036	1.067	0.906	0.921	0.532	0.569
SEM	0.074	0.551	0.574	0.534	0.405	0.486	0.345	0.356	0.302	0.307	0.188	0.201

ND - not done (sample missed).

Table A.5a: Plasma levels of nedocromil sodium (ng/ml) following intravenous infusion.

Subject	Time (minutes) from start of intravenous infusion.										
	0	5	10	15	20	25	30	35	40	45	50
1	0.133	7.724	7.667	9.548	10.264	7.043	6.227	7.749	5.433	4.105	3.445
2	0.102	4.957	4.804	7.985	6.646	7.908	7.146	4.716	3.515	3.237	2.213
3	0.037	5.462	6.731	7.846	8.290	7.705	7.270	5.500	2.566	2.881	2.320
4	0.015	5.380	5.933	7.233	6.766	9.958	6.395	2.865	4.606	2.126	1.850
5	0.057	1.900	7.000	7.722	11.610	9.474	10.874	5.013	3.552	5.270	4.603
6	0.027	7.238	8.718	7.358	10.482	8.490	10.036	6.985	4.581	4.721	3.272
7	0	4.917	5.025	4.483	6.476	12.932	7.221	3.189	3.945	2.409	2.025
8	0.112	7.838	10.342	9.984	11.980	8.159	12.690	5.552	ND	3.525	3.887
9	0	5.796	6.928	5.780	6.911	ND	6.460	4.368	ND	3.562	2.801
Mean	0.054	5.690	7.016	7.549	8.825	8.959	8.258	5.104	4.028	3.537	2.935
SD	0.050	1.830	1.750	1.692	2.263	1.861	2.339	1.592	0.935	1.032	0.934
SEM	0.017	0.610	0.583	0.564	0.754	0.658	0.780	0.531	0.353	0.344	0.311

ND - not done (sample missed).

Table A.5b: Plasma levels of nedocromil sodium (ng/ml) following intravenous infusion.

Subject	Time (minutes) from start of intravenous infusion.									
	55	60	75	90	120	150	180	210	240	270
1	2.847	2.352	1.356	1.178	0.889	0.437	0.329	0.111	0.186	0.090
2	2.405	1.900	0.998	0.975	0.477	0.545	0.334	0.430	0.355	0.280
3	1.550	2.325	1.503	1.465	0.391	0.582	0.139	0.284	0.238	0.220
4	3.379	1.425	0.813	0.539	0.261	0.501	0.091	0.229	0.370	0.110
5	2.537	3.886	2.780	2.048	1.370	0.968	0.275	0.388	0.348	0.350
6	1.787	1.748	0.946	1.043	0.525	0.133	0.321	0.244	0.279	0.560
7	2.453	1.291	0.537	0.548	0.170	0.383	0.155	0.060	0.175	0.070
8	2.860	2.492	1.572	0.816	0.718	0.184	0.250	0.182	0.150	0.140
9	ND	2.537	1.488	1.263	0.620	0.868	0.403	0.599	0.385	0.240
Mean	2.477	2.217	1.333	1.097	0.602	0.511	0.255	0.281	0.276	0.230
SD	0.591	0.774	0.649	0.472	0.363	0.277	0.105	0.168	0.092	0.160
SEM	0.209	0.258	0.216	0.157	0.121	0.092	0.035	0.056	0.031	0.050

ND - not done (sample missed).

Table A.6: Plasma levels of nedocromil sodium (ng/ml) after oral administration.

Subject	Time (minutes) from oral administration.										
	0	15	30	45	60	75	90	120	150	180	240
1	0.130	0.790	0.708	2.402	1.745	1.593	1.339	1.905	0.926	1.598	1.289
2	0.049	0.040	0.839	1.234	0.942	0.954	0.796	0.950	1.485	1.754	1.765
3	0.162	2.758	3.530	3.569	4.035	2.504	2.153	4.475	4.652	3.885	0.338
4	0.036	0.301	0.260	1.783	2.834	1.785	1.269	2.049	1.614	2.732	3.021
5	0	0	1.589	2.254	3.128	2.731	2.822	2.942	2.143	1.345	1.518
6	0.207	0.057	0.149	0.713	2.315	1.796	1.990	2.934	1.322	1.389	0.594
7	0.143	0.932	0.768	0.629	0.786	0.793	0.749	0.932	0.866	0.995	0.910
8	0.027	0.026	0.114	0.403	0.8452	0.579	0.671	0.607	0.980	0.905	2.342
9	0.050	0.014	0.152	5.101	4.841	4.085	2.628	2.578	3.955	3.978	ND
Mean	0.089	0.546	0.901	2.010	2.385	1.869	1.602	2.152	1.994	2.065	1.472
SD	0.072	0.902	1.095	1.542	1.455	1.107	0.823	1.235	1.380	1.183	0.898
SEM	0.024	0.301	0.365	0.514	0.485	0.369	0.274	0.412	0.460	0.394	0.318

ND - not done (sample missed).

Appendix B. Data from chapter 4: Nedocromil sodium pharmacokinetics after respiratory and pharmacological manoeuvres.

Table B.1 Subject details and FEV_1 before and after inhaled methoxamine.

Subject	Age	Sex	Weight (kg)	Baseline FEV_1 (% predicted)	FEV_1 with methoxamine	
					Before	After
1	23	M	75	4.6 (105)	4.6	4.85
2	23	F	73	4.3 (110)	4.75	4.75
3	38	M	82	3.87 (106)	4.1	4.05
4	32	M	70	3.92 (102)	4.1	4.0
5	29	M	98	5.55 (110)	5.75	5.85
6	29	M	82	4.51 (101)	4.7	4.75
7	33	M	75	4.2 (94)	4.8	4.7
8	22	M	78	5.15 (110)	5.15	5.35
Mean	28.6		79.13	4.56 (104.8)	4.74	4.78
SD	5.68		8.69	0.58 (5.63)	0.54	0.61
SEM					0.19	0.22

Table B.2 Inspiratory parameters on first study day.

Subject	BHT (sec)	IV (l)	PIF (l/min)	TF (sec)	VF (l)	FF (l/min)	VF%
1	10.4	5.10	50	1.8	1.31	55	26
1	10.4	5.02	49	1.5	0.76	37	15
2	10.9	4.13	55	1.9	1.13	32	27
2	11.1	4.05	43	1.5	0.93	32	23
3	11.3	3.65	61	1.1	0.67	42	19
3	10.7	4.26	59	1.0	0.57	43	13
4	11.1	4.38	57	1.5	1.10	39	25
4	10.4	4.29	57	1.1	0.69	41	16
5	8.9	5.84	58	1.5	1.08	53	19
5	9.5	5.42	46	1.8	0.85	39	16
6	10.8	3.74	38	1.3	0.82	38	22
6	11.3	3.76	37	1.2	0.68	39	18
7	10.7	4.77	53	1.5	1.03	44	22
7	14.2	4.63	42	1.5	1.04	37	22
8	10.5	5.34	54	1.9	1.20	33	23
8	11.0	5.28	52	1.8	1.02	54	19
Mean	10.83	4.60	50.69	1.49	0.93	41.13	20.31
SD	1.101	0.674	7.543	0.293	0.217	7.311	4.094
SEM	0.275	0.168	1.886	0.073	0.054	1.828	1.024

Abbreviations: BHT - breath-holding time; IV - inspired volume; PIF - peak inspiratory flow; TF - time of aerosol actuation; VF - inspired volume at aerosol actuation; FF - inspiratory flow at aerosol actuation; VF% - percentage of inspired volume at aerosol actuation.

Table B.3 Inspiratory parameters on second (methoxamine) study day.

Subject	BHT	IV	PIF	TF	VF	FF	VF%
1	10.4	5.02	49	1.4	0.75	44	15
1	9.0	5.03	45	1.8	1.18	47	23
2	10.6	3.63	50	1.3	0.97	38	27
2	10.8	4.26	62	1.6	1.43	40	34
3	11.6	3.80	48	1.4	0.66	29	18
3	11.2	4.12	45	1.7	0.94	29	23
4	10.9	4.28	49	1.3	0.71	37	17
4	10.9	3.69	46	1.4	0.79	28	21
5	10.8	5.86	43	1.8	0.92	39	16
5	10.4	5.80	41	1.6	0.79	34	14
6	11.0	4.04	39	1.3	0.78	42	19
6	11.3	4.33	45	1.2	0.80	31	19
7	11.4	4.81	49	1.6	1.12	43	23
7	10.7	4.55	43	1.5	0.93	41	20
8	10.6	5.40	52	1.7	1.02	40	19
8	10.1	5.03	57	1.5	0.97	43	19
Mean	10.73	4.60	47.69	1.51	0.92	37.81	20.44
SD	0.607	0.707	5.828	0.188	0.199	5.935	4.926
SEM	0.152	0.177	1.457	0.047	0.050	1.484	1.231

Table B.4 Inspiratory parameters on third (probenecid) study day.

Subject	BHT	IV	PIF	TF	VF	FF	VF%
1	11.5	4.11	49	1.3	0.76	48	19
1	11.1	3.68	42	1.5	0.96	45	26
2	10.5	3.39	47	1.9	0.98	40	29
2	9.6	4.26	50	1.2	0.75	36	18
3	9.4	4.01	38	1.6	0.75	32	19
3	12.5	4.11	63	1.7	0.80	42	20
4	10.7	4.60	56	1.3	0.86	25	19
4	10.9	4.24	48	1.5	0.79	27	19
5	9.3	5.75	42	1.4	0.88	38	15
5	11.2	5.73	49	2.3	1.29	39	23
6	11.2	3.83	41	1.3	0.78	38	20
6	11.3	4.66	40	1.2	0.81	34	17
7	10.9	4.81	66	1.5	0.99	43	21
7	11.5	4.86	53	1.5	1.07	44	22
8	10.7	5.32	50	1.3	0.85	40	16
8	10.6	4.73	50	1.6	0.84	41	18
Mean	10.81	4.51	49.00	1.51	0.89	38.25	20.06
SD	0.831	0.687	7.840	0.284	0.144	6.266	3.586
SEM	0.208	0.172	1.960	0.071	0.036	1.567	0.897

The tables on the following 3 pages depict the time course of plasma nedocromil sodium concentrations after inhalation of the drug for each subject on each of the study days. Note that the dotted lines indicate the times at which the respiratory manoeuvres were performed. The first was 9 FEV_1 manoeuvres over a 3 minute period, the second was a full inspiration followed by a 30 sec breath-hold, and the third was 1 FEV_1 manoeuvre.

Table B.5 Nedocromil sodium plasma concentrations (ng/ml) on first study day.

Time	Subject 1	Subject 2	Subject 3	Subject 4	Subject 5	Subject 6	Subject 7	Subject 8
0	0	0.016	0.049	0	0	0	0	0.086
5	4.322	5.719	2.365	0.660	4.110	0.594	4.036	6.457
10	3.841	5.124	1.793	1.468	6.218	0.420	4.318	5.767
15	3.419	4.950	2.275	2.301	3.336	0.355	4.828	5.709
20	2.921	7.995	1.317	1.257	2.643	0.312	4.969	5.583
30	2.753	5.573	1.269	1.503	2.531	0.362	4.212	4.712
40	2.514	5.331	1.355	2.014	3.132	0.297	4.106	3.900
50	1.826	5.586	1.755	1.868	3.071	0.425	4.120	3.974
60	2.278	5.065	1.320	2.960	2.687	0.334	4.559	3.433
70	1.610	4.137	2.582	2.138	2.433	0.224	3.590	3.624
73	2.655	4.443	2.032	2.442	4.351	0.567	4.060	6.932
76	1.958	4.326	1.661	2.216	3.696	0.359	4.218	5.888
80	2.301	4.073	1.081	1.580	2.363	0.257	4.182	4.128
90	1.822	3.394	1.010	3.338	2.246	0.253	3.443	2.916
100	1.181	2.901	0.604	0.916	1.961	0.180	3.164	2.990
110	1.314	2.347	0.528	1.268	0.875	0.151	3.269	2.431
113	1.780	3.763	0.685	1.699	1.829	0.269	3.666	3.634
116	1.224	3.006	0.569	1.667	1.296	0.269	3.624	3.111
120	0.842	5.534	0.633	2.315	1.217	0.261	3.417	2.985
130	1.950	2.322	0.485	1.180	0.938	0.095	2.746	2.404
140	0.921	2.042	0.405	1.104	0.772	0.174	2.389	2.196
150	0.803	1.625	0.413	0.773	0.812	0.102	2.379	1.916
153	0.443	1.738	0.504	1.068	0.566	0.130	2.244	2.309
156	1.148	1.832	0.374	0.987	0.391	0.186	2.515	2.160
160	0.511	1.778	0.305	0.905	0.634	0.116	2.106	1.999
165	0.606	2.023	11.000	5.953	0.504	0.109	1.964	2.092
170	1.072	1.850	0.265	0.653	0.559	0.286	1.895	1.860
180	1.789	2.113	0.241	0.836	0.460	0.125	1.613	1.673
200	0.446	1.583	0.205	0.847	0.389	0.161	1.576	1.529
220	0.424	1.386	0.435	0.583	0.173	0.030	1.083	1.185
240	0.102	0.873	0.111	0.674	0.143	0.015	0.797	1.078
270	0.404	0.533	0.147	1.693	0.111	0.009	0.639	1.014

Table B.6 Nedocromil sodium plasma concentrations on second (methoxamine) study day.

Time	Subject 1	Subject 2	Subject 3	Subject 4	Subject 5	Subject 6	Subject 7	Subject 8
0	0	0	0.010	0	0	0.002	0	0
5	4.296	3.296	1.620	2.569	4.241	1.507	2.780	7.094
10	4.509	3.317	1.440	2.352	3.893	1.657	2.888	5.889
15	3.800	3.796	1.810	2.311	4.208	1.550	2.692	5.265
20	3.248	3.896	2.920	2.416	3.734	1.444	2.545	4.412
30	2.815	3.428	1.190	2.123	3.728	1.467	2.383	3.754
40	2.432	3.775	1.340	1.490	3.459	0.989	2.144	3.702
50	2.103	3.896	1.290	2.496	3.344	0.792	2.546	3.680
60	1.802	3.830	1.530	1.906	3.116	0.847	2.643	3.322
70	1.477	4.047	1.180	2.347	2.933	0.858	2.247	6.406
73	2.974	4.051	1.640	3.425	4.633	1.113	3.174	7.131
76	2.171	4.072	1.460	3.173	3.369	1.037	2.836	5.084
80	1.870	3.623	1.380	2.011	2.964	1.013	2.331	3.927
90	1.314	2.363	1.080	1.949	2.275	0.884	1.931	3.853
100	1.184	2.841	0.960	1.624	1.948	0.617	1.733	2.798
110	1.012	2.495	0.850	1.455	1.841	0.569	1.584	2.612
113	1.098	3.301	1.240	1.515	2.219	0.829	1.808	3.636
116	0.943	2.667	2.415	3.175	2.147	0.490	2.423	3.372
120	0.894	2.493	0.760	1.431	1.811	0.418	1.652	2.860
130	0.660	1.854	0.630	1.520	1.503	0.424	1.604	2.658
140	0.571	1.907	0.590	1.024	1.322	0.307	1.526	2.064
150	0.509	1.348	0.720	0.860	1.337	0.251	1.331	2.279
153	0.572	1.739	0.610	1.841	1.261	0.258	1.461	2.251
156	0.521	1.897	0.670	1.020	1.257	0.321	1.222	2.305
160	0.506	1.739	0.800	0.528	1.073	0.381	1.184	1.820
165	0.477	1.415	0.450	0.802	1.108	0.362	0.979	1.943
170	0.328	1.477	0.450	0.746	0.902	0.575	0.765	1.922
180	0.339	1.294	0.500	0.867	1.086	0.459	0.986	2.022
200	0.196	1.224	0.400	0.691	0.905	0.340	0.818	1.618
220	0.111	1.018	0.470	0.514	0.746	0.262	0.875	1.357
240	0.271	0.422	0.480	0.451	0.581	0.210	0.535	1.259
270	0.062	0.314	0.310	0.412	0.472	0.175	0.441	1.009

Table B.7 Nedocromil sodium plasma concentrations on third (probenecid) study day.

Time	Subject 1	Subject 2	Subject 3	Subject 4	Subject 5	Subject 6	Subject 7	Subject 8
0	0	0	0.005	0	0.048	0	0	0.370
5	5.182	7.555	2.520	0.060	4.662	1.949	6.151	12.210
10	3.498	8.235	2.027	0.401	4.153	1.821	6.281	11.276
15	3.230	8.405	2.315	0.599	3.882	1.487	6.561	9.726
20	2.720	7.103	2.378	0.496	3.555	1.261	6.352	11.124
30	2.523	7.062	2.003	0.436	4.028	1.319	5.759	8.330
40	1.124	6.759	1.975	0.481	3.758	2.192	5.496	9.348
50	1.345	6.199	2.699	0.608	3.325	1.499	5.272	10.646
60	1.638	6.377	2.301	0.653	3.323	1.384	5.038	10.146
70	1.577	5.855	2.022	0.388	2.352	1.048	4.399	7.352
73	3.445	7.121	3.372	1.120	4.176	1.884	6.172	15.802
76	2.827	6.399	2.946	0.175	3.685	1.757	5.543	15.990
80	2.183	5.993	2.038	0.673	2.744	1.433	4.792	14.750
90	1.075	5.511	1.858	0.609	2.116	1.099	4.862	9.554
100	0.990	5.017	1.523	0.858	1.882	0.641	3.670	9.930
110	0.605	4.767	1.120	0.325	1.366	0.440	3.328	8.400
113	0.984	5.926	1.130	0.649	2.234	1.077	3.370	9.958
116	1.100	4.701	1.505	0.405	2.053	0.512	3.718	10.682
120	1.123	4.661	1.544	0.458	1.417	0.353	2.712	9.478
130	0.783	4.265	1.218	0.365	0.985	0.697	2.615	7.886
140	0.571	3.638	1.022	0.192	1.216	0.300	2.529	6.780
150	0.481	3.307	0.703	0.407	0.867	0.307	2.054	7.252
153	0.448	3.624	1.031	0.178	0.858	0.196	2.354	8.298
156	0.476	3.784	0.872	>10	0.924	0.226	2.301	6.536
160	0.651	3.414	1.293	0.656	0.780	0.174	2.104	6.078
165	0.434	3.925	0.899	0.153	0.587	0.255	1.860	4.720
170	0.181	3.426	0.354	0.322	0.626	0.230	1.747	5.798
180	0.617	3.246	0.493	0.124	0.871	0.277	1.528	4.494
200	0.448	2.476	0.881	0.362	0.667	0.206	1.609	3.844
220	0.245	2.066	0.309	0.033	0.357	0.224	1.425	2.924
240	0.241	1.854	0.051	0.082	0.197	0.002	2.411	2.216
270	0.314	1.148	0.003	0.073	0.153	0.000	0.586	1.810

Table B.8 Maximum plasma concentrations (Cmax) and time to reach Cmax (Tmax) for the 3 study days.

	Day 1		Day 2 (methoxamine)		Day 3 (probenecid)	
	Cmax (ng/ml)	Tmax (min)	Cmax (ng/ml)	Tmax (min)	Cmax (ng/ml)	Tmax (min)
1	4.322	5	4.509	10	5.182	5
2	5.719	5	3.896	20	8.405	15
3	2.365	5	2.920	20	2.520	5
4	2.301	15	2.569	5	0.599	15
5	6.218	10	4.241	5	4.662	5
6	0.594	5	1.657	10	1.949	5
7	4.969	20	2.888	10	6.561	15
8	6.457	5	7.094	5	12.210	5
Mean	4.118	8.75	3.722	10.625	5.261	8.75
SD	2.138	5.825	1.657	6.232	3.788	5.175
SEM	0.756	2.059	0.586	2.203	1.339	1.830

The tables on the following pages depict the AUC values derived from the nedocromil sodium plasma concentration-time curves. The columns are as follows:

AUC whole study: the $AUC_{0\text{-}270\ min}$.

AUC minus 9 FEV_1 and minus 1 FEV_1: the AUC for the whole study minus the increase caused by the respiratory manoeuvres.

AUC minus breath-hold: the AUC for the whole study minus the increase due to the manoeuvre.

% Δ after manoeuvre: the change in AUC caused by each manoeuvre expressed as a percentage of the AUC for the whole study.

Table B.9 Plasma nedocromil sodium AUC on first study day.

Subject	AUC whole study	AUC minus 9 FEV_1	AUC minus breath-hold	AUC minus 1 FEV_1	% Δ after 9 FEV_1	% Δ after breath-hold	% Δ after 1 FEV_1
1	347.236	339.252	349.603	347.592	2.300	-0.680	-0.100
2	774.083	769.100	764.406	774.321	0.640	1.250	-0.030
3	202.545	207.780	201.013	202.335	-2.580	0.760	0.100
4	309.048	306.560	295.370	305.929	0.810	4.430	1.010
5	382.983	372.569	376.677	384.324	2.720	1.650	-0.350
6	51.452	49.900	49.730	51.057	3.020	3.350	0.770
7	709.144	700.766	703.034	708.157	1.180	0.860	0.140
8	729.776	705.205	719.900	728.256	3.370	1.350	0.210
Median	365.11	355.11	363.14	365.96	1.74	1.30	0.12

Table B.10 Plasma nedocromil sodium AUC on second study day.

Subject	AUC whole study	AUC minus 9 FEV_1	AUC minus breath-hold	AUC minus 1 FEV_1	% Δ after 9 FEV_1	% Δ after breath-hold	% Δ after 1 FEV_1
1	305.574	295.197	304.339	305.096	3.36	0.37	0.12
2	575.314	568.724	568.981	570.827	1.15	1.10	0.78
3	240.040	236.788	232.434	238.765	1.35	3.17	0.53
4	361.013	355.309	355.764	358.936	1.58	1.45	0.58
5	505.745	495.603	502.013	506.253	2.01	0.74	-0.10
6	165.766	163.436	165.572	165.470	1.41	0.12	0.18
7	413.258	406.273	409.373	412.044	1.69	0.94	0.29
8	747.601	752.761	740.409	747.951	-0.69	0.96	-0.05
Median	387.14	380.79	382.57	385.49	1.50	0.95	0.24

Table B.11 Derived AUC values from plasma nedocromil sodium concentration-time curves on third study day.

Subject	AUC whole study	AUC minus 9 FEV_1	AUC minus breath-hold	AUC minus 1 FEV_1	% Δ after 9 FEV_1	% Δ after breath-hold	% Δ after 1 FEV_1
1	288.76	272.44	283.26	287.91	5.65	1.90	0.29
2	1151.63	1143.27	1146.63	1151.63	0.73	0.43	0
3	325.96	317.86	322.17	322.78	2.48	1.16	0.98
4	88.62	86.28	86.69	89.71	2.65	2.19	-1.22
5	450.83	436.97	443.56	449.54	3.07	1.61	0.29
6	180.05	172.72	178.24	181.01	4.07	1.01	-0.53
7	878.52	868.82	877.60	875.56	1.10	0.10	0.34
8	1888.73	1794.28	1865.58	1879.63	5.00	1.23	0.48
Median	388.40	377.42	382.87	386.16	2.86	1.20	0.29

Appendix C. Data from chapter five: method for radiolabelling nedocromil sodium.

The tables on the following pages contain the raw data derived from the aerosol size analyses using the multi-stage liquid impinger. Different impingers were used, and therefore the cut-off sizes for the various stages differ slightly depending on the impinger used. The table headings are as follows:

Location: location within the impinger.

D_{50}: effective cut-off size for the stage/location (anything passing a given stage must be below its effective cut-off diameter).

mg at location: amount of drug per actuation at a given location.

% at location: % of delivered dose at location (drug or Tc^{99m}).

Cum % < by wt: Cumulative percentage less than by weight. The percentage of the cloud delivered to the impinger less than the previous location's D_{50} diameter. For example, for table 5.7, the % on the filter is less than 0.9 μm, and the % on stage 4 and the filter is less than 3.8 μm, &c.

The remaining columns are repeats of the above either for delivered drug or for radioactivity.

Table C.1 Nedocromil sodium radio-labelling data: method 1, fine aerosol.

	Before labelling				After labelling				
Location	D_{50}	mg at location	% at location	Cum % < by wt	mg at location	% at location	Cum % < by wt	Activity %	Cum % < by wt
Adaptor		0.248	14.1		0.148	9.9		14.1	
Throat	22.0	0.713	40.6	100	0.785	52.7	100	51.6	100
1	10.9	0.115	6.5	52.8	0.156	10.5	41.4	10.1	40.0
2	7.0	0.089	4.8	45.2	0.110	7.4	29.8	5.9	28.2
3	3.8	0.253	14.4	39.6	0.174	11.7	21.6	10.7	21.3
4	0.9	0.332	18.9	22.8	0.113	7.6	8.6	7.5	8.9
Filter		0.013	0.7	0.9	0.003	0.2	0.2	0.2	0.2

Table C.2 Nedocromil sodium radio-labelling data: method 1, fine aerosol.

	Before labelling				After labelling				
Location	D_{50}	mg at location	% at location	Cum % < by wt	mg at location	% at location	Cum % < by wt	Activity %	Cum % < by wt
Adaptor		0.213	12.0		0.147	9.3		8.8	
Throat	19.0	0.770	43.5	100	0.827	52.3	100	57.3	100
1	10.7	0.132	7.5	50.5	0.075	4.7	42.4	6.1	37.3
2	6.7	0.143	8.1	42.1	0.137	8.7	37.2	6.2	30.6
3	3.8	0.229	12.9	32.9	0.187	11.8	27.6	9.0	23.8
4	0.81	0.270	15.3	18.2	0.202	12.8	14.6	12.1	13.9
Filter		0.031	0.7	0.8	0.007	0.4	0.5	0.6	0.7

Table C.3 Nedocromil sodium radio-labelling data: method 1, fine aerosol, no surfactant.

	Before labelling				After labelling				
Location	D_{50}	mg at location	% at location	Cum % < by wt	mg at location	% at location	Cum % < by wt	Activity %	Cum % < by wt
Adaptor		0.225	13.6		0.21	11.9		7.8	
Throat	22.0	0.708	42.7	100	0.873	49.5	100	53.2	100
1	10.9	0.117	7.1	50.2	0.130	7.4	43.7	20.9	35.9
2	7.0	0.088	5.3	42.1	0.095	5.4	35.4	6.2	17.0
3	3.8	0.215	13.0	36.0	0.230	13.0	29.3	6.7	11.4
4	0.9	0.283	17.1	21.1	0.219	12.4	14.6	5.2	5.2
Filter		0.022	1.3	1.5	0.008	0.5	0.5	0.4	0.4

Table C.4 Nedocromil sodium radio-labelling data: method 1, coarse aerosol, no surfactant.

	Before labelling				After labelling				
Location	D_{50}	mg at location	% at location	Cum % < by wt	mg at location	% at location	Cum % < by wt	Activity %	Cum % < by wt
Adaptor		0.234	11.0		0.121	7.6		6.4	
Throat	19.0	0.834	39.3	100	0.888	55.4	100	51.3	100
1	10.9	0.444	20.9	55.4	0.307	19.2	40.0	28.0	40.9
2	6.2	0.207	9.7	31.7	0.103	6.4	19.3	5.7	14.7
3	4.4	0.126	5.9	20.6	0.069	4.3	12.3	3.4	9.4
4	0.7	0.242	11.4	13.9	0.1122	7.0	7.7	6.3	6.3
Filter		0.018	0.8	1.0	0.002	0.1	0.1	0.3	0.3

Table C.5 Nedocromil sodium radio-labelling data: method 1, coarse aerosol.

	Before labelling				After labelling				
Location	D_{50}	mg at location	% at location	Cum % < by wt	mg at location	% at location	Cum % < by wt	Activity %	Cum % < by wt
Adaptor		0.188	9.6		0.085	5.8		5.9	
Throat	21.0	0.926	47.3	100	0.965	65.4	100	64.7	100
1	10.3	0.385	19.7	47.7	0.143	9.7	30.6	8.4	31.2
2	6.4	0.182	9.3	25.9	0.114	7.7	20.3	6.2	22.3
3	4.0	0.136	6.9	15.6	0.086	5.8	12.1	6.1	15.7
4	1.0	0.136	6.9	7.9	0.080	5.4	5.9	8.3	9.5
Filter		0.004	0.2	0.2	0.002	0.1	0.1	0.4	0.4

Table C.6 Nedocromil sodium radio-labelling data: method 1, coarse aerosol.

	Before labelling				After labelling				
Location	D_{50}	mg at location	% at location	Cum % < by wt	mg at location	% at location	Cum % < by wt	Activity %	Cum % < by wt
Adaptor		0.238	11.9		0.118	7.3		26.8	
Throat	19.0	0.995	49.8	100	1.09	67.3	100	52.1	100
1	10.9	0.363	18.2	43.5	0.173	10.7	27.4	7.9	28.8
2	6.2	0.143	7.2	22.9	0.090	5.6	15.9	4.0	18.0
3	4.4	0.095	4.8	14.8	0.069	4.3	9.9	3.2	12.9
4	0.7	0.161	8.1	9.4	0.079	4.9	5.3	6.0	8.2
Filter		0.005	0.3	0.3	0.001	0.1	0.1	0	0

Table C.7 Nedocromil sodium radio-labelling data: method 2, fine aerosol.

	Before labelling				After labelling				
Location	D_{50}	mg at location	% at location	Cum % < by wt	mg at location	% at location	Cum % < by wt	Activity %	Cum % < by wt
Adaptor		0.175	9.8		0.223	12.5		13.9	
Throat	19.0	0.981	55.2	100	0.820	46.1	100	46.4	100
1	10.7	0.132	7.4	38.8	0.081	4.6	47.2	4.6	46.0
2	6.7	0.078	4.4	30.5	0.121	6.8	42.0	7.0	40.7
3	3.8	0.130	7.3	25.7	0.215	12.1	34.2	10.8	32.6
4	0.81	0.262	14.7	17.5	0.304	17.1	20.4	16.8	19.9
Filter		0.019	1.1	1.2	0.013	0.7	0.8	0.3	0.4

Table C.8 Nedocromil sodium radio-labelling data: method 2, fine aerosol.

	Before labelling				After labelling				
Location	D_{50}	mg at location	% at location	Cum % < by wt	mg at location	% at location	Cum % < by wt	Activity %	Cum % < by wt
Adaptor		0.170	9.3		0.297	15.1		15.2	
Throat	21.0	0.941	51.3	100	1.026	52.2	100	51.4	100
1	10.3	0.119	6.5	43.4	0.089	4.5	38.5	7.7	39.4
2	6.4	0.134	7.3	36.3	0.136	6.9	33.2	6.9	30.3
3	4.0	0.191	10.4	28.2	0.172	8.8	25.0	7.5	22.1
4	1.0	0.266	14.5	16.7	0.236	12.0	14.7	11.0	13.3
Filter		0.012	0.7	0.7	0.009	0.5	0.5	0.2	0.3

Table C.9 Nedocromil sodium radio-labelling data: method 2, fine aerosol.

	Before labelling				After labelling				
Location	D_{50}	mg at location	% at location	Cum % < by wt	mg at location	% at location	Cum % < by wt	Activity %	Cum % < by wt
Adaptor		0.227	12.9		0.217	11.5		8.4	
Throat	19.0	0.928	52.7	100	1.080	57.1	100	58.4	100
1	10.7	0.083	4.71	39.6	0.087	4.6	35.5	17.0	37.5
2	6.7	0.111	6.3	34.1	0.098	5.2	30.3	5.2	17.2
3	3.8	0.173	9.8	26.9	0.164	8.7	24.4	4.9	11.8
4	0.81	0.2259	13.0	15.6	0.233	12.3	14.6	6.0	6.5
Filter		0.011	0.6	0.6	0.011	0.6	0.7	0.1	0.1

Table C.10 Nedocromil sodium radio-labelling data: method 2, fine aerosol, no sonication.

	Before labelling				After labelling				
Location	D_{50}	mg at location	% at location	Cum % < by wt	mg at location	% at location	Cum % < by wt	Activity %	Cum % < by wt
Adaptor		0.210	11.8		0.244	11.7		9.3	
Throat	21.0	0.899	50.2	100	1.189	57.2	100	48.6	100
1	10.3	0.101	5.7	42.5	0.168	8.1	35.2	23.2	46.4
2	6.4	0.144	8.1	36.0	0.121	5.8	26.0	6.3	20.8
3	4.0	0.162	9.1	26.8	0.146	7.0	19.4	5.7	13.8
4	1.0	0.246	13.9	16.4	0.201	9.7	11.4	6.2	7.6
Filter		0.011	0.6	0.6	0.008	0.4	0.4	0.6	0.7

Table C.11 Nedocromil sodium radio-labelling data: method 2, coarse aerosol.

	Before labelling				After labelling				
Location	D_{50}	mg at location	% at location	Cum % < by wt	mg at location	% at location	Cum % < by wt	Activity %	Cum % < by wt
Adaptor		0.174	8.0		0.295	9.6		11.2	
Throat	19.0	1.186	54.4	100	1.624	53.1	100	59.9	100
1	10.9	0.369	16.9	40.9	0.599	19.6	41.3	11.8	32.4
2	6.2	0.155	7.1	22.6	0.230	7.5	19.6	6.3	19.1
3	4.4	0.113	5.2	14.8	0.125	4.1	11.3	3.9	12.1
4	0.7	0.181	8.3	9.2	0.182	5.9	6.8	6.9	7.9
Filter		0.004	0.2	0.2	0.005	0.2	0.2	0	0

Table C.12 Nedocromil sodium radio-labelling data: method 2, coarse aerosol.

	Before labelling				After labelling				
Location	D_{50}	mg at location	% at location	Cum % < by wt	mg at location	% at location	Cum % < by wt	Activity %	Cum % < by wt
Adaptor		0.163	7.9		0.1545	12.4		13.1	
Throat	19.0	0.953	45.3	100	0.506	40.8	100	41.1	100
1	10.9	0.467	22.2	50.9	0.420	33.9	53.4	32.3	52.7
2	6.2	0.210	10.0	26.9	0.076	6.1	14.7	5.8	115.6
3	4.4	0.117	5.6	16.1	0.045	3.6	7.9	3.3	8.9
4	0.7	0.185	8.8	10.0	0.038	3.1	3.6	4.3	5.0
Filter		0.010	0.5	0.5	0	0	0	0	0

Table C.13 Nedocromil sodium radio-labelling data: method 2, coarse aerosol.

	Before labelling				After labelling				
Location	D_{50}	mg at location	% at location	Cum % < by wt	mg at location	% at location	Cum % < by wt	Activity %	Cum % < by wt
Adaptor		0.117	5.8		0.145	6.5		8.6	
Throat	22.0	1.005	49.5	100	1.313	58.8	100	60.0	100
1	10.9	0.418	20.6	47.5	0.307	13.7	37.1	12.0	34.4
2	7.0	0.149	7.3	25.6	0.124	5.6	22.4	4.4	21.3
3	3.8	0.182	9.0	17.8	0.176	7.9	16.5	7.3	16.4
4	0.9	0.149	7.3	8.3	0.161	7.2	8.1	7.3	8.5
Filter		0.01	0.5	0.5	0.007	0.3	0.3	0.4	0.5

Appendix D. Data from chapter six: SPECT study.

Table D.1: age, height and pulmonary function of subjects.

Subject	Age	Height (m)	Pulmonary function (% predicted)
1	21	1.75	4.6 (105)
2	26	1.85	4.7 (100)
3	22	1.69	3.92 (114)
4	22	1.66	3.9 (103)
5	23	1.80	3.83 (99)
6	33	1.72	3.92 (102)
7	27	1.93	5.55 (110)
8	33	1.69	3.93 (101)
9	30	1.82	4.51 (101)
10	31	1.83	4.2 (94)
Mean	26.8	1.77	(102.9)
SD	4.7	0.09	(5.67)

Table D.2: Percentage of initial activity incorporated into MDI.

Subject	Fine aerosol	Coarse aerosol
1	84.8	85.3
2	87.1	89.3
3	84.9	87.0
4	82.9	87.8
5	85.9	83.7
6	84.8	85.7
7	84.5	88.2
8	83.7	83.6
9	85.0	82.6
10	85.2	79.9
Mean	84.88	85.31
SD	1.13	2.90
SEM	0.36	0.92

Table D.3: Inspiratory parameters for inhalation of fine nedocromil sodium.

Subject	BHT	IV	PIF	TF	VF	FF	VF%
1	9.3	6.17	48	1.6	0.99	41	16
1	8.3	6.52	50	1.5	0.99	46	15
2	11.2	5.13	61	1.3	0.93	44	18
2	11.9	5.52	59	1.7	1.35	58	24
3	10.6	4.34	42	2.4	1.16	31	27
3	10.7	4.45	46	1.5	1.2	48	27
4	11.4	3.78	35	1.8	0.92	28	24
4	12.2	3.68	40	1.7	0.88	29	24
5	10.9	4.62	58	1.8	1.27	38	27
5	11.6	4.73	62	1.7	1.06	41	22
6	10.8	3.04	38	1.8	0.75	26	25
6	9.8	3.92	35	1.8	0.94	27	24
7	6.8	5.75	48	2.0	1.27	30	22
7	6.3	6.04	41	1.8	1.03	31	17
8	9.7	4.12	41	1.7	0.82	39	20
8	10.2	3.88	35	1.7	0.69	33	18
9	11.5	3.26	35	1.7	0.85	34	26
9	11.2	3.25	33	1.6	0.82	31	25
10	11.3	4.83	52	1.5	0.98	41	20
10	11.2	4.83	55	1.3	0.96	49	20
Mean	10.35	4.59	45.7	1.7	0.993	37.25	22.05
SD	1.6	1.02	9.60	0.24	0.18	8.69	3.83
SEM	0.36	0.23	2.15	0.05	0.04	1.94	0.86

Abbreviations: BHT - breath-holding time; IV - inspiratory volume; PIF - peak inspiratory flow rate; TF - time of aerosol actuation; VF - inspired volume at aerosol actuation; FF - inspiratory flow at aerosol actuation; VF% - % of inspired volume at aerosol actuation.

Table D.4: Inspiratory parameters for inhalation of coarse nedocromil sodium

Subject	BHT	IV	PIF	TF	VF	FF	VF%
1	9.8	6.45	62	1.8	1.27	53	20
1	9.4	6.21	65	1.7	1.23	58	20
2	10.1	5.77	43	1.9	1.14	40	20
2	10.2	5.78	50	1.6	0.97	44	17
3	10.7	4.41	55	1.2	0.83	35	19
3	11.9	4.36	44	1.6	0.99	41	23
4	11.3	3.95	37	1.7	0.96	36	24
4	10.9	3.9	40	1.8	0.98	33	25
5	12.2	5.01	65	2.0	1.59	53	32
6	9.8	4.05	37	2.0	0.93	25	23
6	10.3	4.03	35	1.8	0.9	28	22
7	5.5	6.28	51	1.9	0.96	28	15
7	12.6	6.56	51	2.0	1.22	32	19
8	10.6	4.18	37	1.5	0.7	41	17
8	11	4.18	50	1.8	0.93	38	22
9	10.6	4.5	37	1.3	0.78	38	18
9	10.8	4.16	44	1.2	0.72	47	17
10	10.9	3.69	50	1.3	0.77	50	21
10	10.4	4.6	50	1.3	0.94	45	21
Mean	10.47	4.85	47.53	1.65	0.99	40.26	20.79
SD	1.46	0.99	9.51	0.28	0.22	9.21	3.79
SEM	0.33	0.23	2.18	0.06	0.05	2.11	0.87

Abbreviations: BHT - breath-holding time; IV - inspiratory volume; PIF - peak inspiratory flow rate; TF - time of aerosol actuation; VF - inspired volume at aerosol actuation; FF - inspiratory flow at aerosol actuation; VF% - % of inspired volume at aerosol actuation.

Table D.5: Fate of delivered dose after inhalation of fine nedocromil sodium.

Subject	Dose (MBq)	Chest	Impacted	Exhaled	Adaptor	Test shots (MBq)	Delivered Dose (MBq)
1	238.91	2.33	82.78	0.69	14.2	280	310
2	188.73	8.86	78.3	0.43	12.38	210	230
3	216.84	3.17	89.2	0.48	7.12	270	280
4	331.59	4.94	80.82	0.59	13.65	400	320
5	258.48	8.92	79.43	0.16	11.49	280	400
6	223.96	10.35	77.27	0.24	12.14	280	260
7	279.01	9.59	70.35	0.57	19.48	360	520
8	254.72	7.21	80.34	0.4	12.05	290	360
9	241.73	8.18	74.82	2.32	14.69	310	340
10	288.53	15.51	72.29	1.83	10.37	430	350
Mean	252.25	7.91	78.56	0.77	12.76	311.00	337.00
SD	40.48	3.82	5.4	0.71	3.2	66.41	81.52
SEM	12.8	1.21	1.71	0.23	1.01	21	25.78

Note: Dose refers to delivered dose assessed by gamma camera; test shots and delivered dose assessed by radioisotopoe calibrator. Chest, impacted, exhaled and adaptor expressed as % of delivered dose.

Table D.6: Fate of delivered dose after inhalation of coarse nedocromil sodium.

Subject	Dose (MBq)	Chest	Impacted	Exhaled	Adaptor	Test shots (MBq)	Delivered dose (MBq)
1	227.3	13.68	64.6	0.64	21.1	300	350
2	292.39	7.41	51.9	7.79	32.89	300	350
3	243.47	4.09	76.71	8.63	10.56	300	300
4	305.33	3.7	89.78	0.15	6.37	330	372
5	202.95	7.79	78.41	1.11	12.69	320	360
6	221.43	7.03	73.68	0.78	14	330	340
7	284.66	5.07	83.41	4.89	6.61	350	390
8	330.55	7.05	84.66	0.36	7.94	360	410
9	336.71	4.76	77.59	4.2	13.45	480	480
10	397.32	12	74.19	0.19	13.58	440	360
Mean	284.21	7.26	75.49	2.87	13.92	351.00	371.20
SD	61.15	3.3	10.78	3.28	7.96	61.73	48.18
SEM	19.34	1.04	3.41	1.04	2.52	19.52	15.24

Note: Dose refers to delivered dose assessed by gamma camera; chest, impacted, exhaled and adaptor expressed as % of delivered dose; test shots and delivered dose assessed by radioisotope calibrator.

Table D.7: Specific activity expressed as mg of nedocromil sodium detected in the whole chest or right lung after inhalation of fine nedocromil sodium assessed by counts derived from both planar and SPECT images.

Subject	Chest (planar)	R lung (planar)	R lung (SPECT)
1	0.092	0.028	0.042
2	0.349	0.146	0.040
3	0.125	0.056	0.027
4	0.195	0.074	0.026
5	0.351	0.142	0.061
6	0.408	0.172	0.064
7	0.378	0.178	0.050
8	0.284	0.123	0.049
9	0.322	0.122	0.055
10	0.611	0.275	0.082
Mean	0.311	0.132	0.050
SD	0.151	0.07	0.017
SEM	0.048	0.022	0.005

Table D.8: Specific activity expressed as mg of nedocromil sodium detected in the whole chest or right lung after inhalation of coarse nedocromil sodium assessed by counts derived from both planar and SPECT images

Subject	Chest (planar)	R lung (planar)	R lung (SPECT)
1	0.539	0.215	0.079
2	0.292	0.129	0.037
3	0.161	0.079	0.027
4	0.146	0.058	0.019
5	0.307	0.129	0.042
6	0.277	0.134	0.049
7	0.200	0.074	0.035
8	0.278	0.080	0.041
9	0.188	0.071	0.051
10	0.473	0.116	0.070
Mean	0.286	0.109	0.045
SD	0.13	0.047	0.018
SEM	0.041	0.015	0.006

Table D.9: Penetration index derived from planar gamma camera images, coronal or transverse reconstructed SPECT images after inhalation of fine nedocromil sodium

Subject	P 1	P 2	C NC	C C	T NC	T C
1	3.02	1.34	2.25	3.05	2.22	3.22
2	2.13	1.53	3.15	5.68	2.19	3.00
3	1.28	1.34	1.45	1.72	1.63	2.19
4	1.58	1.37	1.84	2.38	1.82	2.33
5	2.54	1.43	2.39	3.05	3.00	4.32
6	2.07	1.55	2.72	3.58	2.91	4.09
7	1.56	1.35	1.80	2.10	1.68	1.93
8	1.63	1.47	1.73	2.06	2.09	2.95
9	1.80	1.49	1.91	2.44	1.91	2.56
10	5.03	1.84	4.42	9.80	5.09	14.07
Median	1.94	1.45	2.08	2.75	2.14	2.98

Abbreviations: P 1 - 1st planar image; P 2 - 2nd planar image (following SPECT); C NC - coronal SPECT, not corrected for blood background; C C - coronal SPECT, corrected for blood background; T NC - transverse SPECT, not corrected; T C - transverse SPECT, corrected.

Table D.10: Penetration index derived from planar gamma camera images, coronal or transverse reconstructed SPECT images after inhalation of coarse nedocromil sodium

Subject	P 1	P 2	C NC	C C	T NC	T C
1	2.50	1.30	3.15	3.84	2.61	3.06
2	2.18	1.43	1.99	2.45	2.19	2.82
3	1.31	1.23	1.58	1.86	1.67	2.07
4	1.45	1.30	1.79	2.33	1.78	2.44
5	2.22	1.61	2.38	3.21	2.44	3.53
6	2.39	1.64	3.24	4.17	2.94	3.62
7	2.00	1.40	2.54	3.71	2.64	3.85
8	1.59	1.34	2.08	2.73	2.58	4.16
9	1.59	1.43	2.58	3.23	2.38	3.45
10	5.68	2.61	6.84	14.05	7.75	17.63
Median	2.09	1.42	2.46	3.22	2.51	3.49

Abbreviations: P 1 - 1st planar image; P 2 - 2nd planar image (following SPECT); C NC - coronal SPECT, not corrected for blood background; C C - coronal SPECT, corrected for blood background; T NC - transverse SPECT, not corrected; T C - transverse SPECT, corrected.

Table D.11: Distribution of voxel activity within the right lung after inhalation of two formulations of nedocromil sodium.

	Standard			Coarse		
	SD	Skew	Kurtosis	SD	Skew	Kurtosis
1	0.511	-0.1494	1.4158	0.5053	0.2929	1.9887
2	0.5868	-0.5372	1.8627	0.5352	-0.5486	2.3158
3	0.4907	-0.7617	2.0925	0.4472	-0.8008	1.8099
4	0.3896	-0.2798	1.5309	0.5001	-0.3855	2.7369
5	0.5639	0.0578	2.3551	0.5325	-0.1880	1.6102
6	0.5478	-0.0121	1.976	0.6695	-0.4333	1.4637
7	0.4449	-0.2077	0.8296	0.6258	-0.4935	1.2885
8	0.4792	-0.133	1.3336	0.559	0.0068	0.9569
9	0.4417	-0.138	1.2985	0.6284	-0.2259	2.1765
10	0.6551	0.5123	1.6689	0.6886	1.1355	3.4141
Mean	0.511	-0.165	1.636	0.569	-0.164	1.976
SD	0.079	0.34	0.448	0.08	0.549	0.726

Table D.12: Median dose position (expressed as shell number) of both aerosols.

Subject	Fine aerosol	Coarse aerosol
1	6.79	6.46
2	6.33	6.71
3	7.21	7.13
4	6.88	7.28
5	6.42	6.73
6	6.42	6.23
7	7.13	6.79
8	6.96	7.00
9	7.11	6.93
10	3.20	2.93
Median	6.84	6.76

Table D.13: Intensity half-distance for both aerosols (expressed as standardised position from right lung hilum).

Subject	Fine aerosol	Coarse aerosol
1	43.3	31.5
2	43.3	53.3
3	60.3	69.3
4	51.7	46.5
5	33.3	43.3
6	33.0	28.9
7	69.3	40.8
8	46.2	38.5
9	40.8	46.2
10	9.9	9.1
Median	43.3	42.1

Table D.14: Pharmacokinetic parameters following inhalation of 2 formulations of radio-labelled nedocromil sodium.

	Fine			Coarse		
Subject	C max (ng/ml)	T max (min)	AUC obs (ng.min/ml)	C max (ng/ml)	T max (min)	AUC obs (ng.min/ml)
2	2.093	45	228.24	1.031	45	118.06
3	0.725	30	117.09	0.873	45	111.48
4	1.503	60	208.37	0.715	60	55.08
5	2.306	7	230.50	2.502	5	110.83
6	2.455	60	360.29	0.942	45	124.27
7	6.079	5	339.04	2.213	10	189.22
8	1.179	15	26.78	1.730	60	155.41
Mean	2.33	31.71	216.76	1.43	38.57	123.48
SD	1.77	23.75	116.88	0.72	22.31	41.54
SEM	0.67	8.98	44.18	0.27	8.43	15.70

Table D.15: Absorption half-life (min) of technetium after inhalation of 2 formulations of radio-labelled nedocromil sodium

Subject	Fine	Coarse
1	14.78	6.44
2	12.46	15.07
3	11.05	10.93
4	11.04	44.14
5	9.39	12.27
6	14.97	49.15
7	17.50	25.11
8	8.59	18.68
9	13.05	14.06
10	5.56	17.86
Mean	11.84	21.37
SD	3.49	14.27
SEM	1.10	4.51

Table D.16: Technetium absorption rate constant after inhalation of 2 formulations of radio-labelled nedocromil sodium.

Subject	Fine	Coarse
1	0.0469	0.1076
2	0.0556	0.0460
3	0.0627	0.0634
4	0.0628	0.0157
5	0.0738	0.0565
6	0.0463	0.0141
7	0.0396	0.0276
8	0.0807	0.0371
9	0.0531	0.0493
10	0.1246	0.0388
Mean	0.0646	0.0455
SD	0.0246	0.0271
SEM	0.0078	0.0086

Table D.17: Nedocromil plasma levels (ng/ml) after inhalation (mins) of fine formulation.

Time	2.5	5	7.5	10	15	30	45	60	90	120	180	240	300	360
Subject														
1	0.270	0.229	0.487	0.886	1.294	0.611	0.593	0.746	0.331	0.743	0.258	0.240	1.440	0.270
2	1.433	1.633	1.420	1.382	1.553	1.572	2.093	1.526	1.084	0.876	0.364	0.154	0.125	0.000
3	0.000	0.071	0.482	0.593	0.215	0.725	0.409	0.377	0.373	0.086	0.282	0.311	0.380	0.465
4	0.620	ND	1.272	1.058	0.698	1.001	0.875	1.503	1.240	0.663	0.547	0.762	0.000	0.000
5	1.958	1.724	2.306	2.178	1.595	1.428	1.595	1.547	1.049	0.680	0.524	0.143	0.130	0.142
6	1.856	1.881	1.848	1.888	1.545	1.497	1.810	2.455	1.875	1.461	1.149	0.295	0.244	0.090
7	3.833	6.079	3.464	2.777	5.969	2.835	2.828	2.073	1.173	1.344	0.226	0.140	0.000	0.000
8	0.000	0.098	0.257	0.000	1.179	0.393	0.039	0.241	0.144	0.000	0.000	0.000	0.000	0.000
10	1.729	21.458	1.387	1.682	6.258	2.162	2.098	2.840	7.821	0.872	0.802	0.459	0.365	0.247
Mean	1.30	4.15	1.44	1.38	2.26	1.36	1.37	1.48	1.68	0.75	0.46	0.28	0.30	0.13
SD	1.24	7.26	1.02	0.85	2.23	0.78	0.93	0.90	2.37	0.49	0.34	0.22	0.45	0.16
SEM	0.41	2.57	0.34	0.28	0.74	0.26	0.31	0.30	0.79	0.16	0.11	0.07	0.15	0.05

ND - not done (sample missed).

Table D.18: Nedocromil plasma levels (ng/ml) after inhalation (mins) of coarse formulation.

Time	2.5	5	7.5	10	15	30	45	60	90	120	180	240	300	360
Subject														
1	2.708	ND	3.443	2.556	2.615	1.785	2.404	2.338	1.283	1.002	0.26	0.717	0.224	0.055
2	0.881	0.937	1.029	0.893	0.64	0.754	1.031	0.834	0.803	0.397	0.183	0.076	0	0
3	0.385	0.277	0.544	0.856	0.478	0.552	0.873	0.861	0.461	0.337	0.249	0.184	0	0.308
4	0.423	0.372	0.44	0.258	0.156	0.295	0.363	0.715	0.464	0.165	0	0.023	0.066	0
5	2.502	1.835	2.03	1.874	1.081	0.727	0.849	1.155	0.539	0.234	0.051	0.029	0	0
6	0.695	0.758	0.634	0.787	0.73	0.748	0.942	0.915	0.622	0.526	0.359	0.062	0	0.006
7	1.545	1.393	2.089	2.213	1.916	2.06	1.2	1.741	0.675	0.495	0	0.373	0	0
8	0.522	0.725	0.607	0.63	0.592	0.149	1.26	1.73	0.549	0.75	0.136	0.099	0.547	0.033
10	0.934	4.776	0.793	0.918	1.028	0.996	1.317	1.328	1.485	0.773	0.521	0.315	0.388	10.746
Mean	1.18	1.38	1.29	1.22	1.03	0.90	1.14	1.29	0.76	0.52	0.20	0.21	0.14	1.24
SD	0.88	1.46	1.02	0.79	0.77	0.64	0.55	0.55	0.37	0.28	0.17	0.23	0.21	3.57
SEM	0.29	0.52	0.34	0.26	0.26	0.21	0.18	0.18	0.12	0.09	0.06	0.08	0.07	1.19

Table D.19: Plasma activity (Kbq/ml) after inhalation (minutes) of fine nedocromil sodium.

Time	0	2.5	5	7.5	10	15	30	45	60	90	120	180	240	300	360
Subject															
1	0	0.77	1.1	1.81	2.63	6.33	10.26	11.09	10.72	9.93	9.14	8.07	6.84	5.79	6.28
2	0	1.72	1.99	2.18	2.57	3.31	4.84	5.3	4.74	4.76	4.76	3.99	3.7	3.61	3.29
3	0	0.29	0.42	1.36	2.86	5.54	8.86	9.57	8.65	10.99	9.22	8.88	7.69	7.91	5.71
4	0	1.5	ND	3.55	4.14	4.7	7.07	7	7.97	6.68	7.53	5.75	5.82	5.41	5.13
5	0	3.54	3.81	4.86	5.67	6.39	8.77	9.03	7.99	9.81	7.9	6.67	6.28	5.82	6.39
6	0	1.11	1.74	2.38	3.29	4.35	6.84	6.76	7.89	6.7	7.61	6.07	5.28	4.56	4.41
7	0	6.86	8.57	10.33	13.23	19.34	31.46	30.93	27.74	23.74	23.48	19.15	18.48	17.96	18.3
8	0	0.5	2.01	4.25	5.83	7.57	8.44	8.97	8.06	7.69	7.73	6.69	5.86	5.81	5.72
9	0	1.83	2.27	2.83	3.93	5.08	8.78	8.43	8.06	6.28	7.09	5.71	5.26	5.49	4.88
10	0	2.41	3.63	5.66	6.35	11.26	11.06	9.85	8.78	12.96	11.06	8.38	7.43	7.36	7.59
Mean		2.05	2.84	3.92	5.05	7.39	10.64	10.69	10.06	9.95	9.55	7.94	7.26	6.97	6.77
SD		1.94	2.40	2.64	3.19	4.74	7.52	7.31	6.38	5.45	5.16	4.20	4.11	4.05	4.22
SEM		0.61	0.80	0.84	1.01	1.50	2.38	2.31	2.02	1.72	1.63.	1.33	1.30	1.28	1.33

Table D.20: Plasma activity (Kbq/ml) after inhalation (minutes) of coarse nedocromil sodium.

Time	0	2.5	5	7.5	10	15	30	45	60	90	120	180	240	300	360
Subject															
1	0	3.01	ND	4.36	4.98	5.82	6.42	7.19	7.19	6.82	5.88	5.03	4.59	4.27	3.95
2	0	2.61	3.04	3.38	3.57	4.2	5.89	7.05	6.3	6.07	5.47	4.67	4.63	5.59	4.05
3	0	0.6	1.23	1.93	3.08	4.98	5.68	5.51	5.81	5.03	4.69	4.17	3.89	4.06	3.16
4	0	0.77	0.75	1.08	1.79	2.49	4.74	5.32	6.84	8.27	7.77	7.43	6.52	6.07	6.1
5	0	3.39	2.93	4.33	4.26	5.59	6.29	7.07	5.65	4.98	5.48	4.69	3.87	3.99	3.85
6	0	0.97	1.59	1.5	2.09	2.06	1.91	2.45	3.42	3.89	3.78	3.43	3.15	2.41	2.36
7	0	4.1	4.26	5.22	6.56	9.65	18.03	19.57	23.08	18.43	16.45	14.11	14.27	13.99	13.53
8	0	0.69	2.57	4.45	6.88	10.03	15.92	16.52	16.82	14.66	12.7	9.81	10.23	9.39	8.04
9	0	1.19	1.47	2.84	3.59	4.04	5.95	6.85	5.91	5.98	5.92	4.78	3.64	4.21	4.68
10	0	1.06	2.13	2.64	3.14	4.76	7.22	7.29	7.44	6.05	5.4	4.67	5.63	4.54	4.49
Mean		1.84	2.22	3.17	3.99	5.36	7.81	8.48	8.85	8.02	7.35	6.28	6.04	5.85	5.42
SD		1.30	1.09	1.40	1.71	2.65	5.06	5.30	6.14	4.73	4.03	3.32	3.55	3.40	3.26
SEM		0.41	0.36	0.44	0.54	0.84	1.60	1.68	1.94	1.50	1.28	1.05	1.12	1.08	1.03

Calculation of total radiation dose incurred by subjects inhaling radioactive aerosols.

Sample calculation based on ICRP recommendations (ICRP 1987).

Lung activity. Based on data for Tc-labelled albumin microspheres used in perfusion studies. Clearance of microspheres from the lung is essentially zero, so the half-life of clearance of activity is that of pertechnetate, 6.04 hr. In this thesis however, clearance of activity from the lung is rapid, with an estimated half-life of 20 minutes (0.3 hr). The activity of microspheres is 0.011 milliSievert (mSv)/MBq of activity in the lung. Dose is related to effective half-life by:

$$\text{Dose} = \text{initial activity} \times \text{half-life}$$

Therefore, assuming a lung activity of 15.51 MBq (subject 10, table D.5), the total dose to the body is given by:

$$\text{Dose} = (15.51 \times 0.012) \times (0.3/6.04) = 0.009 \text{ mSv}$$

Plasma activity. Based on data for pertechnetate. The activity of pertechnetate is 0.013 mSv/mBq, so for an assumed value of 94 mBq (calculated from the maximum plasma activity of subject 7, table D.19 and multiplied by an estimate of plasma volume for an average male - 3 litres), the dose is 1.22 mSv.

Stomach activity. Based on data from gastric emptying studies with little absorption of gut activity. For an assumed stomach activity of 150 mBq, dose is equal to 0.024 mSv/mBq multiplied by 150, giving 3.6 mSv.

The total dose from these calculations is therefore 4.83 mSv, and therefore for both studies the estimated total dose incurred by subjects would be 9.7 mSv.

Note that these calculations are based on a 'worse-case' scenario, with values of activity taken as the maximum recorded for all subjects in lung and plasma, and as a generous overestimate of stomach activity.